Astronomical Polarimeter and Pulse Timer

Group III – Authors

Vincent Miller, *Photonics Engineering*

David Patenaude, *Photonics Engineering and Computer Engineering*

Ethan Tomczak, *Electrical Engineering*

David Urrego, *Computer Engineering*

Project Sponsor

Dr. Stephen Eikenberry, *Professor*

Faculty Reviewers

Mark Maddox, *Professor*
Dr. Sonali Das, *Lecturer*
Dr. Stephen Eikenberry, *Professor*

Senior Design Mentors

Dr. Lei Wei, *Associate Professor*
Dr. Aravinda Kar, *Professor*

List of Figures

List of Tables

Chapter 1 – Executive Summary

Pulsars are rare astronomical objects with uniquely extreme properties, the study of which has revolutionized our understanding of the universe in the past and may well continue to do so in the future. To further the field of astronomy, we will build a polarimeter device to record precise polarization data of the light from optical pulsars, and how it varies over time. In this document, we discuss the research, design, construction, and testing processes needed to build it successfully.

The optics are broken down into two subassemblies that together are mounted to an existing telescope. The polarimeter is a Stokes Polarimeter and collects all scientific data. We find that building a Stokes polarimeter requires a half waveplate, dual Wollaston prisms, and a series of single photon photodetectors and mirrors. The image acquisition and guiding system enables the device to stay pointed at the target star, along with checking for proper alignment. The design makes use of a pinhole mirror for splitting background starlight away from scientific detectors, and a series of lenses to focus this starlight onto a detector. Alternative imaging paths allow us to see an image of the telescope pupil for alignment purposes.

Components such as the analog to digital converter (ADC) and microcontroller unit (MCU) require our own code to record incoming data and convert from an analog signal to a computer-readable digital format. Onboard components utilize code written in *C* to directly interface with data acquisition and control hardware elements such as two switchable mirrors and a rotating half waveplate. An external *Python* package will handle user inputs and data interpretation. For user accessibility, interfacing with this instrument will be done over a standard USB connection.

These components are all powered by a custom-built power supply which can provide 3.3V, 5V, and ±12V simultaneously. These voltages are regulated by a custom PCB, providing stable voltages for all the peripherals. Current requirements were gathered for each component and accounted for in the design of the power supply.

Initial product research is conducted to identify shortcomings in existing astronomical polarimetry, then specific components are selected from the available space of products that fit within our engineering constraints. Using this information, we perform calculations to determine the needed design to construct this instrument. All designs are first tested using relevant simulation software such as LTSpice and Zemax. Performance is validated by constructing a physical prototype of the simulated design. The constructed device is subject to rigorous testing and adjustments to ensure functionality.

Chapter 2 – Project Description

In this chapter, we will describe in greater detail the project as a whole. Part of this will be to give background information and the motivation for the project. We also discuss the overall goals and objectives for the project and give specifications for the project.

2.1 Project Background and Motivation

In this section we look at the background of pulsars, as this is what our instrument will be detecting. From there we give some motivation as to why this project is beneficial to astronomers.

2.1.i Background

Our project is about making an instrument that can measure the polarization and pulse timing of pulsars, which are neutron stars that emit pulses. We plan to accomplish this by attaching our instrument to a pre-existing telescope. To measure the polarization, we intend to make a linear Stokes polarimeter. By attaching this instrument onto the telescope, we can analyze intensity of light after it passes through the polarizers and waveplates, which allows for the polarimeter to calculate the Stokes parameters. These parameters include light intensity, circular polarization, as well as linear polarization. This data reveals the degree and angle of polarization. Light from the Crab Pulsar will also be processed to determine how the light is polarized. Overall, our tool can be used to determine the orientation and degree of the pulsar's magnetic field and analyze the interactions between the pulsar's emitted light and its surrounding environment.

2.1.ii Primary Motivation

The motivation for this project comes from Dr. Stephen Eikenberry, who is a professor at the University of Central Florida, College of Optics and Photonics. His research focuses on astrophysics and the development of instrumentation for Astrophotonics research.

At Dr. Eikenberry's request we are building an instrument to measure the pulse timing and polarization of light from the Crab Pulsar, an optical pulsar approximately 7000 light years from earth. Pulsars are a type of neutron star that emit bright, directed beams of radiation while simultaneously spinning at high speeds. This leads to a pulsing effect where the brightness of the star increases and decreases periodically, as the beam points towards and then away from astronomers on Earth. Among astronomical objects, this regular pulsing behavior is unique to pulsars and could provide valuable data needed to explain how they operate.

All neutron stars, pulsars included, are a highly unusual type of star with extremely fast rotational velocities, strong magnetic fields, and extreme densities. The polarization and pulse timing data provide astrophysicists with vital information needed to study the structure and dynamics of pulsars. Polarization data discloses details about the pulsar's magnetic field such as its structure and strength, this can help explain how the pulsar emits radiation and interacts with particles. Measuring pulse timing can provide the distance of a pulsar from Earth, it can give information on the pulsar's rotation and stability, and measuring changes in a pulsar's timing can indicate internal processes like starquakes and/or interactions with nearby objects. The combination of these two data points can serve astronomers by helping scientists understand the pulsar's behavior, structure, and the space around it. The extreme rotating magnetic fields near the surface of these types of stars interact with outgoing particles and produce linearly polarized light, which is what our project will be detecting. When synchronized with pulse timing measurements, our instrument will provide novel scientific data that will help scientists study these extreme and complex objects. Since pulses from the Crab Pulsar are detectable at visible wavelengths, our project will be built using visual spectrum optical components. It will be mounted onto the existing 20-inch telescope at the University of Central Florida's Robinson Observatory. It is uncommon for pulsars to emit visible light, as there are only a handful of such pulsars known. The Crab Pulsar, being one of these rare exceptions, provides a unique opportunity to study its properties in detail. By focusing on visible light, our project aims to capture high resolution data that can reveal new insight about its emission mechanisms and magnetic field structure, which are characteristics that would be difficult to obtain at other wavelengths. Having a better understanding of this pulsar could greatly contribute to the field of astrophysics in a variety of ways.

2.1.iii Further Applications

The module we will be constructing can be used for many additional measurements by astronomers. This device will have a sufficient sampling rate to be able to measure all kinds of visible stars and exoplanets within our galaxy, helping astronomers gain a more thorough understanding of our universe. For example, using this device on other stars we can use the polarization and pulse timing data gathered to geometrically map the magnetic field of the observed star. In the case of exoplanets, astronomers will be able to map out the orbital path of the observed exoplanet. This can be done because the starlight reflected off the exoplanet will be of a particular polarization. Overall, we would like to see many observatories use this device for a wide range of data collection.

2.2 Existing Projects and Products Comparison

In this section, we look at some of the existing products for measuring polarization of light (polarimeters). We also look at instruments that mount to a telescope, similar to our project.

2.2.i Mini-HIPPI (Miniature High Precision Polarimetric Instrument)

This telescope polarimeter developed by Jeremy Bailey, Daniel V. Cotton, and Lucyna Kedziora-Chudczer displays remarkably similar functionality to the product we would like to develop. The Mini–HIPPI is a telescope mountable stellar polarimeter which has the following design properties: high precision measurements (0.1% error), compact footprint (weight of 650g), large wavelength coverage (nanometer range), and lastly, sophisticated optical design coupled with sensitive detectors. The optics section of the module comprises a ferroelectric liquid crystal (FLC) modulator, a Glan Taylor Prism, and a collection of photomultiplier tube modules [1]. The use of a FLC modulator rather than a wave plate retarder is important to note. FLC modulators allow for fast, real-time application, whereas a half wave plate retarder may want to be selected for higher precision and reliability. Furthermore, for this polarimeter design, the team chose a Glan Taylor prism which limits the measurements to linear polarization states of the input signal. This prism was primarily chosen for simplicity and cost-effectiveness. In summary, the Mini-HIPPI is an excellent project to reference for our project design considering the optics design.

2.2.ii Thorlabs High-Dynamic Polarimeter

An existing product on the market is a pre-built polarimeter. These polarimeters come with different wavelength ranges and an accuracy of ±0.25°. They operate on the principle of using a rotating quarter-wave plate and a linear polarizer hooked up to a photodiode. The use of a quarter-wave plate allows for the instrument to detect circularly polarized light. This particular polarimeter from Thorlabs has a max sampling rate of 400 samples/s [2]. In our case, we would require a higher sampling rate to achieve the temporal resolution to see the pulse features. We are also dealing with incoherent light, which this polarimeter cannot handle.

2.2.iii Radio Astronomy Polarimetry

Polarimetric measurements of various pulsars have been taken before and are most commonly measured at radio frequencies. This is simply because, of the over 3000 known pulsars, the overwhelming majority pulse at radio frequencies. Additionally, radio polarimetry in astronomy can often be done without specialized measurement devices since radio antennas are inherently susceptible to the polarization of the received signal. Specifically, this is the case with the ALMA radio telescope [3]. Unfortunately, radio frequency polarimetry cannot be used to replace visible spectrum polarization data. Visible spectrum light and higher energy light in general provide unique information about the high energy interactions and mechanisms taking place within pulsar magnetic fields.

Overall, it is critical that we do research on existing products and projects related to our project to compare design measures and locate potential obstacles that may slow developmental and prototyping processes. Through the work of others, we can also see if certain methods should or should not be considered regarding our design specifications. Additionally, the research opens the avenue into new technologies that may suffice a requirement we desire. Using this approach will aid our development timeline and will improve the overall quality of our final product.

2.3 Goals and Objectives

Now we look at the goals of our project, and the objectives to achieve them. We start by giving our main goal and the objectives for it. Then we break our goals down into smaller basic, advanced, and stretch goals. Finally, we list our objectives for these goals as well.

2.3.i Goals

Our goal is to enable further study of visible-spectrum pulsars (specifically the Crab Pulsar) by creating an instrument to measure the polarization and pulse timing concurrently of the incident light. This instrument would then be attached to a telescope to gather light from the pulsar. Our overall objectives (or sub-goals) to meet this goal are:

- Design a Stokes polarimeter that can sample at a minimum of 250kHz.
- Design a pupil imaging system for alignment of the instrument to a telescope.
- Provide an image for a telescope's built-in tracking system.
- Design a software package which computes pulse timing for each measured polarization.

The overall goal can be broken down into basic, advanced and stretch goals. Our basic goals are:

- Optics: High efficiency optical coupling out of telescope to initially collect 100% of telescope output, no more than 10% power loss through the system. Near diffraction-limited off-axis aberrations in imaging subsystems. Measure pulse timing at 1µs and 1% polarization measurement accuracy.
- Hardware: Design a power supply unit. Design a PCB containing a data path from peripherals, a physical control panel containing an LCD, sampling start/stop button, and sampling duration control. Implement a MCU to direct control flow and data flow. Include on-board memory and USB I/O for data processing.
- Software: Control flow for hardware; sampling start/stop and sample duration adjustment.

Then some advanced goals:

- Optics: design of a system for imaging the telescope's aperture (exit pupil) for best alignment; designing optical paths to have minimized power loss; increasing sensitivity for higher polarization resolution (to 0.1% accuracy).
- Hardware: Allow for adjustable sampling rate and duration. Include physical controls (buttons, dials, LCD, etc.) on physical instrument.
- Software: Effective and logical data management and precision processing of pulse timing and polarization intensity; program UART/I2C for external (PC) control.

Our stretch goals:

- Optics: To achieve significantly higher (0.01%) measurement accuracy; designing the system to not lose more than 5% of optical power throughout.
- Hardware: Remote sampling and oscillator controls; Low power mode.
- Software: Full GUI program. Utilize Wi-Fi/Bluetooth hardware for more interactivity options.

Our objectives for the above goals are:

Optics:

- To not lose any light from coupling by gathering the full aperture of telescope output.
- Create a separate light path for defocusing to the telescope's aperture (imaging the pupil).
- Use AR coatings for optical surfaces on all light paths to reduce power loss.
- Include Wollaston prisms for separating light based on polarization state.
- Implement single photon avalanche photodetectors with high temporal resolution. These will be sensitive enough to measure optical signals on the order of femtowatts.
- Use low chromatic dispersion half-waveplates with precise polarization control to ensure polarization accuracy.

Hardware:

- Use AC to DC converter to provide power when plugged in. Distribute power throughout module using the necessary voltage regulators and op-amps schemes.
- Create BNC I/O for photoreceiver data input.
- Use a 1 MSPS ADC built into a MCU to convert photoreceiver signal into digital data which can be stored in on-board memory.
- Install a stable and fast clock in our system for high performance.
- Include sufficient flash memory to store sampled data, around 4GB is a good target.
- Include an LCD display to allow user to see and set sample start, sample duration and/or rate.
- Control panel will include a button, switch, and dial which will be read by the MCU to perform control actions.

Software:

- Use GPIO pins to read instrument parameters from hardware interface.
- Adjust hardware configuration (MCU) to match user parameters.
- Implement ".FITS" data formatting for the data coming in.
- Implement serial communication with connected PC.
- Implement pulse time calculation algorithm.
- Implement polarization angle algorithm.
- Make a user-interface for interacting with the data collected, including data plots.

2.3.ii Demonstration and Testing Plan

To demonstrate and test our project we utilized a 520nm laser from one of the CREOL labs. We built an 'artificial telescope' optical setup, which uses this laser as its input. The setup uses lenses and apertures to create an f/8.2 beam. By having a means to demonstrate in a controlled laboratory environment, we can work better on the prototype. Later testing of the instrument will be done at the Robinson Observatory at UCF when a more complete prototype is ready, and the night sky is clear. The telescope at the observatory is a 20" f/8.2 Ritchey-Chrétien reflector telescope.

Since we are interested in measuring fast pulse timing and polarization, we will modulate our light source. For finding polarization, we can use a simple wire grid polarizer to change the source's polarization and measure it with our instrument. By knowing the polarization of the light, we can then compare and measure the error of our instrument.

2.3.iii Illustrations

Below in Figure 2-1 is our overall initial optical design. It involves coupling light out of the telescope and into the instrument, where it is then split into two main paths. One path is collimated before being sent to the polarimeter. The other path is used for imaging the telescope's output and has a separate toggleable path for imaging the telescope's pupil for alignment purposes.

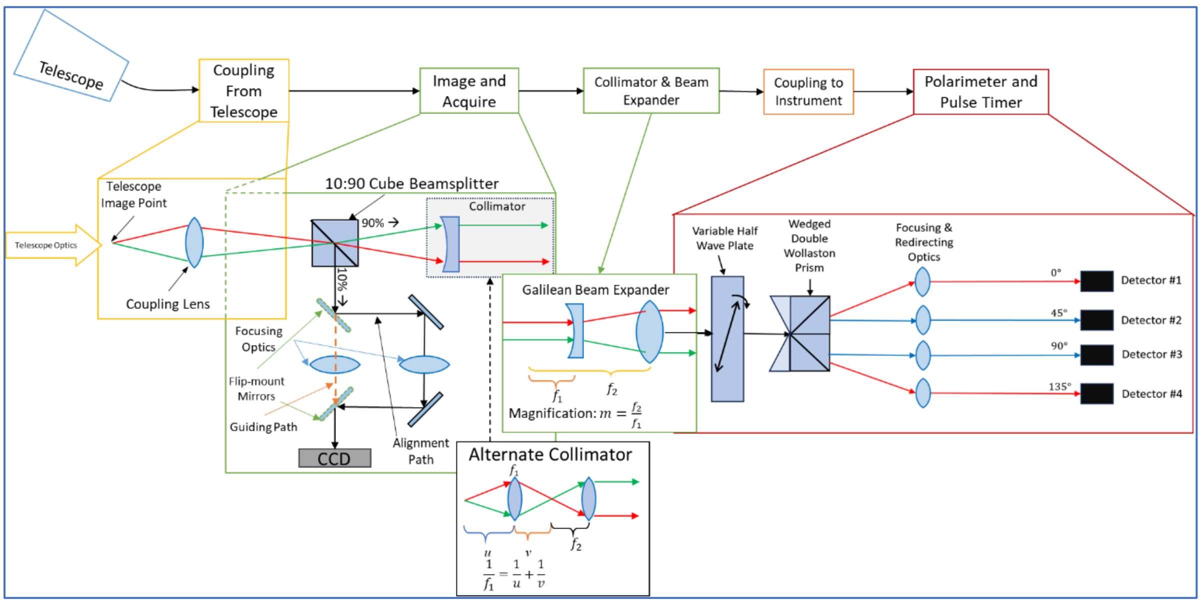

Figure 2-1 *- Initial Optical Design for the instrument.*

2.3.iv Hardware Features and Specification

The physical structure of this device is separated into three components: power supply unit (PSU), printed circuit board (PCB), and the optics coupling and detection module. Figure 2-2 below provides a visual representation. Within the power supply unit, we will house a battery which will supply power to printed circuit board and its peripherals. The design must meet our specification of supplementing the module with enough power for at least one hour before shutdown. In cases in which the module is low on battery, we will also include a 120V AC adapter within our design to charge the module. The module is intended to operate with the power from the adapter but can be disconnected if desired.

The printed circuit board will consist of the following components: controls for adjusting sampling rate and start/stop of data collection and sample duration. Also, some controls will be included for adjusting mirror positions within the module's optics section. MCU must have an ADC module which can sample at a rate of 1MSPS for our desired resolution.

A control board will host the necessary peripherals such as: buttons, knobs, and LCD needed for the previously mentioned functionalities. These control features will help us to collect an accurate sampling of data and allow for resolution adjustment if needed. We will have four distinct plane wave detectors in the optics module which would require approximately 391KB of data for all sensors to read for 50ms. The PCB will contain on-board memory storage of 4GB which will allow for approx. 10,737, 50ms samples before needing to be cleared. A USB 3.0 port will be installed for first programing the MCU for proper functionality, and secondly allowing for data collection from an outside computer. The MCU will have input from the detectors which will be processed by the internal ADC to sample then save the incoming signal from each plane wave detector.

Attaching to the telescope mount itself will be the star tracking equipment, polarimeter and pulse timer, and the necessary coupling optics. Due to the rotation of the Earth, the telescope will need to be constantly adjusted to stay pointing at the target star. We will accomplish this by building a separate optical path from the scientific instruments, where the starlight is instead imaged onto a CCD. The image detected by this CCD will then be sent to the established telescope tracking and control software, which will make all necessary adjustments. This will be sufficient for the telescope to stay on target during our observations. The scientific instrumentation that we will be building is a linear stokes polarimeter that will simultaneously be used to measure pulse timing. This consists of a double wedged Wollaston prism, which will split the incoming light into two pairs of beams, where each pair has orthogonal polarizations. Each path will have its own linear polarizer at a unique angle. By using 0, 45, 90, and 135 angles for the four polarizers, we can determine the signal's Stokes parameters by comparing the intensity readings from each detector. Changes in the total detected intensity will be used to find pulse timing. The variable half-wave plate is continuously cycled to filter out variations in polarization created by the instrumentation itself that would otherwise overwhelm the signal. Coupling optics will be needed to ensure that all light collected by the telescope can be received by the scientific instruments. The telescope in question is a 20" f/8.2 Ritchey-Chretien telescope, and our coupling optics will need to fit this system such that all light enters the system, while also not being overly large to allow extraneous signals (light) in.

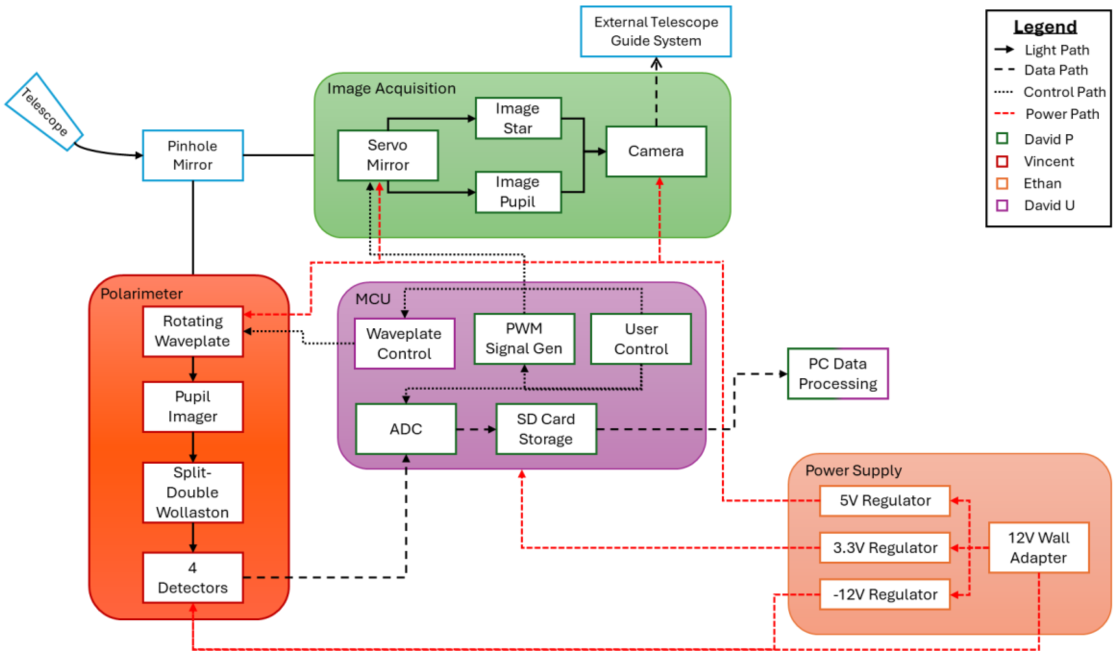

***Figure 2-2** – Hardware Block Diagram*

2.3.v Software Features and Specification

On the software side, we will be acquiring the sensor data and processing it. The acquisition will be from 4 detectors, which require conversion from an analog signal to a digital signal. The digital signal can then be stored in a cache until sampling is complete, where it can be formatted and stored more permanently. We plan on formatting the data as a '.FITS,' which stands for Flexible Image Transport System, which is a common file type used by astronomers.

To get the pulse time, we first find the intensity of the light by combining the intensities from two orthogonal detectors, such as the ones at 0° and 90°. This finds the 1st Stokes' parameter and is used to scale the other parameters. With the intensity, the signal should be oscillating sinusoidally, and so we find the pulse time by measuring the difference between two maxima. The maxima can be found either by enumeration through the data, or by using calculus (derivatives) to find them. The general flow is shown in Figure 2-3 (left).

For finding the polarization, we find the other two Stokes' parameters. The 1st parameter I is the intensity and is used to scale the Q and U parameters. The Q parameter is found by taking the difference of the squares between 0° and 90°. To account for unpolarized light, the 3rd parameter U is found by taking the difference of squares between 45° and 135°. The general flow chart is shown in Figure 2-3 (right) below.

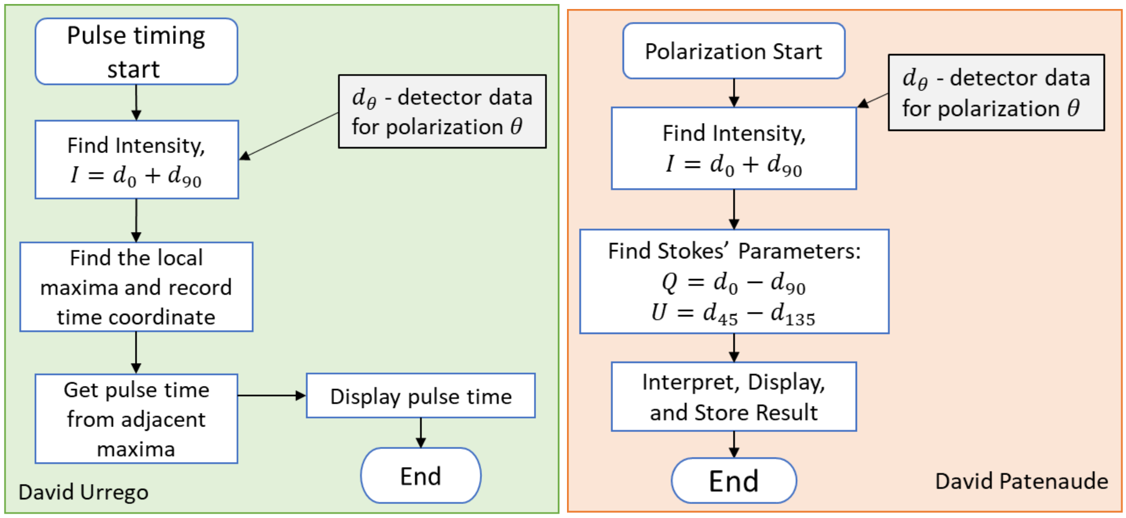

Figure 2-3 *– (left) Flowchart for finding pulse time. (right) Flowchart for finding the polarization.*

Additionally, programming of the microcontroller is also required. This is mainly for control flow and data collection. The control flow section of the flow chart below in Figure 2-4 shows a design that displays systematic data processing and user interaction. It begins with the user pressing a start button that will trigger a reaction of events, the system's first response is to configure the ADC with the set parameters. A start message will be displayed alongside the frequency on the LCD screen. This way the user is always aware of the system's status. The system then generates a signal frequency directed at the wave plate which is crucial for data collection and polarization quality. Once the signal is output a 50ms runtime sample is collected. During this period, the system samples and holds the data in a buffer, and then saves it to the main memory. This efficiently captures and stores the data to maintain integrity and accuracy. From here, the control flow branches into two parallel paths: one where the system ensures sufficient memory space and organization for incoming data through memory allocation, and another where it stops sampling and displays a session termination message on the LCD, informing the user. This structured approach optimizes data handling and memory management while enhancing user experience by providing real-time updates.

In the data management portion of the flowchart, the process begins with memory allocation, a critical step ensuring that sufficient space is set aside for subsequent operations. From memory allocation, the flow branches into two paths. The first path involves assigning address space for detectors 1 through 4, with each detector receiving a set amount of memory. The second path involves tagging the sampling session. These two branches converge into a single step: USB transfer out. This final step involves transferring the allocated data, both the detector address spaces and the sampling session tag, out via USB. This structured flow ensures efficient memory use and smooth data transfer, keeping the system organized and making it easier to analyze and store data later.

The USB transfer leads to the data processing section of the flowchart. The first block in this section is the software package, which splits into two paths. The first path combines the intensity data from single plane wave detectors with its pair, locates data maxima and timestamps, and then calculates the delta between two maxima to determine pulse time. The second path calculates the Stokes parameters from the plane wave detector and uses these parameters to display a graph along with the corresponding polarization. Both paths converge at the final block, which displays the processed data on the monitor, ensuring comprehensive data processing and visualization.

The expected pulses from pulsars will be on the order of 30ms, but to see the features of the pulse, we will sample every 1µs. The detectors will therefore have to be fast and sensitive due to the faintness of the incident light. To measure polarization, the design will feature a modulated waveplate and Wollaston prisms to separate the light into 4 beams, which go through a polarizer before the detector. This set up describes a linear Stokes polarimeter. Sampling at a high frequency and rotating the half-wave plate will eliminate the polarization effects from the telescope system.

To track the pulsar in the night sky, an image is captured and sent to the telescope's built-in tracking software. The input light is split upon entering the instrument using a beamsplitter, allowing an image to be taken on one path, while the other path continues into the instrument. As an optional feature, we will also save the camera's image to our internal storage. This makes it more convenient for the astronomer to retrieve the image for viewing.

Some other features we will implement are the ability to adjust the sampling frequency and the sample duration. By default, we will design for a 1MHz sampling rate, and 50ms duration. We will allow the sampling rate to increase to 2MHz and decrease to 100kHz while allowing the sample duration to increase to 1s and decrease to 25ms. The sampling rate will dictate how fast of an analog-to-digital converter we will need. The sample duration dictates how much storage is needed, although this isn't a huge issue as memory chips are cheap. The main issue is ensuring that the memory is fast enough to not bottleneck the data acquisition. This feature will be implemented by adding some buttons or dials with a basic LCD character display, which allows direct control on the actual instrument. We may also consider making it software controlled via a program on a plugged-in computer. This gives more choice to the astronomer for how much continuous data they may want.

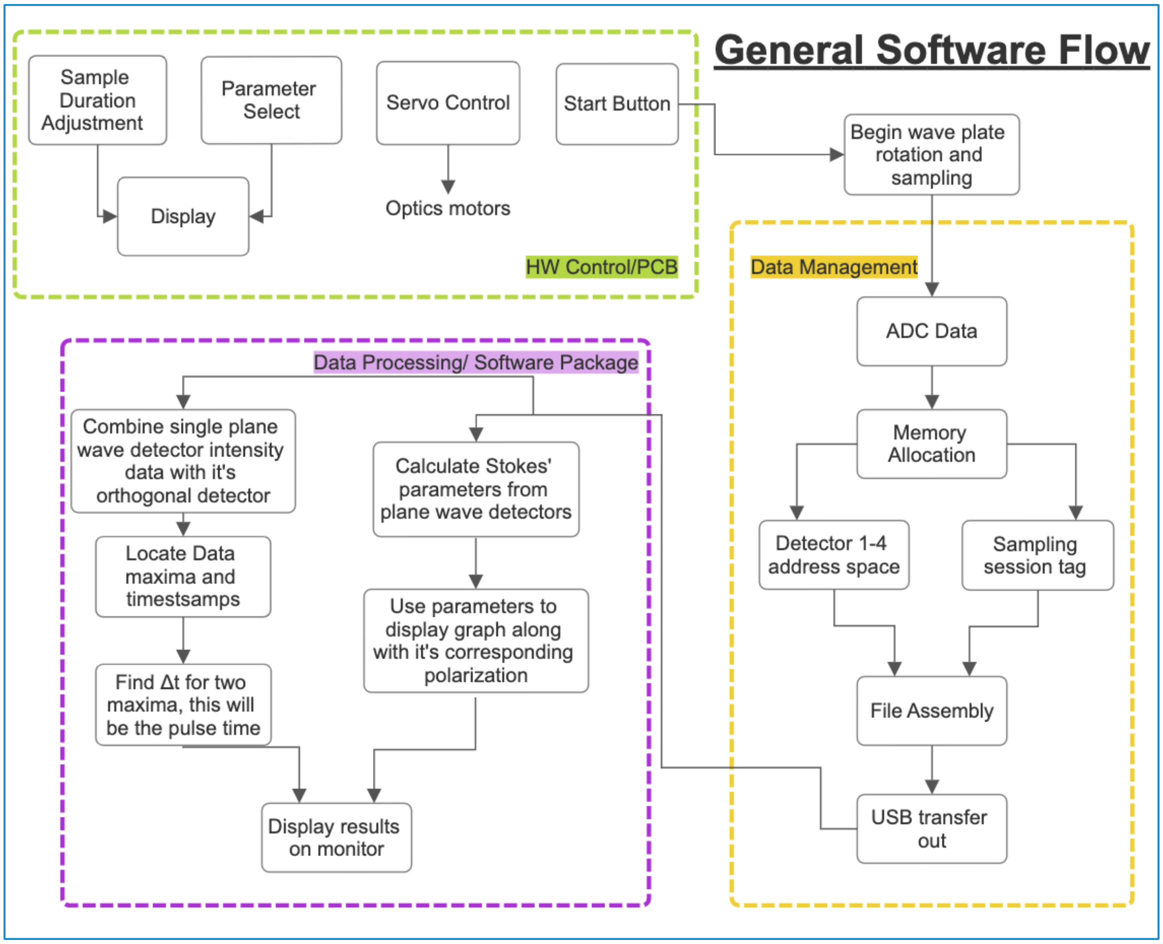

Figure 2-4 *- General Software flow, including control flow, data management, and data processing.*

We also want to ensure minimal optical power loss from reflections and absorption when the light is coupled and manipulated by the instrument. This is an important consideration given the low incident light intensity from astronomical sources. This can be accomplished by minimizing the amount of glass material that the light must travel through, such as lenses and beamsplitters. When a lens is used, an anti-reflective (AR) coating can be used to virtually eliminate Fresnel reflection losses. To ensure minimal losses, the optical power loss will be calculated for the optical design to ensure that sufficient power reaches the detectors.

2.4 Required Specifications

On account of the previous objectives and constraints, table 2.1 provides the functional specifications for our project's design. The highlighted specifications are those that we will demonstrate at the end of Senior Design II.

Table 2-1 - Specifications for Design

Description	Specification	Explaination
1. **Optical Power Sensitivity**	< 1 pW	The signals we measure are weak.
2. Down time between samples	15 seconds or less	Slowest part is transferring data across UART bridge
3. Imaging System Magnification	Magnifications of 0.8 and 0.018	Magnifications to keep images on camera for tracking and alignment
4. 4 Output PSU	3.3V, 5V, ±12V	These voltages are required across the system for proper functionality.
5. **Sample rate of pulse counting**	500 kHz	Enables us to detect signals with high temporal resolution.
6. **Minimum sample duration/time**	100ms	Allows for capture of full pulsar pulse.
7. **Polarization Measurement**	Accurate to 1°	Measure polarization state to 1 degree of precision for high resolution data.
8. **External memory size**	≥4GB	Allows for storing many samples
9. **Instrument size**	20"x20"x10"	Instrumentation must fit onto the available telescope slot.
10. Internal data rate capacity	At least 4 MB/s	Required speed to ensure all incoming data can be properly handled
11. Analog Frontend Speed	1 GHz or better	Required gain-bandwidth to handle detector pulses

2.5 House of Quality

Below is our House of Quality, which correlates the engineering requirements with the customer or market requirements. The diagram also includes the correlation between the engineering requirements as well and has the actual specifications for the engineering requirements at the bottom. For our project, we are trying to balance cost with performance, as we want to achieve a high sampling rate and high accuracy of the polarization and pulse time information. Unfortunately, we are also dealing with weak light and the detectors for weak signals get expensive very quickly.

Correlations	
Positive	+
Negative	−
No Correlation	

Relationships	
Strong	●
Moderate	○
Weak	▽

Direction of Improvement	
Maximize	▲
Target	◇
Minimize	▼

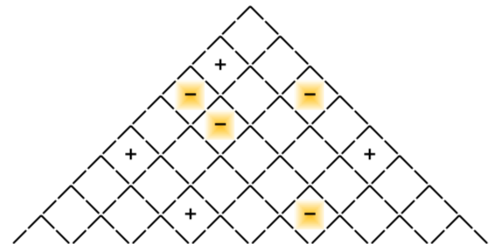

Weight	Customer Requirements (Explicit and Implicit) / Engineering Requirements	Polarization Measurement Accuracy	4 Output PSU	Sample Duration/Time	Sample Rate, ADC Module	On-board memory	Instrument Size	Optical Power Sensitivity	Internal Data rate capacity
	Column #	1	2	3	4	5	6	7	8
	Direction of Improvement	▲	◇	◇	◇	▲	▼	▲	▲
1	Resolution/Accuracy	●	▽	○	●	▽	▽	○	○
7	Ergonomic Mounting	○	○	▽	▽	▽	●	○	▽
2	High Sampling Rate	●	○	●	●	○	▽	▽	○
3	Computational Software	○	▽	○	▽	○	▽	○	○
4	Easy Data Access	▽	▽	▽	▽	●	▽	▽	●
6	Reliability	●	●	○	●	○	▽	●	○
5	Affordability	○	○	▽	●	●	○	●	●
	Target	0.1% Error	3.3V, 5V, 12V, -12V	50ms	1 MHz, 1 MSPS	4GB	6"x9"x11"	10fW	At least 16 MB/s

Figure 2-5 *- House of quality, showing customer requirements and engineering specifications.*

Chapter 3 – Technology and Parts Research

In this chapter, we report the findings of our research on the different technologies that we can use for completing our project. We then discuss products that we will use for the project.

3.1 Technology Comparisons

In this section, we look at the different technologies that we can use for the project. We group the technologies together and look at the advantages and disadvantages of each one. We then decide which one fits the best with our project and specifications.

3.1.i FPGA vs. MCU

We begin by looking at the difference between a Field-Programmable Gate Array (FPGA) versus a Microcontroller (MCU). These are the two main technologies that can be used for embedded systems. Each has its own strengths and weaknesses. Deciding whether to use an FPGA or an MCU for a project like the Crab Pulsar Polarimeter and Pulse Timer involves looking at factors like performance, flexibility, power use, cost, and how hard they are to develop with.

Field-Programmable Gate Arrays (FPGAs) are semiconductor devices that have a bunch of programmable logic blocks connected through programmable links. Unlike fixed-function chips, FPGAs can be reconfigured after they are made, allowing designers to create custom hardware functions. FPGAs are great for performance because they can do many things at once, making them highly efficient for tasks that can be done in parallel. This is particularly useful for real-time signal processing where multiple operations need to happen at the same time. Additionally, FPGAs are very flexible because their hardware functions can be updated or changed without altering the physical device, which is helpful during development and testing. FPGAs can integrate custom peripherals tailored to specific application needs, allowing for highly specialized hardware setups. Moreover, because of their parallel architecture, FPGAs offer low latency for certain types of computations, which is important in real-time applications.

However, FPGAs have some downsides. Designing for FPGAs requires knowledge of hardware description languages (HDLs) like VHDL or Verilog, which can increase development time and costs due to the complexity of hardware design. FPGAs generally use more power compared to MCUs, which can be a problem in battery-operated applications. The initial cost of FPGAs and their development tools can be higher than those for MCUs, making them less attractive for budget-sensitive projects. Additionally, the design cycle for FPGAs can be longer because of the complexity of hardware design and the need for thorough testing and validation.

On the other hand, Microcontrollers (MCUs) are integrated circuits designed to perform specific control functions. They typically consist of a processor core, memory, and peripherals all in one chip. MCUs are widely used in embedded systems for their simplicity and cost-effectiveness. MCUs are easier to program, and use compared to FPGAs, as they often use high-level programming languages like C or C++, which are more accessible to a broader range of developers. MCUs are designed to be power-efficient, making them ideal for battery-powered applications where energy use is a key factor. They are generally less expensive than FPGAs, both in terms of the initial hardware cost and the development tools required. MCUs come with a variety of built-in peripherals such as ADCs, DACs, timers, and communication interfaces, which simplify the design process. The development cycle for MCUs is typically shorter due to their simpler architecture and the availability of extensive libraries and development tools.

However, MCUs also have their limitations. They operate sequentially and may not handle tasks that need to be done in parallel as efficiently as FPGAs, which can be a drawback in applications requiring high-speed processing. Unlike FPGAs, MCUs have fixed hardware functionality, which means they cannot be reconfigured to change their fundamental hardware architecture. MCUs may have higher latency for certain types of operations due to their sequential processing nature, which can be a limitation in real-time applications requiring rapid response times. Additionally, while MCUs have a range of built-in peripherals, they lack the ability to implement completely custom hardware configurations as FPGAs do.

Given the specific needs of the Crab Pulsar Polarimeter and Pulse Timer project, we have decided to use an MCU for several reasons. The polarimeter is intended to operate for extended periods, potentially in remote locations where battery life is crucial. The lower power consumption of MCUs makes them ideal for such applications, ensuring longer operational times without frequent recharging or battery replacements. Budget constraints are always a factor in project development, and MCUs offer a cost-effective solution without compromising the necessary performance for our application. The lower initial cost and affordable development tools make MCUs a practical choice.

Utilizing an MCU allows the team to leverage existing skills and resources, reducing the learning curve associated with FPGA development. This leads to a shorter development cycle and faster time to completion, test, and prototype. MCUs come with built-in peripherals such as ADCs for signal conversion, timers for precise event handling, and communication interfaces for data transfer. These features align well with the requirements of our polarimeter, simplifying the hardware design and integration process. While FPGAs offer superior parallel processing capabilities, the performance of modern MCUs is sufficient for our data processing needs. By carefully optimizing the code and leveraging the MCU's capabilities, we can achieve the required real-time data acquisition and processing.

In practical terms, the Crab Pulsar Polarimeter and Pulse Timer require precise, real-time data processing capabilities to measure the polarization and pulse timing of light from the Crab Pulsar. The instrument needs to handle high-frequency data sampling and processing while maintaining low power consumption for extended use. MCUs are particularly well-suited for this task because they can efficiently manage the high-frequency data sampling needed to capture the pulsar's light variations. With integrated peripherals, MCUs can directly interface with sensors and other components, streamlining the data acquisition and processing pipeline.

Moreover, the cost-effectiveness of MCUs is a significant advantage. Given that our project operates under budget constraints, the lower cost of MCUs compared to FPGAs allows us to allocate resources to other critical areas of the project, such as high-quality sensors and optics. This financial flexibility can enhance the overall performance and accuracy of our instrument. The lower initial investment in MCU hardware and development tools is also beneficial, enabling us to quickly prototype and test our designs without incurring prohibitive costs.

Another critical factor is the development simplicity offered by MCUs. Our team's proficiency in high-level programming languages like C and C++ aligns perfectly with the development environment for MCUs. This alignment reduces the time and effort required to develop and debug the software, allowing us to focus more on optimizing performance and ensuring the robustness of our system. The availability of extensive libraries and community support for MCUs further accelerates the development process, providing access to pre-built functions and solutions that can be integrated into our project.

The built-in peripherals of MCUs play a crucial role in simplifying our design. For instance, the ADCs in MCUs allow us to convert the analog signals from our detectors into digital data for processing. Timers can be used to precisely control the sampling intervals, ensuring accurate time measurements of the pulsar's pulses. Communication interfaces like UART, SPI, or I2C facilitate data transfer between different components of our system and external devices, such as a computer for data logging and analysis. These integrated peripherals eliminate the need for additional external components, reducing complexity and potential points of failure.

While FPGAs offer unparalleled performance for parallel processing tasks, the nature of our project does not demand such capabilities. The real-time data processing requirements can be effectively met by modern MCUs, especially when the software is carefully optimized to leverage the available processing power. By focusing on efficient code design and leveraging the MCU's features, we can achieve the necessary performance without the added complexity and cost of FPGA development.

In conclusion, while both FPGAs and MCUs offer distinct advantages, the specific needs of the Crab Pulsar Polarimeter and Pulse Timer project make an MCU the more suitable choice. The MCU's power efficiency, cost-effectiveness, development simplicity, and integrated peripherals align well with our project requirements, ensuring a practical and efficient solution. By selecting an MCU, we can achieve our goals of precise polarization and pulse timing measurements while maintaining the flexibility and efficiency needed for extended use in an astronomical research setting. This choice allows us to deliver a high-quality instrument that meets our objectives while adhering to budget constraints and leveraging our team's strengths in software development.

3.1.ii Beamsplitter Technologies

Here we look at the different ways in which a beam can be split onto multiple paths. Some preliminary options are block beamsplitters, plate beamsplitters, and pinhole mirrors. Of these types of splitters, they can be either polarizing or non-polarizing, meaning they can split the light based on polarization state or not. First, we will look at plate beamsplitters.

3.1.ii.a Plate Beamsplitters

A plate beamsplitter is a piece of flat glass that has a special dielectric coating on it that reflects some fraction of the incident light. The exact ratio of reflected to transmitted (R/T) light can be designed through the design of the coating. Typically, these beamsplitters are used at a 45° angle of incidence (AOI) to give a 90° difference in the output optical paths. When the transmitted light goes through the glass, the light will refract and end up shifted or offset from the incident light [4]. Since the glass will have two boundaries with air, Fresnel reflections will occur on the back surface create a 'ghosting' effect. This effect diminishes the efficiency. To eliminate this effect, an anti-reflective (AR) coating may be applied to the back side of the beamsplitter, which will increase the efficiency of the beam splitter [4]. Another means of eliminating the ghosting is to use a 30 arcmin wedge, or some combination of the two [5]. The wedge makes it so that any amount that is reflected will diverge away.

While plate beamsplitters can be made for both polarizing and non-polarizing applications, the dependence on angle of incidence for polarized light makes it so that the reflection or transmission differs between *s*-polarized and *p*-polarized light [6]. The Fresnel reflection equations describe this effect, and it is plotted in figure 3.2 for uncoated N-BK7 glass (n=1.5168). Therefore, a non-polarizing plate beamsplitter will end up reflecting different intensities of parallel and perpendicular components of the incident light's polarization. This is seen in some of the product datasheets from the different Thorlabs products.

From Thorlabs, they have 10:90 (R:T) plate beamsplitters with an AR coating for 400-700nm (visible light) operation. They have a couple of different sizes available, including a rectangular plate. Part number **BSN04** has a half-inch diameter and 3mm thickness. It also features the 30 arcmin wedge to further reduce the ghosting effect. The difference in transmitted and reflected *p*-polarized and *s*-polarized light is <35% [5]. The BSN products all share the transmission profile shown in figure 3.1 below, which shows how they differ. These are the specs that help populate the comparison table. Other manufacturers share similar specifications as the Thorlabs beamsplitters.

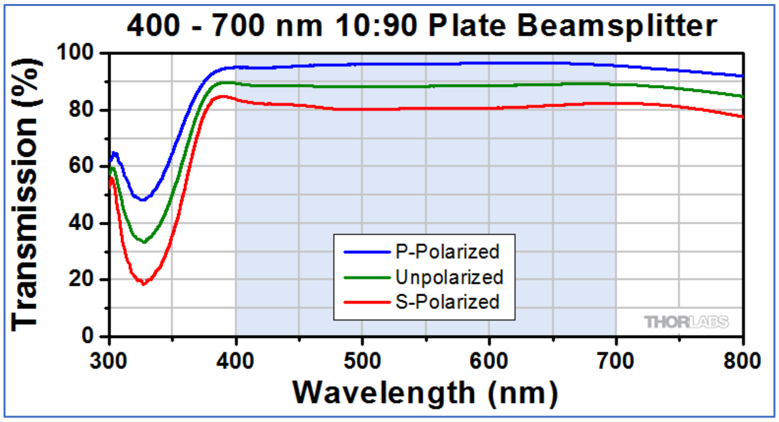

Figure 3-1 *- Plot of transmission for a 10:90 plate beamsplitter, showing both the p- and s-polarized light. Reprinted from ThorLabs, Inc. #BSN product series*

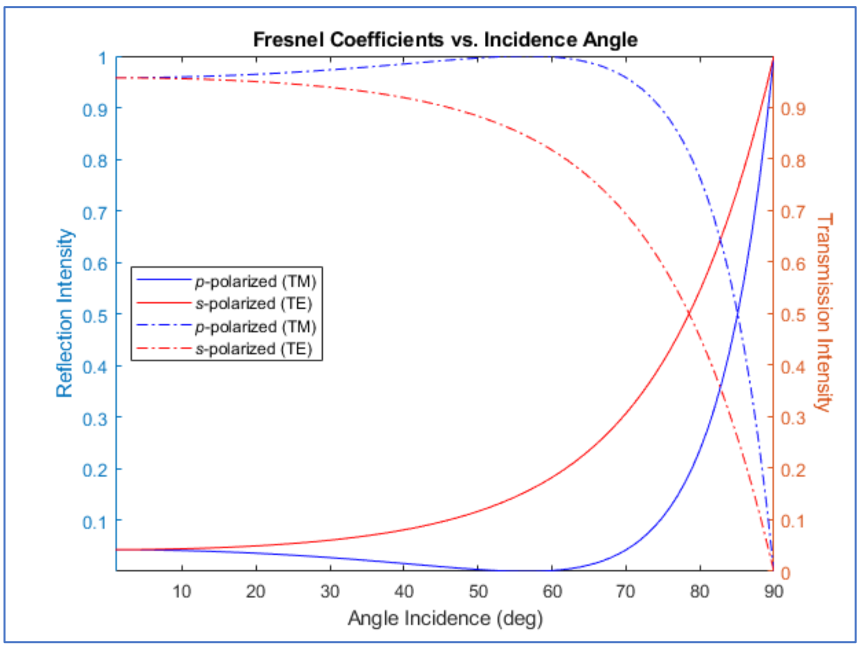

Figure 3-2 *- Plot of Fresnel reflection/transmission of parallel (p) and perpendicular (s) polarized light for n=1.5168. This is for uncoated glass and is provided as an illustration of how the reflections of orthogonal polarizations differ with angle of incidence.*

3.1.ii.b Cube Beamsplitters

Now we look at cube beamsplitters, which are two 90° prisms cemented together with a coating along the prisms' hypotenuse. These are designed for a 0° AOI, and typically have AR coatings to prevent reflection losses. Since a 0° AOI is used, the polarizations do not deviate from each other very much, as shown in figure 3.3. Furthermore, the transmitted beam is not displaced from the incident beam as much as the plate beamsplitter deviates them [5] [6].

Cube beamsplitters are susceptible to high optical power (such as a pulsed laser) when cemented together, but optical contacting allows for the higher power [5]. In our use case, high power won't be an issue, as we are dealing with faint incoherent light from a star.

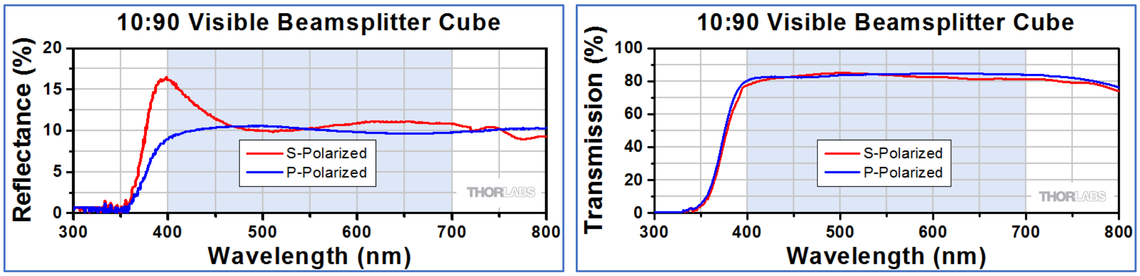

Figure 3-3 *- Reflection and Transmission of a beamsplitter cube. Retrieved from Thorlabs product page: Reprinted from ThorLabs, Inc. #BS0 product series*

Reflected and transmitted beam deviation is listed as ±5 arcmin, which is better than the displacement of a plate beamsplitter. The overall power transmitted and reflected is >85%, but the difference in *p*- and *s*-polarized light transmitted or reflected is <10% [5]. We visually see this difference is minimal from figure 3.3 above. Other manufacturer specifications also fall into similar ranges as these Thorlabs beamsplitter cubes.

3.1.ii.c Pellicle Beamsplitters

Pellicle beamsplitters are made from a nitrocellulose membrane stretched to be only a few microns thick. This effectively eliminates the ghosting problem of plate beamsplitters. The downside is that the membrane is delicate and flammable, and therefore is only suitable for low-power applications [5].

The thin film nature of the nitrocellulose material makes it so that the transmission and reflection oscillate from multiple-beam interference. The classic example of this is a Fabry-Perot Etalon which uses the same mechanisms as that of a laser cavity. In all of these cases there is a 100% transmission (0% reflection) resonance at certain frequencies of light, which repeats based on the free-spectral range (FSR). Since we are operating over the visible spectrum (400-700nm), these variances would unevenly transmit/reflect the different wavelengths.

3.1.ii.d Pinhole Mirror

The pinhole mirror is a mirror with a very precise (~50µm) ellipse in the center of it. The ellipse is made through a photolithographic process, where the ellipse is etched through a chemical process before being blasted by UV-light. Based on where the light hits the ellipse, some will be reflected, while the rest is transmitted. This would allow it to act as a beamsplitter with a variable R/T ratio based on alignment. The pinhole mirror operates by focusing the light onto the ellipse and based on the geometry of the beam and pinhole, a certain ratio of light will reflect while the rest transmits. The advantage of this method is that the light stays in air, and so there is no dispersion of light. There are also no polarization effects on the transmitted light, which is important for our application. Overall power loss would also be low. The downside of the pinhole mirror is that it would take time and expertise to manufacture one using the facilities in CREOL. As such, as an upgrade or stretch goal, we will investigate manufacturing one for senior design 2.

3.1.ii.e Comparisons between Beamsplitter types

Below is a table (3.4) that compares the different beamsplitter types mentioned in the previous sections. The data is taken from general product families for 10:90 beamsplitters. ChatGPT was used to start the research and included a pro/con of some of these different types [GPTA]. Its response is detailed in Appendix C for [GPTA].

Table 3-1 *- Comparison of Beamsplitter Types*

Specification	Type of Beamsplitter			
	Plate	Cube	Pellicle	Pinhole Mirror
AOI	45°	0°	45°	45°
Relative Size	Compact	Bigger	Compact	Compact
Performance	<1% Power loss	<15% loss	Variable	Little to none (mirror-based)
Polarization Performance	No more than 35% R or T difference	<10% difference	Variable	Minimal/None
Beam Displacement	Yes	No	Minimal	No
Durability	Normal	Robust	Fragile	Normal
Cost	$100-200	$175-250	$100-150	Unknown

Of the specs compared, the polarization performance is one of high importance since we will be measuring the polarization of the transmitted beam. If the beamsplitter affects the polarization too much, then the polarimeter will not accurately reflect the polarization of the pulsar’s light. Although any deviation could be accounted for in the data processing, minimizing the deviation of the polarizations would be ideal. In this case, a cube non-polarizing beamsplitter accomplishes this, at the downside of losing at most 15% of the total power. While this is concerning for a low light application, by minimizing losses elsewhere, and using sensitive detectors, it should still accomplish what we desire.

3.1.iii Switchable Mirrors

As part of the exit pupil imaging system, there are two paths that the light can take, the alignment path for pupil imaging, and the default path for taking an image for tracking. To toggle the optional path a form of switchable mirror is required. Our options are to find a mirror that has a togglable reflective coating, or to mechanically move the mirror with a stepper motor (or something similar).

3.1.iii.a Transreflective Mirrors

Transreflective mirrors are mirrors that can toggle their reflectivity based on an electrical signal. These mirrors utilize thin film solid-state devices, allowing them to toggle their reflectivity. One product from Kent Optronics has >87% reflectance in the mirror state, and with an AR coating, 95% transmittance in the clear state [7]. The mirror works well in the visible light spectrum (400-700nm), which is what we are dealing with for this project. There was no pricing information readily available for this product. Additionally, there is no mention of the product's effect on polarization, although it is being used to change imaging paths where polarization-preservation is not as important.

3.1.iii.b Motorized Mirrors

A mirror that has a motorized mount typically allows for the angle of the mirror to be adjusted. These adjustments allow for a few degrees of rotation, with very high precision. Such mounts are expensive and are better used for beam-steering applications. However, there are motorized flip mounts that flip a mounted optical component from a 0° state to a 90° state. This would suit our needs to allow for two optical paths, one path where a mirror redirects the light by 90°, and the other path where the light continues unabated. Unfortunately, these come at a premium. Fortunately, they do make unmotorized mounts at a much-reduced cost [8].

Using an unmotorized mount comes with the downside that a mechanical means of flipping them must be devised. A simple lever-based approach may be a possible design. Alternatively, we can make a 3D printed mount and use a motor to move the mirror into or out of the optical path. There are 2 main types of motors for this application, one being the stepper motor, and the other being a servo. The servo is the simpler option, only requiring a PWM input, but is limited in its operation. A servo is designed to operate over a 180° rotation (±90° from center). They are often small which makes them useful in a variety of ways, especially for RC hobby toys. Our other option is a stepper motor, which requires its own IC for power, as it is more current demanding. The stepper motor can rotate bi-directionally, but only with a specific number of steps per rotation. For example, a basic stepper motor has 64 steps, resulting in 5.625° per step. Stepper motors are also not limited to a specific angular range, and so can be used in open-loop systems. In these cases, the stepper's position is known by how many steps it has taken [9].

3.1.iii.c Comparisons of Switchable Mirrors

Since this part of the design is not as critical as other parts, we want to minimize the costs of getting switchable mirrors. As such, our main criterion is cost. This means that we will be getting flip mirror mounts and designing a means to flip them using a motor. Our choice of motor will depend on how much torque we require for flipping the mirror. The other consideration is how much current the motor uses, as this will require our power supply to be designed to handle it.

Table 3-2 *- Comparison of switchable mirror technologies.*

Specification	**Transreflective Mirror**	**Motorized mirror mount**
Power transmitted	95%	100% (mirror is out of path)
Power Reflected	>87%	99%
Power required	100-260V/20Hz square wave	3-5VDC plus PWM signal

Cost	"at a competitive price"	Pre-built: expensive (~$1000); Designed ourselves: <$100

3.1.iv Battery Technologies

3.1.iv.a Lithium-ion (Li-ion)

Lithium Battery technology is widely used in many electronic products, especially applications which require stable voltages and reliable lifespan. Li-ion batteries are materials like LiCoO2, LiMn2O4, LiFePO4, NMC, or NCA in the cathode, and silicon, graphite, or lithium titrate for the anode. Furthermore, the current collectors in the cathode and anode are aluminum and copper, respectively. These batteries use lithium salt as an electrolyte between the cathode and anode. Lasty, Li-ion batteries require a separator material typically a thickness of 20µm and contain tiny pores that allow the ions to pass through during charging and discharging processes. The most common separator is called a "shutdown" separator and allows for the pores to seal shut if the battery wanders outside of the operating temperature or in the event of a short, effectively preventing damage [10]. Additives are often added to these batteries to prevent malfunction, deuteriation, or increase performance of the battery itself. These additives may include fire retardant, SEI-forming (Solid Electrolyte Interphase), and stabilizing chemicals. Overall, Li-ion batteries offer a high energy capability within a small footprint, are great for maintaining stable voltages which are essential for keeping sensitive components stable, and lastly Li-ion batteries have an excellent charge retention capacity ensuring a long lifespan of charge.

3.1.iv.b Lithium Polymer (Li-Po)

Lithium polymer batteries are a subcategory of lithium-ion batteries that offer many advantages over a typical Li-ion cell. Li-Po batteries are assembled virtually the same as Li-ion. However, rather than a liquid electrolyte a Li-Po battery utilizes a solid or gel polymer as the electrolyte component of the battery. To create these types of electrolyte materials, lithium salts are dissolved into high molecular density polymer host materials, resulting in the final product becoming a dual ionic conductor. These batteries however are susceptible to faster degradation due to a concentration polarization formed by movement of anions and cations [11]. Li-po Batteries allow for a thinner and more compact footprint on devices making this battery a great choice in many microelectronics and portable devices. Along with a decreased size, many Li-Po batteries can be manufactured in many shapes also allowing for more ergonomic use in products. The main disadvantages with Li-Po batteries are that the cost of manufacturing is more expensive as compared to a typical Li-ion battery. When compared to a liquid electrolyte lithium battery, Li-Po's performance is largely failing when it comes to charge density and cycle number. Overall, Li-Po although very versatile for small devices, really does not meet any standard we need with our project [12].

3.1.iv.c Nickel-Metal Hydride (NiMH)

Nickel Metal Hydride batteries are a precursor battery technology compared to lithium-ion batteries and have been in use since the early 1970s. Typical NiMH batteries are made using a metal hydride anode, a KOH electrolyte, and a separator material like a Li-ion.

NiMH batteries offer great energy density and specific energy outputs as compared to NiCd batteries [13]; however, it is important to note the energy density of a Li-ion battery is greater than a NIMH cell. Furthermore, NiMH batteries often cost almost half the price to manufacture over Li-ion batteries [14]. In addition, NiMH batteries have been shown to allow for hundreds of reuse and recharge cycles which makes it a very reliable source of power. Lastly, NiMH batteries are susceptible to many operating malfunctions at low temperature [13]. Overall, NiMH batteries may suffice our project requirements in terms of cost; however, we might want a battery in which as greater energy density for a longer cycle life.

3.1.iv.d Nickel-Cadmium (NiCd)

Similar in composition to NiMH batteries, NiCd batteries are composed of a nickel cathode and a cadmium anode, in which the cadmium electrode has a higher charge capacity. NiCd batteries are great in performance when it comes to durability, lifespan, charge retention, and flat discharge rate. However, these forms of batteries are expensive to manufacture and if the battery is disposed of improperly it can lead to extreme environmental damage. This is due to the properties of cadmium which is a highly toxic metal and can cause many issues [13]. In summary, for our project there is no real use to having this form of battery technology due to it's higher cost. Additionally, the module will only require small power consumption, so need for a very large charge capacity.

3.1.iv.e Summary

After researching and reviewing many battery technologies, Li-ion batteries seem to fit the best with our project's application. This battery technology will ensure a steady and stable power supply that can be recharged and maintained effectively. In addition, Li-ion battery cost is inexpensive, and these batteries are offered in various energy and power specifications which meet our design criteria.

Table 3-3 *- Summary of Battery Technologies*

Battery Technology	Pros	Cons
Li-Ion	• High Energy Density • Robust component	• Lower voltage output when load draws high current
Li-Po	• Available in higher voltages than Li-ion • Low discharge temperature • Can be manufactured in many footprints	• If damaged is susceptible to thermal runaway
NiMH	• Less prone to memory effect as compared with NiCd	• Expensive for large scale implementation

	• Nontoxic materials used to manufacture	• High self-discharge rate
NiCd	• Flat discharge rate	• Manufactured with highly toxic materials

3.1.v Charge Controllers

In addition, with having a battery unit utilized within this product, we must ensure the battery supplies the correct current and voltage to the PCB. Charge controllers manage just that. Charge controllers also allow for the proper charging of the battery cells and ensure that there is no overcharging which may cause a potential safety issue and system failure. Overall, adding this component to our system will protect and extend the battery's lifespan through overcharge protection, voltage regulation, and current limiting. Types of charge controllers include: shunt regulators, series regulators, PWM regulators, and MPPT controllers.

3.1.v.a Shunt Regulator

Shunt regulators fall under the classification of a linear regulator and are designed to maintain constant voltage level from an input source. This design of a charge controller can generate a stable output voltage through using an additional output resistor which draws excess current from the output to ground, hence shunting/limiting the input current of the power supply (e.g. 12V DC supply). Once the desired voltage level of the battery has been reached the regulator shunts any excess current to ground, which prevents the battery from overcharging and ultimately extending the battery's lifespan. A downside to this design of a charge controller is that due to the constant connectivity of the power supply, the constant current may cause a large power loss, in turn heating the device. This may cause complications to surrounding components and could potentially cause a safety hazard if not managed properly. Due to the heat loss this form of charge controller is considered less efficient as compared to other options, however, it is cheap and simple to implement in designs [15].

3.1.v.b Series Regulator

Like the shunt regulator, a series regulator is also classified as a linear regulator and considered an on/off controller. The series regulator is designed to behave as a switch connected from the input source to the battery. The switch will only be engaged when the battery voltage level drifts below the desired reading and will consequently disconnect once the battery is at desired operating levels. The controller is implemented with a relay or transistor which will behave as the switching mechanism, mainly relay circuits. The switching can be done in pulses to ensure no overcurrent flow into the battery cell and helps maintain the battery's integrity. The pulse duration is determined depending on the cell's state of charge (SOC) and condition.

3.1.v.c PWM Regulator

PWM regulators are very similar to the series regulator, but in this application the switching mechanism is purely controlled through a transistor. This transistor is placed in series between the supply and battery cell and will switch on and off at a high frequency with pulses of varying duty cycles/widths. The PWM regulator monitors the SOC and condition of the battery and determines the correct pulse width needed to supply proper charging to the battery cell. This design of a regulator behaves as a series regulator when the pules are 100% or 0% width (on or off), however, to configure a PWM regulator as such there is factors that must be considered such as if the connected load is sensitive to noise, the PWM may introduce additional noise into the circuit due to its high frequency switching operation.

3.1.v.d MPPT Regulator

Maximum power point tracking (MPPT) regulator can be considered as a more advanced PWM regulator. The MPPT regulator attentively monitors the source output voltage and output current. This device then calculates the output's proper initial power point and constantly adjusts the output's operating point. This operation principle allows for great efficiency, especially for large systems, by providing power loss prevention through the adjusting operating point. Although this controller has improved efficiency it is more expensive than a traditional PWM charge controller. In addition, it is important note this design of a charge controller is intemperate to small systems, this is because the efficiency seen for smaller devices vs larger is seemingly minute [16].

3.1.vi Polarimeter Technologies

Polarimeters are devices used in determining the polarization state of incident light beams. Measuring the polarization of light is crucial for many fields of optics far beyond the focus of this product. This interest means that the problem of measuring polarization has a wide variety of established solutions.

3.1.vi.a The Simplest Polarimeter

Since a polarimeter is simply any device that can measure the polarization of light, there are a large variety of devices and techniques that can all be considered polarimeters. The simplest such device is a rotating, or otherwise variable, polarizer placed between a light source and a detector. Since the output optical power through a polarizer is dependent on the incident light's polarization angle relative to the polarizer's, rotating the polarizer will produce an easily detectable change in measured intensity. Output intensity can then be considered with respect to the known polarizer angle to determine the original polarization of the light.

This design benefits from having a very high theoretical maximum resolution. Polarization resolution is limited by the resolution of the detector and the precision to which the polarizer angle is known, both of which are dependent on the chosen equipment and could theoretically be very high. Additionally, this would also work for very weak signals, as a detector with high sensitivity could be used without issue.

This configuration would not be viable for use with a light source variable in intensity and polarization. Changes in optical power could not be attributed solely to rotating the polarizer. For the Crab Pulsar, a source whose intensity and polarization are constantly changing, this device would not be usable.

3.1.vi.b Integrated Polarimeters

Integrated polarimeter devices operate on similar principles to the polarimeter as discussed previously. Instead of rotating the polarizer, a rotating wave plate is added to the optical path that constantly modulates the light's polarization state. Then, a detector records the variations in intensity relative to the wave plate angle to determine polarization state.

This design benefits strongly from its simplicity. On the user's end, the device only needs to be positioned to detect signals and then plugged in to function properly. Problematically, this design is not applicable to a wide variety of circumstances. Products such as this come with the requirement that input light must be monochromatic and coherent. Monochromaticity and coherence are useful properties to have in a light source that is being measured, but their presence is rare outside of circumstances specially engineered to produce them. Naturally occurring light sources, such as a star, will be neither monochromatic nor coherent. Monochromaticity could theoretically be achieved by spectral filtering, but doing so would also eliminate most of the signal we are trying to measure and is not an option.

Similarly, these integrated polarimeters are not designed with low light applications, such as astronomy, in mind. The detectors in these devices will not be sensitive enough to detect weak signals as needed, and since they are built as a singular device the sensitivity cannot be tweaked to fit our needs. Ultimately, an integrated polarimeter would make for a poor choice considering our technical requirements.

3.1.vi.c Stokes Polarimetry

Stokes parameters are a set of values that describe the polarization state of light. They consist of four parameters: I, Q, U, and V. The parameter I represents the total intensity of the light, while Q and U describe the linear polarization. The V parameter represents the circular polarization. Together, these parameters provide a complete description of the light's polarization state.

The Intensity term I describes the total optical intensity measured by the polarimeter, irrespective of its polarization. This is determined by measuring the intensity of two orthogonal polarization states, then taking the sum. This is generally done with the two orthogonal polarizations being 0° and 90°. This parameter is then normalized to 1, and the other three Stokes Parameters are adjusted accordingly.

The first linear polarization term Q describes the linear polarization, with respect to the vertical and horizontal axes. This is calculated using the difference of the intensities of the 0° and 90° polarization states. As such, it has a possible range of values $-1 \leq Q \leq 1$.

The second linear polarization term U describes the linear polarization as well, but with respect to the ±45° axis. This accounts for ambiguity that may exist in determining the Q parameter. Take unpolarized light for example. The optical power measured coming out of both polarizers would be equal and the Q parameter would then be zero. However, this is the exact same result that you would see if the incident light was instead polarized to 45°. The U parameter solves this issue, since it is measured by taking the difference of intensities for two polarization states oriented at 45° from horizontal. In this case, +45° polarized light would give a U value of 1, while Q would be 0. Unpolarized light would result in both Q and U parameters being 0, removing any ambiguity.

The final parameter V describes the ellipticity. This is the degree to which the light circularly polarized, where values of 1 or -1 correspond to being perfectly left or right-handed circular polarization, with values in between being elliptical.

Alternative formulas for calculating each parameter do exist, however the provided technique is well suited for our polarimeter design as planned.

3.1.vi.d Stokes Polarimeters

A Stokes polarimeter is any device that is used to measure these Stokes parameters. This generally involves measuring the intensity of light after it passes through certain polarizing optics, such that the measured optical power encodes information on the initial polarization state.

One design involves using two polarizing beamsplitters to split light into four distinct beams. The polarizing beamsplitters each individually split incident light into two orthogonally polarized beams. Each beam path has an associated photodetector. The intensities measured by each of the four detectors can then be used to calculate the Stokes parameters. The primary benefit of the Stokes polarimeter is that it is highly variable and can be easily designed to suit the designer's needs. Polarization optics, detectors, and beam paths are all variables that can be adjusted as needed, which is an important feature to consider for our project.

A Stokes polarimeter that we would design would make use of two polarizing beamsplitters to separate light into four beams with distinct polarization states. The axes of each polarizing beamsplitter would need to be oriented at 45 degrees to the other, producing output angles of 0 degrees, 45 degrees, 90 degrees, and 135 degrees. At the end of each beam path, we would place a photodetector that is built for measuring extremely weak optical signals.

A major downside of the Stokes Polarimeter is the associated cost from needing to build four separate optical paths, each with their own set of detectors and lens or mirror optics which necessarily multiplies the associated price tag by a factor of four, regardless of what components we choose. Compounding this, the detectors we will have to use are not cheap, running at least one thousand dollars.

3.1.vi.e Polarimeter Comparison and Summary

While it would be ideal from a development perspective to be able to use an existing integrated polarimeter product, this will not be viable. These devices are not built with our relevant specifications in mind, so we cannot use them. Overall, the Stokes Polarimeter is the best option available, as it allows us to measure very faint signals with high accuracy. The variability in sensitivity and accuracy/precision enables us to use our own components as necessary to reach the required targets. The only downsides are its cost and increased design complexity, but these problems can certainly be solved.

Table 3-4 *- Comparison of Polarimeter Types*

Specification	**Type of Polarizer**		
	Stokes Polarimeter	**Simple Polarimeter**	**Integrated Polarimeter**
Sensitivity	Variable	Variable	Detector Limited
Data Accuracy	Variable	Low	Detector Limited
Installation	Requires Construction	Requires Construction	Simple Installation
Cost	High	Low	High

3.1.vii Polarizing Beamsplitter Technologies

In this section, we will analyze different components and techniques that may be used to separate light based on its polarization state. Polarizing beamsplitters are not intended to split light into two paths based on fractions of the input intensity like the more traditional beamsplitters discussed previously. They are also not meant to separate light based on wavelength like is done by a dichroic beamsplitter. Instead, the two beam paths produced by a polarizing beamsplitter each contain an orthogonal component of the polarization state of any input light.

In the design of this project, some method of splitting light into different optical paths based on polarization will be crucial since it is a requirement for building the Stokes Polarimeter we have chosen.

3.1.vii.a Extinction Ratio

The extinction ratio in optical components is a critical parameter that quantifies the effectiveness of a device in distinguishing between two orthogonal polarization states. It is defined as the ratio of the transmitted power of the desired polarization state to the transmitted power of the undesired polarization state. A high extinction ratio indicates that the optical component can effectively separate or filter out the unwanted polarization, ensuring that only the desired polarization state is transmitted with minimal cross-contamination. This metric is particularly important in applications requiring high polarization purity, such as ours, where the performance and accuracy of the system are heavily dependent on the quality of polarization separation.

3.1.vii.b Brewster Windows

When light hits a dielectric surface at Brewster's angle, the reflected light is the component polarized perpendicular to the plane of incidence (S-Polarized) and contains only this polarization. The transmitted beam is partially P-polarized. This principle can be used to separate polarizations in many applications. However, a Brewster window, which is an optical component specifically designed for this purpose, is not suitable for our use since the transmitted beam is only partially polarized.

3.1.vii.c Polarizing Plate Beamsplitters

Polarizing plate beamsplitters operate using thin film coatings layered onto a transparent substrate. These coatings are engineered to have distinct transmissive and reflective properties for S-polarized and P-polarized light. When a light beam is incident onto the polarizing plate, the S-polarization state is mostly reflected, while the P-polarization state is mostly transmitted through the component.

Polarizing plate beamsplitters benefit from their compact size and low absorption. The thinness of these components means that there is very little optical absorption by either the film or substrate materials. However, the wavelength dependence is a serious issue. Most polarizing plate beamsplitters are only designed to operate within a somewhat narrow spectral region, either the absorption or extinction ratio suffers when outside of the specified band, as can be seen in the figure below.

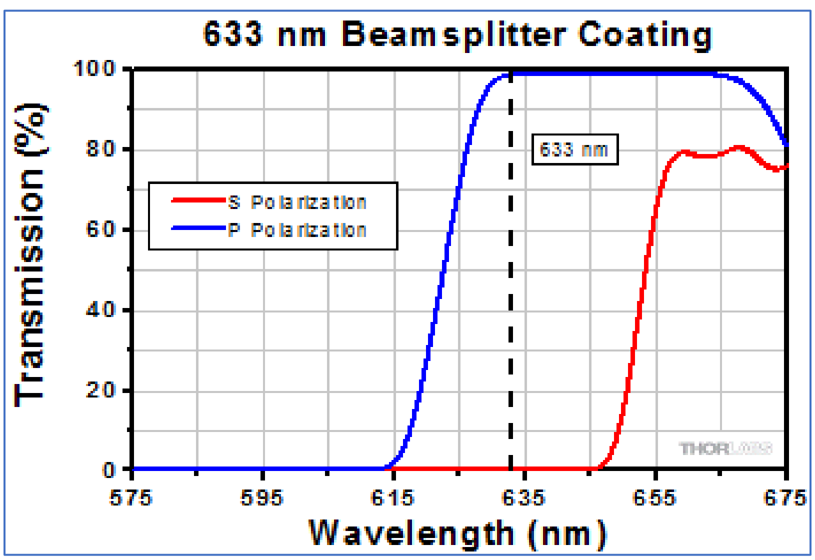

Figure 3-4 *– Typical Transmission of a sample Polarizing Plate Beamsplitter with respect to wavelength. Reprinted from Thorlabs, Inc. #PBSW-633*

This conflicts with our need for broadband beam splitting, since we intend to detect signals over the whole visible spectrum, not a narrow portion. We would therefore need to use a broadband polarizing plate beamsplitter to avoid this issue.

The extinction ratio unfortunately leaves a lot to be desired for any polarizing plate beamsplitter, even those specially designed for broadband usage. Using the above figure as an example, the extinction ratio may be near perfect at a specific wavelength, but for broadband waveplates it is simply impossible to maintain that performance for a wide wavelength band. As a result, the extinction ratio drops significantly, and orthogonal polarizations will be mixed together in the output beams. These two issues combined mean that polarizing plate beamsplitters will need to have a significant advantage over alternative technologies in order for them to be practical.

3.1.vii.d Polarizing Prisms

Polarizing prisms are a set of technologies that split a light beam into its orthogonal polarization components by leveraging the birefringent properties of certain materials. Common types of polarizing prisms include the Rochon and Wollaston prisms, each designed to exploit the different refractive indices for the ordinary and extraordinary rays within a birefringent crystal. At visible wavelengths, this material is typically calcite, quartz, or magnesium fluoride [17]. When a light beam enters the prism, it is separated into two beams with orthogonal polarization states due to the difference in velocity for the polarized components within the birefringent material.

Unlike other polarizing beamsplitter technologies, this separation is achieved with extremely high precision, and the outgoing beams can make polarizing prisms invaluable for applications needing high polarization purity, such as ours. They typically have an extinction ratio above 10,000:1, though may be as high as 100,000:1 depending on product specifics. High performance is maintained over a broad spectrum which can be seen in the figure below. While chromatic dispersion in outgoing rays is unavoidable when using these prisms, the magnitude is minor and can be accounted for by use of achromatic optics elsewhere in the system. Ultimately, chromatism will not impact our product capabilities or overall design since we are not taking images or spectral measurements. An additional consideration is the shape of the prism. These products are typically sold as cubes, but it is possible for them to be shaped as rectangular prisms with one dimension being much thinner than the others. A thinner beamsplitter would be beneficial since it would minimize absorption losses.

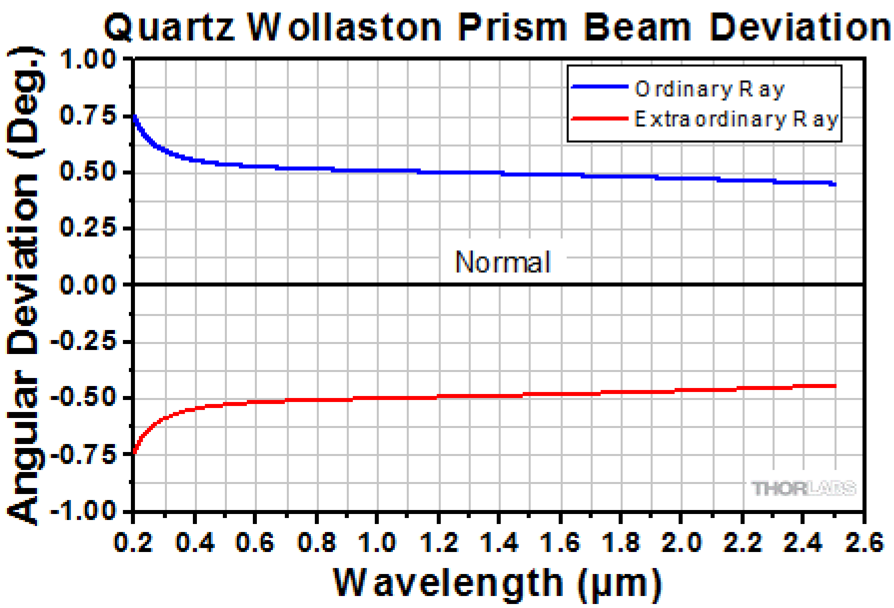

Figure 3-5 *– Angular deviation of a sample Wollaston Prism with respect to wavelength. Reprinted from Thorlabs, Inc. #WP10-A*

3.1.vii.e Wollaston Prisms

Wollaston prisms consist of two birefringent crystal prisms cemented together along their hypotenuses. The two crystals are oriented with their ordinary and extraordinary axes perpendicular to each other, creating an interface between the two at which the ordinary and extraordinary components of input light become swapped when transmitting into the second crystal. The angled interface and differing refractive indices cause both ray components to diverge. [18]

Outgoing rays will be separated by a certain separation angle, which is a product-specific parameter. Since the prism we choose will be used for splitting beams onto separate optical paths, the separation angle is a necessary parameter to consider. There will need to be adequate spacing between beams to ensure enough physical space for us to place detectors or other optical components, but excessive spacing would only make the instrument larger for no reason. Both ray paths have very similar optical path lengths due to the similar refractive indices and equal deviation angles, and as such the output beams will have extremely similar absorption losses which would improve the quality of data we can collect.

3.1.vii.f Rochon Prisms

Rochon prisms are quite similar to Wollaston prisms. The only difference between the two technologies is that Rochon prisms leave the output ordinary ray angle without deviation, while the extraordinary ray is deflected at the full separation angle. This is accomplished through aligning the optical axis of the first crystal along the propagation path. As a result, both the S and P-polarizations are ordinary rays. The second crystal is aligned perpendicular to the optical axis so that at the interface, the P-polarized ray becomes the extraordinary ray and is then deflected due to the change in refractive index, while the original S-polarization remains ordinary and is undeflected [19].

An undeviated polarization component is primarily useful for applications where the polarizer itself would be moved or rotated since this keeps one ray on a constant path. As such, Rochon prisms are better suited for applications where only one polarization component is needed. Relatedly, output beams from Rochon prisms have different optical path lengths for ordinary and extraordinary beams, as the extraordinary ray will necessarily have a longer optical path within the crystal, introducing unbalanced attenuation between outputs.

Table 3-5 *– Prism and Polarizing Plate Beamsplitter Technology Comparison*

Prism and Plate Polarizing Beamsplitter Comparison		
	Pros	**Cons**
Prism Beamsplitters	• Very high extinction ratio (>10,000:1) • Broad spectrum operation possible without sacrificing extinction ratio • Minimal wavelength dependence	• Relatively high optical absorption • Higher weight • Not practical for wide beam diameters • Higher price (~ $600 - $1,000)
Plate Beamsplitters	• Very high extinction ratio at specific wavelengths (>10,000:1) • Low optical absorption • Can easily be used for wide beam diameters • Lower price (~ $400)	• Extreme wavelength dependence • Poor extinction ratio outside a narrow bandwidth

3.1.vii.g Conclusions and Comparison

Table 3.6 summarizes the different polarizing beamsplitter technologies in a more concise format below. Following the table, is a summary of what works best for our project.

Table 3-6 *– Polarizing Prism Beamsplitter Technology Comparison*

Polarizing Prism Beamsplitter Comparison		
	Pros	**Cons**
Wollaston Prisms	• Balanced attenuation of outputs	• Harder to implement mechanically

Rochon Prisms	• Easier to implement mechanically	• Unbalanced attenuation of outputs • Possibly reduced data quality

When choosing between the Wollaston and Rochon prisms, quantitative performance characteristics such as extinction ratio or chromatic aberrations do not need to be considered for the sake of comparisons. The similarity of the two technologies means that performance specifications and prices will likewise be very similar. Relevant considerations will be qualitative.

Equal output attenuation in Wollaston prisms is a valuable property. All polarimetric measurements we will be taking are reliant on comparing the optical power of individual polarization components. Instrumental effects altering our measurements degrades data quality. This could theoretically be solved by performing further analysis and calibration with the final product, but it is better to avoid problems altogether wherever possible. Moreso, Wollaston prism products are more popular and easier to acquire. The only downside to using Wollaston prisms is that it will be more difficult position optical components such that beam paths do not overlap. This problem is certainly solvable though and is not worth lowering data quality by using alternatives. For these reasons, Wollaston prisms are the best choice.

3.1.viii Photodetectors

Photodetectors will be needed for us to convert light into a readable electrical signal. These devices generate an analog electronic signal whose strength is dependent on the incident optical power and specific parameters of the detector itself. Since light from the Crab Pulsar is very faint, we will require photodetectors with a very high sensitivity and low noise. Additionally, the optical wavelengths we intend to use will require a detector with high sensitivity at similar wavelengths.

3.1.viii.a Avalanche Photodiodes

Avalanche photodiodes are popular choices for use in detecting faint optical signals. Unlike more traditional semiconductor devices, avalanche photodiodes operate using the impact ionization effect, where the detector is subject to a strong reverse-biased electric field. Whenever a photon is absorbed and produces an electron-hole pair, the strong field present accelerates charge carriers to high energies which enable further collisions to produce secondary charge carriers. In effect, this creates a source of gain internal to the detector material, known as conversion gain, as opposed to an external amplifier circuit which would be excessively noisy for use with femtowatt scale signals [20].

However, avalanche photodiodes are typically integrated with an external transimpedance amplifier since the photodiode’s own internal gain is high enough to produce a signal that can be safely amplified without introducing significant noise. The conversion gain is typically above 10^9 V/W, while the external transimpedance gain is at least 1kV/A.

Since avalanche photodiodes are sensitive to even very small signals on the order of picowatts or femtowatts and are resilient to noise, this technology is a good fit for use in this project.

3.1.viii.b Single Photon Avalanche Photodiodes

Single Photon avalanche photodiodes (SPADs) are a subtype of avalanche photodiode specially designed for use in single photon counting with high timing precision. They operate using impact ionization as well but are distinct in that they are reverse biased well above breakdown voltage, often referred to as "Geiger Mode". The increased voltage allows even individual photons to trigger an avalanche of charge carriers to produce a detectable pulse. [21].

SPADs are renowned for their high quantum efficiency and low dark count rates, making them ideal for applications in low-light conditions. Their timing resolution, often in the range of tens to hundreds of picoseconds, allows for precise temporal measurements as well [21].

Since they are closely related to avalanche photodiodes, the two technologies have many similar characteristics. Both devices use the same or very similar materials in the detector design, and as such have similar quantum efficiencies and sensitivities to different wavelengths. The external device operation is also quite similar, so implementation into our design will be nearly identical for either.

The price of a SPAD is typically several times that of a regular avalanche photodiode, which may prove to be prohibitive. Although their extreme sensitivity may prove to be a requirement. Additionally, SPADs are prone to after-pulsing, where the impact ionization effect continues well after the photon has been detected, creating a false positive detection. The probability of this occurring is typically less than 1% but may vary higher or lower depending on the specific device.

3.1.viii.c Noise Equivalent Power

It is important to consider the noise equivalent power (NEP) of any photodetector we are considering using. NEP is the input optical power that will create the same signal output as the detector's internal noise. Simply put, it is the minimum measurable optical power at a given frequency, as any less power would become indistinguishable from detector noise. It is given in units of $W/\sqrt{Hz}$, where Hz represents the signal frequency (bandwidth), and is unrelated to wavelength [22]. Silicon based avalanche photodetectors typically have NEPs in the range of 200fW to 3fW. This range, especially in the lower end, will fit our usage case well.

3.1.viii.d Responsivity

Responsivity is a measure of a photodetectors sensitivity to changes in incident optical power, represented as the ratio of generated photocurrent (A) to optical signal (W). An ideal photodetector would have a large responsivity value that is constant for all wavelengths. In practice, photodetector responsivities will change as a function of wavelength due to the absorbance spectrum of the detector material. We will need to carefully consider the responsivity spectrum of our photodiodes in comparison with the optical spectrum of the signal we intend to measure, in order to maximize our measurement sensitivity.

3.1.viii.e Minimum Detectable Optical Power

The minimum detectable optical power (MDP) of a photodiode is the smallest amount of optical power that the device can detect with a signal-to-noise ratio (SNR) of at least 1. This parameter is needed for determining the sensitivity of photodetectors. MDP is derived from a combination of both responsivity and noise equivalent power as in the following equation:

$$P = NEP(\lambda)\sqrt{BW}$$

Where BW is the measurement bandwidth, and NEP(λ) is the noise equivalent power, which itself is a function of wavelength.

Relatedly, these input parameters themselves are determined by several factors, including the photodiode's dark current, noise characteristics, and the bandwidth of the detection system. A lower MDP indicates a more sensitive photodiode, capable of detecting weaker signals. The MDP is often expressed in terms of power per unit to account for the physical dimensions of the photodiode and the spatial distribution of the incident light [22].

3.1.viii.f Photodetector Comparison and Summary

A comparison of photodetector technologies is provided in **Table 3-7** below.

Table 3-7 - Photodetector Technology Comparison

Technology	Pros	Cons
APD	• 1µs timing resolution • Lower cost ~$1000	• Lower sensitivity • High NEP >10fW
SPAD	• High sensitivity ~1000 photons/s • Single Photon Resolution • Very high timing resolution 1ns	• Prone to false positive detections • 1ns timing resolution is excessively high for our purposes • High cost >$5000

3.1.ix Half Wave Plates

Wave plates are optical devices that can change the polarization state of light. They make use of the fact that orthogonal polarizations have different refractive indices in some materials such as quartz and certain polymers. Wave plates have a fast and a slow axis, where light polarized along the fast axis has a lower refractive index than along the slow axis, slow axis has a higher refractive index. When light propagates through a material with these properties, it introduces a phase delay since light aligned to the slow axis will propagate more slowly. The total phase delay is described by the following equation:

$$\Gamma = \frac{2\pi d(n_s - n_f)}{\lambda}$$

Where d is waveplate thickness, n_s and n_f are the refractive indices along the slow and fast axes, respectively, and λ is the wavelength. Γ is the total introduced phase delay. In a half wave plate the thickness is engineered such that the phase delay is equal to π/2, which converts incident light to a linearly polarized state along the fast axis.

3.1.ix.a Multiple Order Waveplates

A multiple order half waveplate is a waveplate where the phase delay is not exactly equal to π/2, but rather a higher multiple of π/2. Any integer multiple of this phase delay will produce the same effect as any other. The specific value depends on the thickness, and it is significantly easier to manufacture components with larger thicknesses. This means that multiple order waveplates are significantly cheaper and easier to handle than the zero-order alternative.

Since refractive index and by extension phase delay are wavelength specific, different wavelengths experience different retardations. The primary downside of multiple order waveplates is that the increased thickness leads to a larger retardation error when used at wavelengths beyond what it is specifically designed around, due to the increased space for error to accumulate. Retardation error is a measure that describes the change in retardation for a shift in wavelength and should be minimized for a quality waveplate. For the same reasons, multiple order waveplates are more susceptible to temperature dependent retardation error as well.

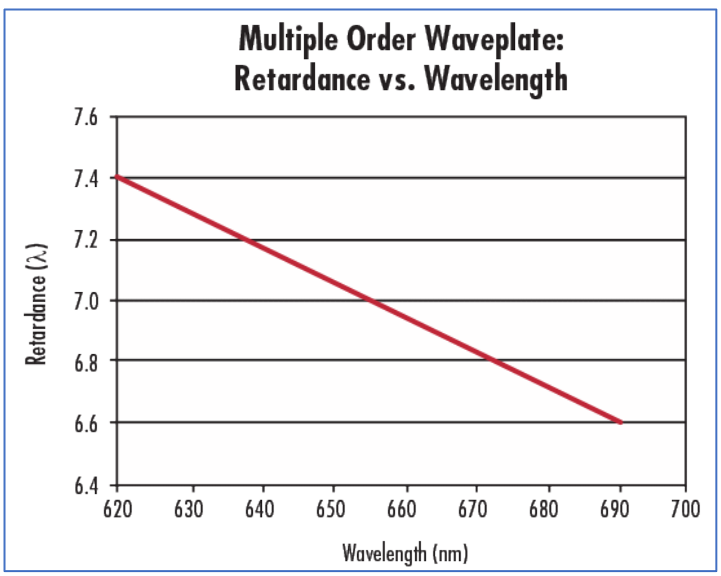

Figure 3-6 *- Plot of wave retardance with respect to wavelength for a 7.25λ multiple order waveplate with center wavelength 632nm. Sourced from [Understanding Waveplates and Retarders | Edmund Optics]*

3.1.ix.b Zero Order Waveplates

Zero order waveplates are built to have the minimum possible thickness needed to achieve the necessary phase delay. This means that the thickness is such that Γ is exactly equal to $\pi/2$ at the center wavelength. Since they are as thin as possible the retardation error at other wavelengths is similarly minimized.

Zero order waveplates are extremely thin, in the order of 25μm, but the exact thickness is dependent on product specifics. As a result, these components are both more difficult to manufacture and handle, which leads to dramatically increased cost. However, they have much better performance over a range with respect to both temperature and wavelength dependent retardation error. This significantly improved performance can justify the added cost in situations where it is needed.

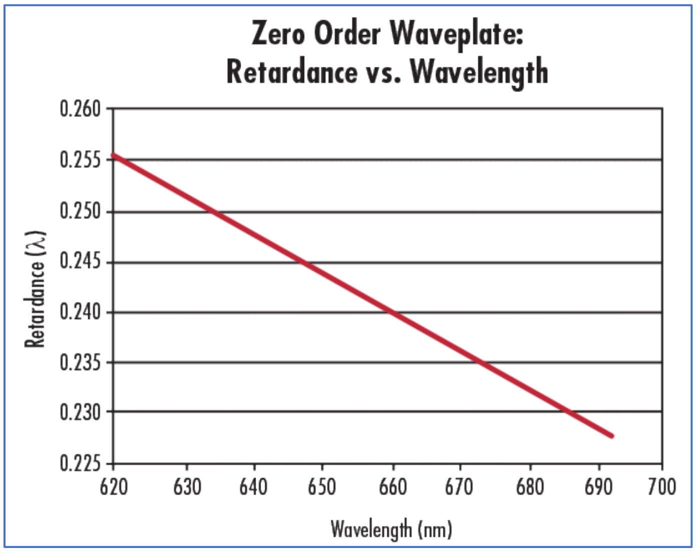

Figure 3.5 *- Plot of wave retardance with respect to wavelength for a 0.25λ zero order waveplate with center wavelength 632nm. Sourced from [Understanding Waveplates and Retarders | Edmund Optics]*

3.1.ix.c Achromatic and Superachromatic Waveplates

Achromatic waveplates are designed to polarization state of light across a wide range of wavelengths. Unlike traditional multi or zero-order waveplates, which are typically effective only at a specific wavelength, achromatic waveplates maintain consistent performance over a broad spectrum, eliminating or otherwise minimizing wavelength dependent retardation error. This is done by layering multiple materials, typically quartz and magnesium fluoride, with distinct birefringent properties such that the error from one material is cancelled out by another's.

This is a similar technique to what is used in the more familiar design of achromatic lenses, in which two materials with different wavelength dependent refractive indices are picked, shaped, and joined together. With respect to waveplates, the plate thickness is varied instead of the curvature of the lenses.

A subtype of this component is the Superachromatic Pancharatnam waveplate, which operates on the same principle, but is designed to minimize error over an extremely broadband range. This is accomplished by stacking three or more individual waveplates together. Superachromats are often designed to maintain precision in both the visible and near infrared spectrum simultaneously, as can be seen in the plot below.

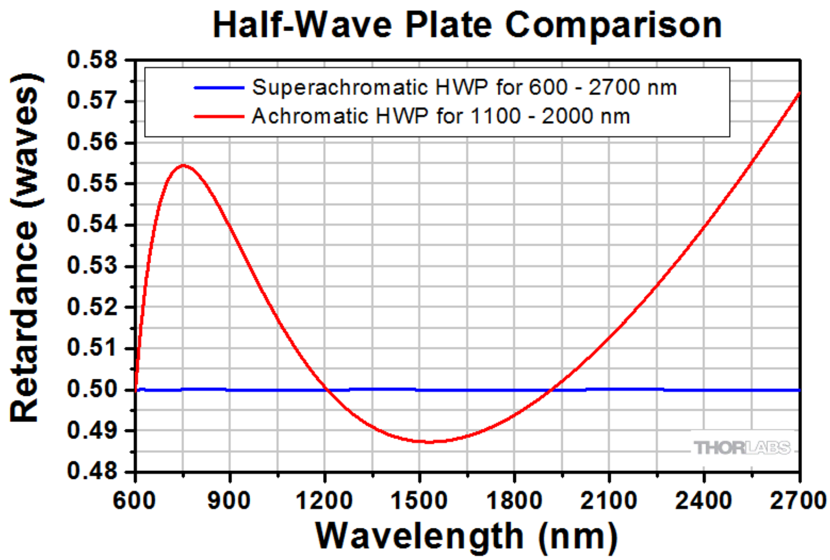

Figure 3.6 *– Plot of wave retardance vs. wavelength for an achromatic and a Superachromatic half waveplate. Reprinted from Thorlabs, Inc. #SAHWP05M-1700, AHWP05M-1600*

This makes them particularly useful in applications requiring precise control of polarization across multiple wavelengths. Since our product is meant for use with stars, which are broadband light sources, superachromatic waveplates may prove crucial to providing the polarization accuracy we require. The price of achromatic and especially superachromatic waveplates is higher than their non-wavelength corrected counterparts, as achromats are often twice as expensive, and superachromats may be more than six times the price non-chromatic corrected or even a regular achromatic half waveplate.

3.1.ix.d Variable Waveplates

Continuously varying the output polarization angle for a half waveplate is a requirement for our polarimeter to function. One way to accomplish this is by using a variable waveplate. This functions the same as normal half waveplates, except the output polarization angle is a function of the input voltage. They typically operate using the same technology as liquid crystal displays. In a liquid crystal, the orientation of the crystal's molecules can be affected by an external voltage. Applying a voltage reorients individual crystal units which has a predictable effect on the refractive index. These are usable as wave retarders since most liquid crystals have birefringent properties.

The major benefit of variable waveplates is their high modulation rate. Fast polarization modulation improves the quality of collected data. We require a minimum modulation rate of 1 Hz, although ideally, we would want this to be as high as 100 Hz. A typical product has a switching time less than 30ms, which corresponds to frequencies greater than 33 Hz, well within acceptable bounds.

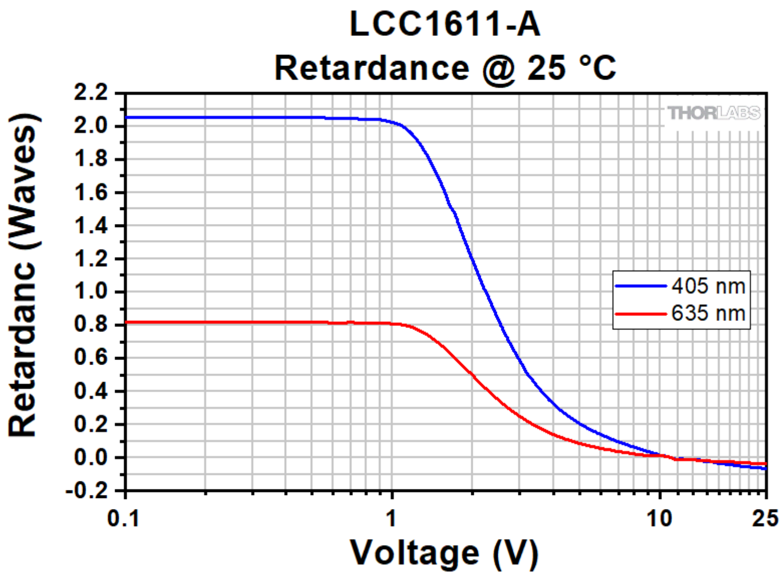

Figure 3.7 *– Plot of wave retardance vs. applied voltage for a sample typical variable half wave retarder. Reprinted from Thorlabs, Inc. #LCC1611-A*

Wavelength dependence still needs to be considered and proves to be a major issue with variable waveplate technology. The Pancharatnam design which underlies superachromatic waveplates is not applied to electrooptically modulable waveplates. The chromatic dependence of the final product is primarily a result of the liquid crystal's innate properties, and little can be done to alter this. As a result, it seems unlikely that liquid crystal variable waveplates will be a viable technology for us to use.

3.1.ix.e Waveplate Comparison and Conclusions

When considering which technology to use, we can quickly eliminate both the zero order and multi order waveplates. The fact that they are designed with use for a specific wavelength in mind immediately disqualifies them for our purposes. Variable liquid crystal waveplates have a similar problem. This leaves us to consider achromats and superachromats. These are specifically designed with broad spectra in mind. The superachromats provide a lower retardation error but come with a much higher price. Ultimately, regular achromats can perform well enough for our purposes, so we will use them.

This opens the problem of modulation. Achromatic waveplates are not electronically controllable, therefore we will need to find a solution for mechanically rotating our waveplate at high precision and frequency.

Table 3-8 - Comparison of Waveplate Technologies

Waveplate Technology	Pros	Cons
Variable Liquid Crystal	• Fast modulation • Moderate price ~\$1300	• Very high wavelength dependence ~λ/2
Multi-Order	• Low price ~\$250	• Very high wavelength dependence > 2λ • Not suitable for broad spectrum • Requires mechanical rotation
Zero Order	• Low retardation error over narrow range • Low price ~\$500	• Not suitable for broad spectrum > 2λ • Requires mechanical rotation
Achromatic	• Low wavelength dependence < λ/50 • Moderate price ~\$1000	• Requires mechanical rotation
Superachromatic	• Very low wavelength dependence < λ/100	• Requires mechanical rotation • Very High Price >\$3000

3.1.x Oscillators

Concerning our design, which includes a half wave plate retarder, we must consider how we will supply the correct signal to the wave plate for the correct switching time. This will ensure a quality signal to the photodetectors. The wave plate requires an oscillating signal for proper functionality, so we must look at what methods can be used to make an oscillator. An oscillator can be thought of as an amplifier in which positive feedback is used to create an output signal with desired frequency without the use of an additional AC input signal. Primarily we will focus on LC and crystal oscillators and discuss which may be better for our application.

The redesigned waveplate system moves away from applying a changing voltage to a static waveplate, instead leveraging a piezo-electric rotation mount developed by Thorlabs. This setup features a waveplate fixed to the rotation mount, enabling precise control over its rotation speed. By adjusting the speed of rotation, the system can effectively meet varying sampling requirements while maintaining the desired polarization state, ensuring improved versatility and reliability in polarization-dependent applications.

3.1.x.a LC Oscillators

This design of an oscillator circuit offers many advantages regarding low cost, compatibility, and power consumption. This device utilizes a DC voltage input and outputs an AC signal that can be tuned to achieve an output with a desired frequency. The oscillation frequency relies on the inductance and capacitance reactance values. The output frequency can be computed by the following equation:

$$f = \frac{1}{2\pi\sqrt{LC}} \text{ (eq. 3.1)}$$

Although cheap to manufacture and easy to tune the output frequency, LC oscillators are susceptible to output variation across temperature ranges. This effect is primarily caused by the materials that compose the capacitors; inductors are still affected however a capacitor's value will vary dramatically as temperature sweeps. Furthermore, LC oscillators have a slower start-up response time as compared to a crystal oscillator, this may affect the performance of any components that require the oscillator. The output signal produced by a small DC voltage i.e., 5V, 12V will require an op-amp to produce the necessary amplitude required for the half wave plate to operate. In summary, LC oscillators, although cheap and easily tunable, are most likely not the best option for our application as we want the start-up response to be rapid so that the half wave plate retarder is operating as intended as the sampling begins.

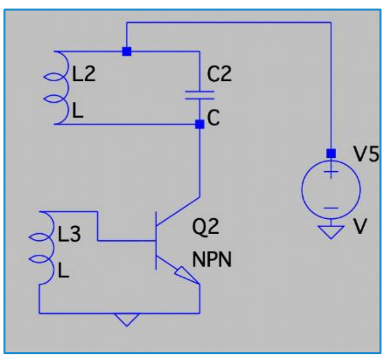

Figure 3-7 *- LC oscillator schematic, made in LTSpice.*

3.1.x.b RC Oscillators

RC oscillators, much like LC oscillators, are comprised of typical electronic components mainly, a resistor and capacitor as the name suggests. This is yet another easy and cheap way of creating an oscillator circuit. This scheme takes advantage of the phase shifting properties of a capacitor and regenerative feedback. Typically, these oscillators are created with more than just the two passive components. Often either a BJT transistor or op-amp is used to create the feedback necessary to have an overall 360-degree phase shift between input and output. The output frequency can be tuned by playing with the resistive and capacitive values and the frequency output is related to the following equation. R being the resistor value, C being the capacitance value, and N being the number of feedback stages. This form of oscillator is best used for creating square wave signals rather than sinusoidal and typically operate in the low frequency range as opposed to how LC circuits produce good high frequency signals.

$$f = \frac{1}{2\pi RC\sqrt{(2N)}}$$

3.1.x.c Crystal Oscillators (Quartz)

Crystal Oscillators, although more expensive to implement, offer great advantages over LC oscillators. Both oscillator's working principles are virtually the same, if you apply a DC voltage input into the crystal device it will output an AC signal. This occurs because of the piezo-electric effect. Due to the material properties, crystals maintain fixed output frequencies. This limitation can be counteracted though frequency division allowing the output signal to be lowered. Typically, crystal oscillators are made with quartz, allowing them to be more robust and stable across various temperatures. Crystals also allow for a fast response time upon start up, making them very good for fast process applications. A popular configuration of the crystal oscillator is to use it in conjunction with an MCU, and used for a clock and will control the flow of instructions processed by the MCU [23]. Overall, a crystal oscillator is going to be a better fit for our design and application. Using this oscillator will ensure that all systems within the module are running swiftly for the sampling process, mainly starting up the half wave plate retarder. We will use a crystal oscillator with the MCU we plan to include on the PCB.

Table 3-9 *- Comparison Oscillator Technologies*

Oscillator Technology	Pros	Cons
LC	• Tunable frequency • Low cost to manufacture • Simple design scheme • Capable of high frequency outputs • Robust component	• Temperature/Environment sensitive • High phase noise and distortion • Component tolerance may affect output frequency • Slow response time
RC	• Low frequency outputs • Easily tunable • Moderate to simple design scheme • Cheap to manufacture	• Limited output frequency • Low precision • Stability varies with environment • Longest response time
Crystal (Quartz)	• Low Phase noise • Accurate and stable output frequency • Small component footprint • Fast response time	• Higher cost to manufacture • Fragile component • Fixed frequency • Complex design scheme

3.1.xi Voltage Regulators

Voltage regulators are primarily used within the power supply unit of many electronic devices. This component aids in stabilizing power supplies (e.g. battery cells), preventing unstable voltage levels, and allow for ease of power management across very sophisticated circuits. This component is essential in our design to maintain a stable power delivery across the entire module. The main types of voltage regulators consist of switching, linear, and low dropout regulators.

3.1.xi.a Switching Regulators

Switching regulators are a power efficient component which uses a periodic on/off series component to allow for selecting the operating function of the device. This type of regulator can take a wide range of input voltages from 2V minimum to +100V [24] and either increase or decrease the output voltage and/or alter the phase 180 degrees. The common configurations of this regulator consist of buck, boost, or boost-buck. When used as a buck converter the output is attenuated to a lower voltage than the input. Boost converters are just the opposite where the output voltage is greater than the input. Lastly, while used in a boost-buck configuration the regulator allows for both of previous cases to be selected, this is the most complex design for a switching regulator [25]. Switching regulators tend to be offered in small package sizes allowing for a more condensed footprint on a PCB. Disadvantages of this type of regulator include having a significant addition of noise to the output signal. In addition, switching regulators tend to be more expensive than a linear regulator; this is due to the component's design complexity.

3.1.xi.b Linear Regulators

Linear regulators operate differently than switching regulators in that the device's internal resistance alters depending on the load connected to the output. Within this device there is no internal mechanism to control between fully conducting and off. Linear regulators take an input voltage which needs to be adjusted to be larger than the desired output signal. The output to input voltage ratio is extremely minute making a linear regulator a great option for reducing Electromagnetic Interference (EMI) in a regulator scheme. This characteristic is great for powering devices with low power consumption and allows the system to operate effectively [26]. The main disadvantage of this type of regulator is that whatever power has been lost between the input and output is given off in the form of heat dissipation which may cause complication to the integrity of the PCB and the components around it.

3.1.xi.c Low Dropout Regulators

Low dropout regulators operate under very similar conditions to a linear regulator but differ by attempting to compensate for the output to input voltage loss. Typically, a linear regulator can have a 1 to 2 V drop between input and output. Whilst LDO regulators try to have only a drop of about a volt. For example, if a power supply was at 2.7 V the regulator could still manage to supply 2.5 V to the load [27]. Often LDO is used within many portable devices to ensure effective power distribution and management. Lastly, it is important to note that the better quality of output to input loss increases the price of this regulator device.

Table 3-10 - Comparison of Voltage Regulation Schemes

Voltage Regular Technology	Pros	Cons
Switching Regulator	• Configuration allows for Buck, Boost, or Buck-Boost • Wider range of input voltages (2V to +100V) • Lower power loss compared to linear regulators	• Susceptible to high EMI from input to output • Complex design scheme
Linear Regulator	• Low EMI from input to output • Simple design scheme • Cheap to manufacture	• Configuration only Bucks • Higher power loss if dropout voltage is large
Low Dropout Regulator (LDO)	• Low noise output • Reduced dropout voltage	• More costly to manufacture over a typical linear regulator

3.1.xii Op-Amp Technologies

Within the following section we will discuss different types of op-amp chip designs and what applications each variant would be best suited for implementation. The few classifications that we're going to discuss include general purpose, precision, high-speed, low-noise, and high output current op-amps.

3.1.xii.a General Purpose

General purpose op-amps are really a board categorization of the following listed amps. However, these devices have been designed for applications ranging from industrial to automotive applications. General purpose op-amps should be an affordable option for a designer whilst offering the broadest performance requirements. These op amps should offer relatively good performance but can be susceptible to having CMRR values that are not too great and may not be the best choice in harsh environment applications. It is important to note that the output noise on these amplifiers is not the best, but still provide a great option for easy signal gain or logic operations.

3.1.xii.b Precision

Precision op-amps have been designed to achieve high accuracy while also providing low voltage offset and drift. These op amps are also created with high CMRR and PSSR values (>100dB) allowing for the outputs of these amplifiers to reject lots of noise. These amps are often designed to have an output offset less than 100 µV, offset drift around 1 µV/°C or less, and noise less than 1 μV p-p. These amplifiers are great for instrumentation and measurement circuits, Analog to Digital converters, and high-fidelity voltage references [28]. Precision op-amps have been designed to achieve high accuracy while also providing low voltage offset and drift. These op amps are also created with high CMRR and PSSR values (>100dB) allowing for the outputs of these amplifiers to reject lots of noise. These amps are often designed to have an output offset less than 100 μV, offset drift around 1 μV/°C or less, and noise less than 1 μV p-p. These amplifiers are great for instrumentation and measurement circuits, Analog to Digital converters, and high-fidelity voltage references [28].

3.1.xii.c High-Speed

“High-speed" op amps are designed to handle high frequency signals and to give a fast response. This design of an op amp is constructed with a gain bandwidth product of 50 MHz or greater. This allows for a wide bandwidth of input signals, whilst preventing distortion due to having a high slew rate [29].“High-speed" op amps are designed to handle high frequency signals and to give a fast response. This design of an op amp is constructed with a gain bandwidth product of 50 MHz or greater. This allows for a wide bandwidth of input signals, whilst preventing distortion due to having a high slew rate [29].

3.1.xii.d Low Noise (LNA)

LNA op-amps have been designed to preserve the signal to noise ratio (SNR). These op amps are typically used in low input applications allowing for very accurate outputs that are protected from internal noise distortion. These op amps are used in lots of RF applications and are intended for high fidelity signal processing [30].

3.1.xii.e High-Output Current

High output current op-amps typically allow for output currents of 100 mA or greater whilst connected to low impedance loads. This design of an op-amp can be used for applications such as: LED driving, current pump configurations, and use as a reference buffer and many other applications. Typical op-amp designs do not allow for high current outputs unless designed with lots of external circuitry to compensate. This form of an op-amp allows for easy integration as opposed to extra “clad-trap” circuitry needed for high output currents to be implemented [31].

Table 3-11 *- Op-Amp Pro/Con Analysis*

Op-Amp Specification	**Pro**	**Con**
General Purpose	• Cheap to manufacture • Simple design scheme • Compact footprint • Large input range	• Noisy outputs • Slow slew rate • Often doesn’t include rail-to-rail output
Precision	• Medium slew rate • Low noise on output • High accuracy	• Smaller input range • Moderate power consumption

	• Low input frequency application	• Complex design scheme
High-Speed	• High slew rate • Large GBW • Fast response • High input frequency application	• Higher manufacture cost • Medium to high noise • High power consumption
Low Noise	• High CMRR • High PSRR • High SNR • Good for small signal applications	• Higher manufacture cost • Complex design scheme • Moderate to high power consumption • Limited output current
High-Output Current	• "Boosted" output current • Reduced footprint, includes components needed for high output current	• Higher manufacture cost • Most have a high slew rate

3.1.xiii Crystal Oscillators

When doing research on finding what crystal oscillators we could use in conjunction with the ESP32 MCU, we must keep in mind what frequency requirements we must meet for sampling, and the overall compatibility scheme the crystal requires to operate properly with the MCU.

Table 3-12 - Table of Crystal Oscillator Comparisons

Crystal	**Kyocera Avx DT1610SB32768C0HPWAA [link]**	**Kyocera Avx MC3225K32K7680C13ASH (XTAL oscillator circuit) [link]**	**Abracon LLC ABM8G-40.000MHZ-18-D2Y-T [link]**	**Raltron Electronics RH100-40.000-12-F-1010-TR [link]**
Frequency	32.768 kHz	32.768 kHz	40 MHz	40 MHz
Tolerance (ppm)	20	90		
Coupling Capacitance (pF)	7	N/A	18	12
Mounting	Surface mount	Surface mount	Surface mount	Surface mount
Cost	$0.61	$1.16	$0.67	$0.21

3.1.xiv Lens Material and Shape

In this section we look at some of the common glasses used to make lenses as well as how the shape of a lens affects aberrations. Since the lens material is the medium in which light will travel in, it is important to pick a good material with low absorption and dispersion. Refractive index changes with wavelength, and so for light with multiple wavelengths (like white light), the different wavelengths will experience different light bending. This effect is called dispersion and is the cause for chromatic aberration. Glass comes in a few varieties based on the index of refraction, dispersion properties and wavelength spectrums (UV, visible, IR). The two more common types are crowns and flints which are used together to eliminate/reduce chromatic aberrations. A popular supplier of optical glass is Schott.

3.1.xiv.a Lens Material

Crown glass is a very popular variant due to its low dispersion, and relatively cheap cost. The optical clarity is also great. The most common variant is N-BK7 from Schott. It features a low index of refraction and high Abbe number (low dispersion). It is the go-to material for an initial optical design. The N- prefix denotes that it is made without environmentally harmful compounds, like lead or arsenic. The B is for boron while the K is for crown.

Flint glass often has a low Abbe number, meaning that it has higher dispersion. The most common use case is in the design of an achromatic doublet lens, which is a lens with little dispersion effects. Achromats use the combination of a crown and flint glass so that dispersion from the crown is cancelled by the flint. An example Schott flint is N-SF11, with an Abbe of 25.68 at the d-line (587nm).

There are also high-index materials that use Lanthanum (La) to increase the index of refraction. Crown and flint varieties exist that have a higher index of refraction. The reason a higher index may be desired is the reduced curvature that a lens would require for the same optical power. For a single surface, the power (K) is: $K = (n' - n)c$ where n' is the index of the material, and n is for the prior material. A greater difference in index and the less curvature there will be. Since curvature is tied with aberrations, a lower curvature results in less aberrations overall. An example material would be N-LAK34.

Another useful material is UV-Fused Silica (UVFS) which has the advantage of having a broader transmission spectrum from ultraviolet (UV) to near-infrared (NIR). It is also more resilient to scratching. The index of refraction is also lower than the popular N-BK7, being 1.458 at 587.6nm (compared to 1.5168 for N-BK7).

A useful way to compare glasses is to use a glass map or Abbe diagram. An Abbe diagram would have the index of refraction on one axis, and the Abbe number on the other axis. An abbe diagram is shown in figure 3.4 below.

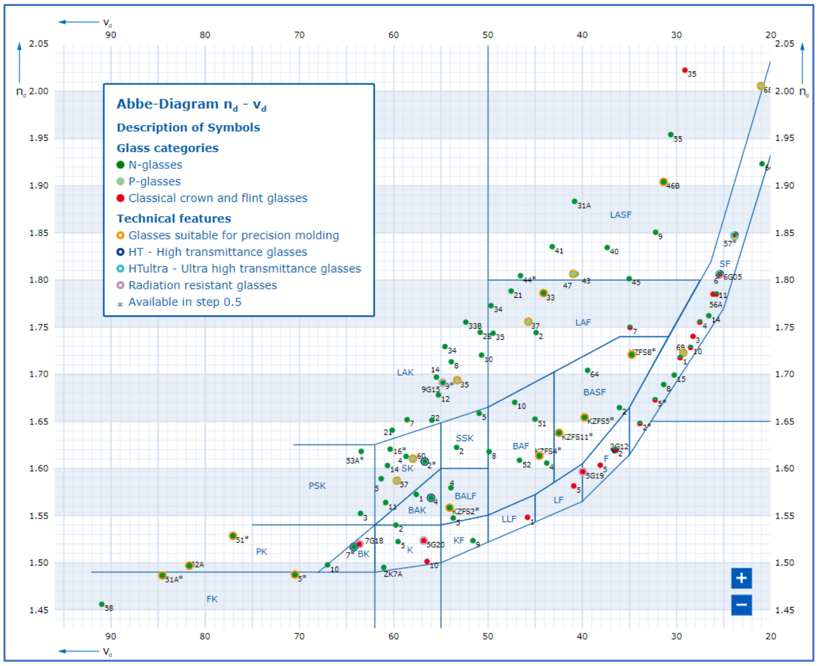

Figure 3-8 - Schott's Interactive Abbe Diagram showing their different glass materials available. Take from https://www.schott.com/en-us/special-selection-tools/interactive-abbe-diagram

Table 3-13 - Lens Material Choice Pros & Cons

Material Class	Pros	Cons
Crown	Low dispersion, great clarity, low cost	More specialized glass may outperform it
Flint	Good clarity, low cost	High dispersion,
High-Index	Reduces curvatures and aberrations; good clarity	Higher cost, greater reflection loss (uncoated)

*cost of materials not definitively researched.

Overall, the performance of N-BK7 is good, at a very reasonable price point, even with anti-reflective coatings. N-SF11 is generally used in combination with a crown material for making achromatic doublets/triplets. Since we will likely buy off-the-shelf achromatic lenses, material choice is less of a concern, as compared to the specifications of the lenses.

3.1.xiv.b Lens Shape

Another consideration is the shape of a lens, as it affects the aberrations of the image. The Seidel coefficients are a measure of the aberration(s) a design has. It can be derived that these coefficients depend on the shape factor and conjugate factor of a lens. The shape factor (B) and conjugate factor (C) are defined below:

$$B = \frac{c_1 + c_2}{c_1 - c_2} = \frac{R_1 + R_2}{R_2 - R_1}$$

$$C = \frac{u + u'}{u - u'} = \frac{m + 1}{m - 1}$$

Where *c* is curvature, *R* is radii of curvature, *u* is marginal ray angle, and *m* is magnification. Some sources like to denote the shape factor as *X* and the conjugate factor as *Y*. The main aberration we are concerned with is spherical aberration, which reduces how focused a point can get. To be aberration-free would mean having a point focused to be smaller than the diffraction-limited spot size, which is related to the radius of an airy disk. It can be found that plano-convex lenses are better for infinite conjugates (imaging from infinity), while a bi-convex lens is good for relay imaging (finite conjugates). This can be seen in the figure below.

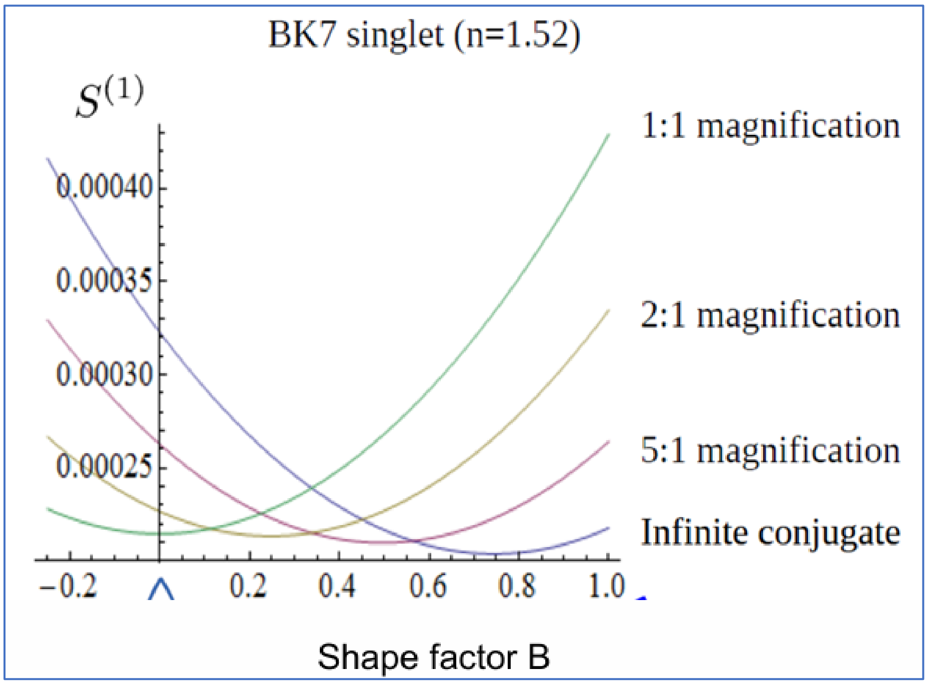

Figure 3-9 *- Spherical aberration vs. shape factor for different conjugates (magnifications) for a BK7 singlet. Retrieved from lecture notes/material for OSE4240 – Introduction to Optical Design.*

3.1.xv Software Technologies

In this section, we look at some of the programs and programming languages that are available for us to use during the designing and implementation of the project.

3.1.xv.a Languages

As in the real world, there are many languages that can be used to program (communicate) with a computer. These vary in their capabilities based on how primitive (low-level) or fluent (high-level) their syntax is. For example, *C* is very primitive, with only basic keywords, requiring the programmer to develop their own data structures, and handle their own memory allocation (with *malloc*). *Python* on the other hand is very high-level, having lots of data structures built-in, and syntax similar to English: "for *x* in *range(0,5)*:" will loop values of *x* from 0 to 4.

3.1.xv.b C Programming Language

Due to the simplicity of *C,* it is the language of choice for most microcontrollers. It is also very close to the hardware level, which is what makes it the most ideal. Some microcontrollers, like Arduinos, use a form of C++, which is an object-oriented *C* language. *C* has been around for a long time, being one of the first programming languages. This is partly why it lacks complexity as machine back then were much simpler. *C++* was designed later to include more advanced programming features, such as objects, inheritance, and other object-oriented features, concepts and ideas.

3.1.xv.c Java Programming Language

Java is a language developed by Oracle and is designed for portability. Portability in this case is defined as being transferrable to other operating systems or machines without having to develop code that is specific to those operating systems. This is achieved under the hood by running *Java* code in a Java Virtual Machine (JVM). *Java* is an object-oriented programming (OOP) language, which means that variables are objects. Objects belong to a class, and a class can be thought of as a blueprint or schematic for objects. Classes define data members and methods (functions) for objects, and inheritance allows for relationships between classes (like parent and child). *Java* follows a strict structure in the sense that variables are type-checked during compilation, as opposed to during runtime like *Python*.

Java is a high-level language and is good for programming across multiple platforms (operating systems). By taking advantage of good OOP practices, like abstraction and polymorphism, *Java* can be used for many programming purposes. It has a lot of packages that have many classes that can be used out-of-the-box, like a HashMap or a StreamReader. These packages offer versatility and additional resources for programming. Unfortunately, since *Java* is high-level, it is far abstracted from the hardware level, and so does not do good as an embedded system language. The data structures in *Java* would require more memory and processing power than *C*.

3.1.xv.d Python Programming Language

Python is a scripting language, and so it is not compiled like most other languages. *Python* is compiled at runtime by the Python interpreter. This means runtime errors are more common as type checking does not occur until runtime. *Python* also has support for object-oriented programming (OOP), just like *Java*. *Python* has lots of functionality built-in and can be expanded with packages that can be installed. Packages like *NumPy* and *matplotlib* allow for easy programming of arrays and numerical computations, as well as plotting of functions and data.

Despite the benefits, *Python* is more intensive to run on a machine, requiring a reasonable processor and memory (RAM). As such it is less useful for microcontrollers and microprocessors.

3.1.xv.e HTML/CSS/JavaScript Programming

For websites, *HTML* is the language that gives the structure of the site, while *CSS* styles it to make it look good. *JavaScript* enables for dynamic web content. For our team website, we will use these languages to produce a professional looking site for our project's documentation.

3.1.xv.f Language Comparison

A comparison of the languages for writing embedded code, and data processing code is summarized in **Table 3-14** below. For the languages looked at, we will be using *C/C++* for embedded (microcontroller) programming. These languages are the best for this kind of application due to their low system requirements. They also have many libraries that provide additional functionality when programming for embedded systems.

Since we will also be developing a software package for processing of our data, we will use *Python* for its ease of use and powerful packages that can help us program faster. Some of these packages allow for MATLAB-like plotting of data and for fairly easy GUI creation. This makes *Python* easier than *Java* for these reasons but also because scripting languages are also just simpler and easier to work with.

Table 3-14 *- Comparison of Programming Languages*

Language	HW Level	Formal Structure	Object-Oriented	Scripting
C	Low	✓	×	×
C++	Low	✓	✓	×
Java	High	✓	✓	×
Python	High	×	Can be	✓

3.1.xv.g Software Applications

For software that will be used for the project, we will use the Arduino IDE for embedded software programming with an Arduino chip. Using this IDE is recommended for programming Arduino-based boards. To program for the ESP32 chip, an additional library or package needs to be installed first. For other programming tasks, like building our website and our (Python) software package, we will use Visual Studio (VS) Code from Microsoft. There is even an extension for Arduino programming in VS Code called *Platformio* that can be used to enable the use of more powerful features in VS Code. We ended up using the ESP-IDF framework for writing the MCU code within VS Code. This framework gives the most control over the MCU and its peripherals.

For logistics, we will use Discord for team communication and VoIP calling. We will also be using GitHub as our code repository, which also solves the problem of source control when many authors are contributing. Microsoft OneDrive is used alongside Office 365 products (Word, Excel, PowerPoint, etc.) for document writing and sharing. For optical design, Zemax is used to test, optimize, and verify the performance of our paraxial designs. For making 3D printing models, a CAD software like SolidWorks, or OnShape will be used. For hardware CAD software, we will use Autodesk Fusion360 or Eagle for PCB schematic capture and layout. We will also use PSpice and LTSpice for other circuit simulations.

3.1.xvi Memory Technologies

For our Crab Pulsar Polarimeter and Pulse Timer project, selecting the appropriate memory technology is essential due to the high-resolution data capturing requirements and the need for reliable long-term storage. We will evaluate four types of memory technologies: SRAM (Static Random-Access Memory), Flash Memory, DRAM (Dynamic Random-Access Memory), and FRAM (Ferroelectric Random-Access Memory). Each of these memory technologies has its own strengths and weaknesses that must be carefully considered to ensure optimal performance for our instrument.

SRAM is known for its extremely high speed and low latency, making it ideal for applications that require quick data access and processing. It consumes very little power when idle, which is advantageous for operations that do not need constant access. Furthermore, SRAM's reliability is high due to its static nature, allowing it to withstand numerous read and write cycles over time. However, SRAM is quite expensive per gigabyte compared to Flash and DRAM, making it less cost-effective for applications requiring large storage capacities. Additionally, SRAM has a lower storage density, meaning it occupies more physical space for the same amount of data compared to other memory types. This limitation makes it impractical for our project, which needs to store extensive amounts of data from pulsar observations, despite its high speed and low latency benefits.
DRAM, in contrast, offers faster read and write operations than Flash, which is beneficial for real-time data processing. Its higher storage density compared to SRAM allows for more compact storage solutions, enabling the storage of larger amounts of data in a smaller physical footprint. However, DRAM's volatility is a major drawback for our project. Since data stored in DRAM is lost when power is turned off, it is unsuitable for long-term data storage unless continuous power is assured or additional backup mechanisms are implemented. Furthermore, DRAM requires constant refreshing to maintain data integrity, resulting in higher power consumption, which is disadvantageous for our project, especially considering the remote and potentially battery-powered nature of the instrumentation. The volatility and high-power consumption of DRAM make it less suitable for our project, given the need for reliable long-term data storage in remote locations.

Flash Memory is the most suitable option for our project due to its balanced features. Flash memory is non-volatile, meaning it retains data even when the power is turned off, which is crucial for our data logging needs where data integrity over extended periods is essential. It offers high storage density, providing ample storage capacity within a reasonable physical space, which is vital for storing the extensive data collected during our pulsar observations. Moreover, Flash is more cost-effective per gigabyte compared to SRAM and DRAM, aligning well with our project budget and making it a practical choice for extensive data storage. However, Flash does have its challenges. It has slower write speeds compared to SRAM and DRAM, which could be problematic for real-time data capture. To mitigate this, we can use a buffering strategy with faster memory like SRAM or DRAM to handle real-time data capture, with periodic writes to Flash to ensure data integrity and efficiently manage write operations. Additionally, Flash has a limited number of write/erase cycles, which could impact its durability over the long term. Proper management of write operations and balanced wear leveling can help extend the lifespan of Flash in our application.

FRAM (Ferroelectric Random-Access Memory) offers several benefits that make it a contender for our project. FRAM is non-volatile, meaning it retains data without power, similar to Flash. It also offers fast write and read speeds, making it suitable for real-time applications, and its high endurance means it can handle many read and write cycles, making it highly durable. However, FRAM is more expensive per gigabyte compared to Flash and typically has lower storage density. While FRAM's non-volatility and durability are advantageous, its higher cost and lower storage density compared to Flash limit its practicality for extensive data storage needs in our project.
In summary, each memory technology has its own set of advantages and limitations relative to our project requirements. SRAM provides high speed and low latency but is costly and occupies more space. DRAM offers very high speed and storage density but is volatile and consumes a lot of power. FRAM provides non-volatility, fast speeds, and high endurance but comes with a higher cost and lower storage density. Flash Memory, on the other hand, balances capacity, cost, and non-volatility, making it the optimal choice for our Crab Pulsar Polarimeter and Pulse Timer project. Its ability to store large amounts of data reliably over long periods, despite slower write speeds, fits well with our project's requirements. By implementing data buffering and managing write/erase cycles effectively, we can ensure efficient and durable data storage. This choice lets us meet our performance, cost, and reliability goals, ultimately contributing to our project's success.

3.2 Product Comparisons

Now we look at some of the products that we need for the design based on the technologies we've chosen. We look at 3 different products from at least 2 different manufacturers so that we have options when it comes to ordering. It also provides redundancy in case one manufacturer is out of stock.

3.2.i Voltage Regulators

Within the following section we compare a few voltage regulator products. We will look at both linear and switching regulators. This comparison will research more than one manufacturer to ensure we can choose the best component for our design requirements. Here, we will primarily focus on the voltage regulators needed to connect our power supply unit to the rest of the PCB and optics as well as to power the MCU and ensure that the processor has enough power to use all peripherals.

Table 3-15 *- Comparison of Linear Voltage Regulators*

Type:	**Linear**	**Linear**	**Linear**
<u>Specification</u>	TI TSP7A49	Analog Devices LT3080	Analog Devices ADP7142

Input Voltage Range (V)	3 - 36	1.2 - 36	2.7 - 40
Output Voltage Range (V)	1.194 - 33 (Adjustable)	0 – 36 (Adjustabl e)	1.8 - 5 (Fixed)
Max Output Current	150 mA	1.1 A	200 mA
Noise (µVrms)	15	40	11
Dropout Voltage (mV)	260	350	200
PSSR	54 dB at 1kHz	75dB at 120Hz, 55dB at 55kHz, and 20 at 1MHz	88 dB at 10 kHz, 68 dB at 100 kHz, 50 dB at 1 MHz
Size	HVSSOP; 3 mm x 4.9mm. VSON; 3mm x 3mm	8DIP 3mm x 3mm	LFCSP 2mm x2mm
Cost	$2.90	$2.20	$1.29

Table 3-16 – Comparison of Switching Voltage Regulators

Type:	**Switching**	**Switching**	**Switching**	**Switching**
Specification	TI LM2576 [link]	AD MAX175	TI LM2675 [link]	TI TPS564257
Input Voltage Range (V)	45 (max)	4.5 - [60-Vout]	8 - 40	3 - 17
Output Voltage Range (V)	1.23 - 37	-0.9 - -36	2.1 - 37	0.6 - 10
Max Output Current (A)	3	1	2.1	4
Switching Frequency (kHz)	52	400k - 2.2M Adjustable Frequency	250	600
Size	TO-263 10.16mm x 15.24mm. TO-223 10.16mm x 8.47mm	SOT583 1.6mm x 2.1mm	PDIP 9.81mm x 9.43mm	SOT5x3 1.6mm x 1.6mm
Cost	$1.74	$1.58	$1.76	$0.62

Following product research, we decided to design our voltage regulator power management scheme using primarily Texas Instruments LM2675-ADJ voltage regulators. This option was chosen because of the maximum output current capability of 3A offered by these regulators. The LM2675 was a great choice for prototyping as well as the IC is available in a dual in-line package which made it easy to breadboard test. Next, we originally chose the LM2576-ADJ as our regulator for the inverted 12V signal. However, even after following the manufacturer's recommendation on the inverting output scheme, it was unsuccessful during prototyping. The LM2576-ADJ was originally chosen because of the inversion scheme provided in the datasheet, packages suitable for breadboard testing, and a relatively high output current of 0.7A while in the inverting configuration. Lastly, the Analog Devices MAX17577 has been chosen to replace the LM2576-ADJ for the inverting regulator. This IC was chosen because the design is specifically meant for inverting outputs while supplying a high output current of 1A. The MAX17577 is only offered in surface mount packages though, so testing with a breadboard is not an option. Rather we must test the regulator when incorporated on a PCB. No linear regulators were chosen in this design to limit power loss, as linear regulators typically have high dropout voltages, which lead to higher power dissipation.

3.2.ii Beamsplitter Products

When looking at beamsplitters, our goal is to reduce any distortions of the polarization and minimize power loss. We found that these form a tradeoff, as reduced polarization deviations come with higher power loss. Our main beamsplitter considerations are plate beamsplitters versus cube beamsplitters. Our other consideration is the splitting ratio, which in our case should be skewed more towards transmission. This way, more power goes to the instrument for measuring polarization and pulse time.

For plate beamsplitters, they act like a mirror, as they operate at an angle of incidence of 45° to reflect light 90° from the transmitted light. Due to their minimal thickness, the power loss is very minimal at <1%. Unfortunately, at a 45° AOI, the Fresnel reflection coefficients for perpendicular (TE) and parallel (TM) polarizations deviate more than desired. In this case, the deviation for reflected and transmitted polarizations is <35% ($|T_{TE} - T_{TM}| <$ 35% and $|R_{TE} - R_{TM}| <$ 35%). This holds for different splitting ratios as well. These specifications are for Thorlabs non-polarizing plate beamsplitters. The other manufacturer considered is Edmund Optics. Edmund Optics has a 10/90 beamsplitter as well as a 20/80 beamsplitter to be considered. The documentation for Edmund Optics components lacks certain information that is handy from the Thorlabs specifications. As such, some information might not be fillable for their products. Also considered is a beamsplitter from Newport. Newport unfortunately only offers a 50:50 splitter, while we ideally look for a 10:90 or 30:70 split.

Table 3-17 *- Comparison of Different Beamsplitters*

Specification	Thorlabs BSN10	Thorlabs BS025	Newport 10BC17MB.1	Edmund Optics #13-420
Size	Ø1" 5mm thick mirror	1" (25.4mm) cube	1" (25.4mm) cube	25mm cube

AOI	45°	0°	0°	0°
Splitting Ratio (R/T)	10:90 $R: 10 \pm 8\%$ $T: 90 \pm 8\%$	10:90 $R: 7 + 10\%/-7\%$ $T: 87 \pm 10\%$	50:50 $R_{avg}: 45 \pm 5\%$ $T_{avg} = 45 \pm 5\%$	30:70 $T: 65 \pm 10\%$
Power Loss	< 1%	< 15%	< 20%	Not Enough Info. Guess: ~ <20%
Polarization Performance	<35% deviation for *s*- and *p*-polarized	< 10% deviation for *s*- and *p*-polarized	<10% deviation for *s*- and *p*-polarized	<6% deviation for transmission only
Coating Range	400-700nm	400-700nm	400-700nm	430-670nm
Cost	$140.17	$251.85	$282	$258.00

We choose the Thorlabs beamsplitter cube (BS025) over the plate beamsplitter due to the better polarization performance. We choose Thorlabs over Newport and Edmund optics because they are the cheapest, but also have the splitting ratio we want (10:90) and have good documentation. In our actual design we use a smaller version of the BS025 cube, to reduce the design footprint. This beamsplitter is 10mm and is also around $50 cheaper. The product number is BS037.

3.2.iii Switchable Mirrors

Since proper motorized mounts are rather expensive for their purpose in the project, we look at manual mounts that flip, enabling the mirror to be taken into or out of the optical path. To make our product more professional, we will use a motor to electronically change the position of the mount. As previously mentioned, we will consider stepper motors and servo motors.

Servo motors are simple to control and small. The main drawback would be its torque output, but they do make ones with high torque for more money. A popular servo, the Tower Pro™ SG90 servo allows for 180° rotation at a speed of 60° in 0.12 seconds. It also features 1.6 kg-cm of torque. A higher torque product is the MG995 servo (also from Tower Pro). This servo has between 8.5 kg-cm (at 4.8V) and 10 kg-cm (at 6V) of torque, depending on the voltage supplied. This servo is limited to only ±60° from center (120° total) and can rotate 60° in 0.2s (4.8V) or 0.16s (6V). We will be using 5V to operate our components, as we will have a 3.3V and 5V rail from our power supply.

Stepper motors on the other hand, require their own driver board/IC to supply the necessary current. Stepper motors will provide a constant torque under idle conditions, which consumes power. The 28BYJ-48 stepper motor has 64 steps for a full 360°, resulting in 5.625° per step. There are a few different torques reported on its datasheet, making it unclear which is its maximum. Going by friction torque, puts the motor at 600-1200 gf-cm (or 0.6-1.2 kg-cm). Also reported is the in-traction torque, which has a lower bound of 34.3mN-m, which is only 0.3497 kg-cm. According to one website, 34.3mN-m is the torque, and it rotates at 15 RPM [9].

A higher torque option is the StepperOnline Nema 17 bipolar stepper motor (part number: 17HS19-2004S1), which has 59N-cm of torque (6.02 kg-cm). The step angle is 1.8° and is rated for 12-24V and 2.0A. The rotation speed of the motor is variable based on the supplied power. As the speed increases though, the torque will decrease.

The table below compares the relevant specifications between the servo motors and the stepper motors detailed above. A driver board (ULN2003) is included with the 28BYJ-48 stepper motor.

Table 3-18 - Comparison of different servo and stepper motors.

Specification	SG90 Servo	MG995 Servo	28BYJ-48 Stepper	Nema 17 Bipolar Stepper
Rotation Angle (total)	180	120	5.625°/step	1.8°/step
Stall Torque (max)	1.6 kg-cm	10 kg-cm	34.3 mN-m or 0.3497 kg-cm	59 N-cm or 6.02 kg-cm
Rotation Speed	60°/0.12s	60°/0.2s	15 RPM = 90°/s	Varies
Gear Material	Plastic	Metal	Metal	Metal
Operating Voltage (Rated)	4.8-6.0V	4.8-7.2V	5V	12-24V (24V recommended)
Cost / units	$18.77 / 10 ($1.88 each)	$26.99 / 6 ($4.50 each)	$9.99 / 5 ($2 each)	$13.99 / 1

The driver board for the stepper motor should also be considered. For the lower power 28BYJ, the included ULN2003 can provide up to 500mA. For the Nema 17, it can take up to 2A, which would require a different driver board. This kind of current draw would also require an additional design of the power supply to handle that kind of current. One possible driver board to use in this case is the L298N, which can handle up to 2 amps of drive current.

Due to the simplicity of servo motors, we will choose one for flipping a mirror. A mirror and its mount will not be too heavy and so high torque isn't required. We also only need around 90° of rotation, and not the open loop that steppers provide. Therefore, we choose the SG90 servo because it has the torque that we need and is the cheapest.

3.2.iv Display

A display unit will need to be chosen and implemented within our project primarily to display control settings and allow for the user of the system to adjust sample duration and rate as well as outputting other menu screens to help the user 'tune' the device in an easy manner. The 20x4 LCD is chosen, as it is simple to program with a library, and provides more text space than the 1602. The increase in cost is not much of a factor.

***Table 3-19** - Comparison of Display Technologies*

Display	**1602 LCD**	**2004 LCD**	**2.4" OLED LCD**
Segments	• 2 segments of 16 characters	• 4 segments of 20 characters	• 128x64 pixels
Size (mm^2)	• 84 x 44	• 98 x 60	• 2.42" diagonal
Additional Features	• I2C compatible	• I2C compatible	• SPI, or I2C
Cost	• ~ $4	• ~ $8	• $14

The 2004 LCD was chosen for its larger display size compared to the 1602. Additionally, the I2C compatibility is a great option for keeping the wiring scheme simple whilst also having compatibility with our MCU of choice, the ESP32.

3.2.v Battery Products

Choosing to include a battery in our design means we must pick the best fit for the application. Specifically, we are going to use a lithium-ion battery for its great charge density capability and compact size. Lithium-ion batteries are also rechargeable which makes it a great option for extending the lifespan of our instrument. The main criteria we are trying to satisfy when it comes to the battery selection are compact size, proper output amperage (1~2 A), and proper voltage output (3.3V). The main use of the battery will be when the instrument is disconnected from the main power supply.

***Table 3-20** – Product comparison of batteries*

Battery	**SparkFun Electronics PRT-13852**	**Jauch Quartz LI18650JP1S1P+PCM+2**	**Adafruit Industries LLC 2750**
Output Voltage (V)	3.7	3.6	3.7
Capacity (mAh)	40	3250	350

Discharge Rate (mA)	8	N/A	N/A
Size	20.0mm x 11.0mm x 3.0mm	20.0mm x 72.0mm	36.0mm x 20.0mm x 5.6mm
Cost	$4.95	$15.74	$6.95

The Adafruit Industries LLC 2750 lithium-ion battery was selected to be used as the systems isolated power source. This li-ion battery provides a compact package whilst also providing sufficient voltage and current ratings intended for our purposes. This battery is relatively inexpensive, and the power demands required by the MCU are not tremendous, allowing for this battery option to provide the correct amount of power needed for the MCU to perform data transfer and software updating without need for the primary 12V wall plug power supply.

3.2.vi Op-Amp Products

When choosing the correct op-amp we must consider the application of the op-amp within the circuit design. For example, we will use an op amp to amplify and buffer the DAC sinusoidal output required for the half wave plate retarder. Furthermore, we will also use an op-amp circuit to boost the signal of the photodetectors which will require an op-amp with low noise due to the small signal inputs.

Table 3-21 - Op-amp Product Comparison

Type:	Precision	Precision	Precision	Ultra High-Speed	General Purpose
Specification	AD86(28/29/30) [link]	TI OPA211(A) [link]	TI OPA140 AIDBVT [Link]	TI OPA847 [link]	TI LM741 [link]
Offset Voltage (µV)	1 - 5	30 - 150	120	100-500	1000 - 5000
Supply Voltage (V)	0 - 5	4.5 - 36	2.24 - 18	-5 - 5	10 - 44
Max Output Current (mA)	30	30	37	100	25
Slew rate (V/µs)	1	27	20	950	0.5
Noise (µVp-p) (0.01-10 Hz)	0.5	.08	5.1 e-3	0.85e-3	N/A

Size	SOT23 2.9mm x 1.3mm	SON-8 3mm x3mm	SOT23 2.9mm x 1.3mm	SON-8 3mm x3mm	PDIP 9.81mm x 9.43mm
Cost	$1.30	$2.86	$1.80	$2.75	$0.25

The op amps chosen for the project include the Texas Instruments TL081 and OPA148AIDBVT. The Tl081 was chosen as a general-purpose op amp for breadboarding purposes, this op amp was available within the university laboratory and allowed for ease of prototyping the ADC front-end circuitry. For use in our actual product, we will choose to utilize the OPA188AIDBVT as it is an ultra-low-noise precision op-amp. These features will allow us to have negligible voltage offset and noise added to our photodetector signal ensuring we have a high-fidelity signal input to the ADC. This will help keep our data accurate and less susceptible to errors and provides the user with quality sampling data.

In redesigning the signal amplification for the PDA44 photodetector, we selected the OPA847, an ultra-high-speed amplifier with a gain-bandwidth product of 3.9 GHz. This choice is driven by the need to accurately reproduce the 4 ns, 50 mV pulses generated during dark counts, which occur at a frequency of approximately 5 kHz. The detector's harmonic frequency is 250 MHz, and faithfully recreating the signal requires preserving both the 3rd and 5th harmonics, with the highest frequency reaching 1.25 GHz. The OPA847's exceptional bandwidth ensures that these critical high-frequency components are amplified without distortion, maintaining signal fidelity for precise analysis.

3.2.vii Oscillators

For our instrument to properly function we must include an oscillator which will generate an adjustable frequency signal that will be utilized by the multiple ADC channels to achieve high speed sampling of our input. We are striving to achieve a sample rate of 1 MSPS. Whilst looking for the correct crystal oscillator we must consider the coupling capacitance as well as the crystal’s set frequency. We must also consider methods that the MCU will use to “alter” the frequency that the crystal clock signal will produce.

Table 3-22 - Comparison of crystal oscillators.

Product Name	**Abracon ABS07-32.768KHZ-T**	**ECS-.372-12.5-34B-TR**	**Abracon ABM3B-40.000MHZ-B2-T**	**TXC 7B-40.000MEEQ-T**
Frequency	32.768 kHz	32.768 kHz	40 MHz	40 MHz
Load Capacitance (pF)	12.5	12.5	18	18
Frequency Stability (± ppm)	20	20	50	30

Size (SMD)	3.2 x 1.5 mm	3.2 x 1.5 mm	3.2 x 2.5 mm	5.0 x 3.2 mm
Cost	$0.69	$0.53	$1.05	N/A

The oscillator selected was the Abracon ABM3B-40MHZ-B2-T. The choice for this crystal was primarily due to the natural frequency it provides. The ABM3B-40MHZ-B2T provides an impressive 40 MHz frequency typically recommended for use with the ESP32 MCU as an external clock source. The use of the crystal oscillator allows to have a stable high frequency clock signal the will be utilized by the ADC module to ensure an accurate sampling rate of 1 MSPS or one sample every microsecond. Additionally, the load capacitance is a typical value for external crystal clock sources which makes implementation on this external source simple.

The ESP32-Mini module includes an internal 40 MHz crystal oscillator, which has been selected for use in the design instead of incorporating an external crystal oscillator. This decision simplifies the overall circuit design by reducing the need for additional external components, minimizing the board's size and complexity. Leveraging the internal crystal also streamlines assembly and cost considerations while maintaining reliable performance for timing and communication requirements within the project.

3.2.viii Polarimeters

As is discussed in the technology research section, off-the-shelf polarimeter devices will not be suitable for our uses. Existing products lack the sensitivity to weak optical signals, temporal resolution, and polarization resolution that we require. As such, we will be building our own polarimeter from scratch. This will be a Stokes polarimeter and requires us to construct an optical system making use of polarizing beamsplitters, rotating achromatic half wave plates, and single photon avalanche photodetectors. Discussions and comparisons for each of these individual parts is done in the following sections.

3.2.ix Photodetectors

When considering photodetectors, there is no clear winner between Avalanche Photodiodes (APDs) and Single Photon Avalanche Photodiodes (SPADs). The single photon resolution SPADs is technically the best fit for our uses, but the pricing makes this difficult to justify unless such extreme sensitivity is strictly necessary. Our need to purchase four of whichever detector we choose greatly magnifies the associated price. To use APDs would cost us roughly $5,500, but to use SPADs would cost us at least $20,000.

We will only consider products with peak sensitivity to visible spectrum light, which typically means silicon-based detectors. Additionally, detectors will need to accept free space optical coupling, as optical fiber inputs will introduce instrumental polarization that cannot be filtered or removed.

For most performance specifications, it is not useful to directly compare SPADs and APDs due to their different operational uses. For example, NEP is not a listed specification for SPADs since it is not a valid parameter for quantifying discrete counting systems. The NEP of an APD and dark count rate and after-pulse probability in a SPAD both quantify the noise level and minimum signal detection for each product. For the ease of comparison, the equivalent parameters are listed next to each other where necessary.

3.2.ix.a Avalanche Photodiodes (APD440A2, APD410A2, APD430A2)

Thorlabs' line of avalanche photodiodes features detectors that are useful for applications needing fast response times and high sensitivity. These APDs are designed for use in fields like telecommunications, medical diagnostics, and scientific research for reliable optical signal detection. They have an accessibly low cost within the range of $1,300 to $1,600, which is suitable for us given the budget. Unfortunately, the Noise Equivalent Power of this product line is too high. Even the product with the best NEP of the product line will not work. This trend is reflective of a technological limitation of existing avalanche photodiode products. To solve this problem, we will now consider Single Photon Avalanche Photodetectors for our use.

3.2.ix.b SPDMH2 SPAD

The Thorlabs SPDMH2 Single-Photon Detection Module is a highly sensitive tool designed for a wide range of applications in scientific research. This product can detect single photons with high efficiency and very low noise, making it ideal for applications requiring single photon counting. The SPDMH2 has a relatively small overall size that will allow it to fit into our design without much issue. It boasts a fast response time, enabling real-time data acquisition and analysis. Additionally, this instrument has no issues with stability and can be used for extended lengths of time without any problems.

It has an extremely low dark count rate at 100 Hz on average, giving it an extremely high signal to noise ratio relative to our use case. It is meant for use with visible spectrum and near infrared light. Peak detection efficiency occurs at 670nm, where it can detect approximately 70% of incident photons. It boasts a very low after-pulse rate of 0.2%. Considering only these specifications, this product is an excellent fit for our project. Unfortunately, it costs $5692.37, which is simply too high given our budget. That would bring the total detector price tag up well over $20,000, not including any other components. As such we cannot use this product.

3.2.ix.c PDA44 SPAD

The Thorlabs PDA44 is a photodetector designed for a broad range of applications in photonics and optical research. This device has a high sensitivity and wide spectral response, making it suitable for detecting optical signals across various wavelengths. Additionally, this product has a relatively low signal to noise ratio resulting from its 5 kHz dark count rate which does a lot to enable quality and reliable data collection using this product.

While the dark count rate is higher than many other single photon counting alternatives, the PDA44 has the lowest dark count of the Thorlabs PDA SPAD product line.

Additionally, its 1.3 mm by 1.3 mm detector area will make focusing light onto the usable detector surface a quick and easy process. The primary benefit of this device however, its low cost of only $1,632.00. This leads to a total detector cost of approximately $6,500, which fits into our budgetary constraints. Ultimately, we will develop or project to make use of this product since it can perform at the level we require and fits within our economic constraints.

Table 3-23 - Comparison of Photodetector Products

Specification	SPADSs		APDs		
Part Number	**SPDMH2**	**PDA44**	**APD440A2**	**APD410A2**	**APD430A2**
Supplier	Thorlabs	Thorlabs	Thorlabs	Thorlabs	Thorlabs
Min. NEP	-	-	2.5 fW/√Hz	150 fW/√Hz	90 fW/√Hz
Dark Count Rate	100 Hz	5000 Hz	-	-	-
After-pulse Probability	0.2%		-	-	-
Conversion Gain	-	-	1.25 GV/W	12.4 MV/W	0.5 MV/W
Transimpedance Gain	-	-	25 – 50 MV/A	0.25 – 0.5 MV/A	0.002 – 0.005 MV/A
Output Pulse Amplitude	3 V	2V	-	-	-
Wavelength Range	400 nm – 1000 nm	320 nm – 900 nm	200 nm – 1000 nm	200 nm – 1000 nm	200 nm – 1000 nm
Active Detector Dimensions	100 μm ø	1.3 mm x 1.3 mm	1000 μm ø	500 μm ø	200 μm ø
Detection Efficiency at Peak Wavelength	70% @ 670 nm	40% @ 450 nm	-	-	-
Responsivity at Peak Wavelength	-	-	25 A/W @ 600 nm	25 A/W @ 600 nm	50 A/W @ 600 nm
Price	$5692.37	$1,632.00	$1,300.32	$1,457.58	$1,457.58

3.2.x Half Waveplates

In this section we will consider available products in order to determine which specific half waveplate we will use. The primary factors we will consider are the retardation error relative to wavelength, spectral bandwidth, anti-reflection coatings, and of course, price. These four parameters are extremely important since they will be the limiting factors for part quality and usability. Some less crucial but still relevant parameters are the clear aperture and transmission, which do not directly define our system limitations, but do factor into our design considerations.

Other factors such as the retardance error with respect to angle of incidence will not be considered, as we intend to design our system such that these factors are not relevant in any significant way.

3.2.x.a AHWP10-580

Thorlabs' AHWP10-580 half waveplate is built for use within the spectral range of 350 nm to 850 nm. While this range is somewhat excessive considering our target range of 400 nm to 700 nm, this is not a problem. The product still maintains a very low retardation error within the stated range, at less than one 300th of a wavelength at 633 nm. It is built out of quartz and UV Sapphire, and the transmission of visible spectrum light varies but is high overall, with a minimum of approximately 96% transmission and a maximum of approximately 98%. This is good for our purposes, and the 2% deviation will not be an issue. Additionally, it has a 0.89" diameter clear aperture, which is plenty large enough to accommodate the planned beam diameter of <10 mm. It is priced at $1,059.22, which is high, but not problematic. The product comes pre-mounted and slots into an SM-1 screw thread.

This product would be an excellent choice. It maintains high performance of our needed wavelength range and is not prohibitively expensive. The transmission losses are fairly standard and are in line with what we expect for any high-quality optic using an anti-reflective coating.

3.2.x.b AHWP10-600

The AHWP10-600 is fairly similar to the waveplate previously discussed, with some minor yet relevant differences. The intended spectral range has 50 nm removed from each end, giving it a range of 400 nm to 800 nm. Since our required bandwidth is 400 nm to 700 nm, this is a considerable issue. When operating at the extreme edges of the intended bandwidth, most products will still maintain decent performance, but it will noticeably degrade as you approach the limit. As such, this product has a retardation error comparable to the AHWP10-580 in all regions except the blue end of the spectrum, where performance diverges significantly.

Transmission data for this product states that it reaches a minimum of 97% over the visible spectrum, and at some wavelengths reaches as high as 98.5%. This is achieved by use of Magnesium Fluoride instead of Sapphire in its construction, as even UV-grade sapphire has not the best material for transmitting shorter wavelengths of light. The clear aperture is 0.89" in diameter, and it also comes pre-mounted into an SM-1 threaded optical mount. Its price is $1,059.22 again, which is in our budget. Despite some minor drawbacks, this product is still an excellent choice. Its only issue is that it is slightly out-performed by the AHWP10-580 in all key parameters.

3.2.x.c 39-033

The Edmund Optics 39-033 half waveplate is designed for use within the spectral range of 450 nm to 650 nm and has a similar range for its applied anti-reflective coating. The waveplate is constructed from crystalline quartz and Magnesium Fluoride, making it quite comparable with most half waveplates in terms of transmission. Its transmission is approximately 96% at minimum and at maximum close to 98% across its operating range. The relatively narrow spectral range will prove to be problematic. While it loosely fits with our requirements, it still loses the outer edges of the spectrum. Despite this, it has an excellent retardation error.

Additionally, the 39-033 half wave plate has a clear aperture of 0.78”. This size is adequate for our design specifications, although smaller than most competing products. The product is priced at $980.00. The waveplate is also available pre-mounted, but not screw threaded for direct integration into rotation mounts. Ultimately this product will not work for us. It loses out on the outer edges of our needed spectrum, even though it has good performance otherwise.

3.2.x.d Conclusion

After considering available half waveplate products, a trend becomes clear. The price of visible spectrum achromatic half waveplates does not vary much across the product space, remaining at approximately $1,000 regardless of specific characteristics. Therefore performance, not price, will be the deciding factor in our product selection.

Edmund Optics’ 39-033 half waveplate is decent, but not good enough. It has a very good performance when considering transmission and retardation error but falls short in its usable spectral range. The 450 nm – 650 nm range is only two thirds of what we require. We will need to choose a different product that better fits our use case.

The AHWP10-600 is a good product that fits our requirements fairly well. It matches our spectral range and has generally good performance. It fails to maintain performance as the wavelength approaches 400 nm unfortunately, and in this parameter, it loses out to a very similar but noticeably better product.

The AHWP10-580 is the clear winner and will be the waveplate we purchase and use going forward. The slightly excessive usable spectral range ensures that the range we really care about has excellent performance. Its visible transmission is a few percent lower than its competitors, however it is still in line with what we expect to see from an anti-reflective optic.

Table 3-24 *- Half Waveplate product comparison*

Specification	**Part Number**		
	AHWP10-580	**AHWP10-600**	**39-033**
Supplier	Thorlabs	Thorlabs	Edmund Optics
Retardation Error	<λ/300	<λ/200	<λ/300
Spectral Bandwidth	350 nm – 850 nm	400 nm – 800 nm	450 nm – 650 nm

Transmission	96% - 98%	97% - 98.5%	96% - 98%
Clear Aperture	Ø0.89”	Ø0.89”	Ø0.78”
AR Coating Bandwidth	350 nm – 850 nm	400 nm – 800 nm	450 nm – 650 nm
Mounting	Mounted, SM-1 Thread	Mounted, SM-1 Thread	Mounted, No thread
Price	$1,059.22	$1,059.22	$980.00

3.2.xi Lenses

From the lens material discussion, N-BK7 is a good choice for our main lens material, as it has good performance at a low cost. For our design, a variety of lens shapes will be needed. For changing the image location, bi-convex singlet lenses do a good enough job, while for collimating, plano-convex lenses will result in less spherical aberrations. Thorlabs also has ‘best-form’ singlet lenses which are designed for infinite image conjugates, i.e., when the light comes from infinity. These lenses come in different sizes, focal lengths, and coatings. Costs are reasonable, at only $42 for a 1” diameter lens (with AR coating).

The preliminary design calls for 6-7 singlet lenses. Once the general design is laid out, optimizations can occur to reduce spherical aberration through lens splitting and lens bending. Through these techniques, additional lenses would be added, as well as different shapes (like meniscus). Thorlabs helpfully compares their different lenses for sale and suggested applications of the different lens shapes. For relaying the image, a bi-convex shape is best, while for collimating, a plano-convex shape is better [32]. A quantitative analysis of aberration is provided in Table 3-26 below. Initially, 3 bi-convex lenses, 1 best-form, 1 plano-convex, and 1 plano-concave lens will be used.

Table 3-25 - Lens Comparison by Manufacturer

Specification	Thorlabs	Edmund Optics	Newport/MKS	Thorlabs
Shape	Bi-Convex	Bi-Convex	Bi-Convex	Aspheric
Diameter	1” or 25.4mm	25mm	25.4mm	25.0mm
Focal Length	100mm	100mm	100mm	50.0mm
f/#	~4	4	4 (3.9)	2.0
Coating Range and Performance	400-1100nm, $R_{avg} < 1.0\%$	400-1000nm, $R_{avg} \leq 1.25\%$	430-700nm, $R_{avg} \leq 0.75\%$	350-700nm, $R_{avg} < 0.5\%$
Material	N-BK7	N-BK7	N-BK7	N-BK7
Part Number	LB1676-AB	45-892	KBX064AR.14	AL25550G-A
Cost	$42.00	$50.00	$55	$349.39

From Table 3-25 above, we see that the different manufacturers have slightly different AR coatings. One thing to note is the AR coating performance is per surface. We also see how an aspheric lens, with diffraction-limited performance is much more expensive than spherical lenses. This table mainly compares the differences between lens manufacturers for the same lens shape, size, and focal length. The most notable difference is the AR coatings. Most manufacturers have multiple different coatings, each with different performance characteristics.

Now we look at how the different lens shapes affect spherical aberration. For this, we use the Zemax files that Thorlabs provides for each of their lenses. We will look at their best-form lens, plano-convex lens, and biconvex lens. Each of these lenses has a 1" diameter, and 100mm focal length. They also have the same coating (Thorlabs A for 350-700nm). The spherical aberration (SPHA) is measured as the Seidel coefficient in units of waves, which uses the primary wavelength of 587.6nm (sodium d-line). The lens product numbers looked at are: LBF254-100, LB1676-A, LA1509-A.

Table 3-26 - Lens Shape comparison

Lens Shape	Infinite Conjugate			1:1 Conjugate		
	SPHA (in waves)	RMS Spot Size	GEO Spot Size	SPHA	RMS Spot Size	GEO Spot Size
Best-Form	7.4369λ	65.897μm	153.41μm	11.9676λ	152.18μm	359.09μm
Bi-Convex	11.6564λ	77.964μm	185.04μm	8.03974λ	131.936μm	307.59μm
Plano-Convex	7.996λ	67.22μm	157.36μm	15.8203λ	176.92μm	411.20μm

To reduce chromatic aberration, which is a shift of the focal length for different wavelengths, achromatic doublets or triplets can be used. Thorlabs sells two types of achromatic triplets, one for finite conjugates (Steinheil) and one for infinite conjugates (Hastings). Our primary lens will relay imaging at 1:1 magnification, while the collimating lens will have an infinite conjugate. Our lens for imaging the object will also be relay imaging and will use a Steinheil achromatic triplet. Below is a comparison between some achromatic doublets and the achromatic triplets. One thing to note is that the doublets are designed for an infinite conjugate (object at infinity), while the Steinheil triplet is best for 1:1 imaging. The aberration data is from Zemax using the F, d, C wavelength preset. The entrance pupil diameter was set to 5 for each lens, which improves their aberration because the rays enter at the center of the lens more. This made each lens be near the diffraction limit for spherical aberration (for on-axis rays).

Table 3-27 - Comparison of Achromatic Lenses Available

Specification	Thorlabs Achromat Doublet	Thorlabs Steinheil Achromat Triplet	Edmund Optics Achromatic Doublet	Newport Achromatic Doublet
Diameter	12.7mm	12.7mm	12.7mm	12.7mm
Thickness	6.0mm	10.0mm	6.75mm	6.85mm
Focal Length	19.0mm	20.0mm	19.1mm	19.0mm
Coating Range & Performance	400-700nm $R_{avg} \leq 0.5\%$	400-700nm $R_{avg} \leq 0.5\%$	400-1000nm $R_{avg} \leq 1.25\%$	430-700nm $R_{avg} \leq 0.5\%$

Material	N-BAF10/N-SF6HT	N-SF8/N-BAF52	N-BAF10/N-SF6	N-BAF10/N-SF14
Spherical Aberration	0.72285λ	0.4218λ	0.64255λ	0.6158λ
Chromatic Aberration (Focal Shift)	73.947μm	49.899μm [Diff. Limited]	66.293μm	56.139μm
Part Number	ACN127-020-A	TRS127-020-A	#49-785	PAC019AR.14
Cost	$60.59	$73.95	$86.00	$117

From Table 3-27 above, we see that the achromatic triplet does the best at correcting chromatic aberration and is near diffraction limited. This is for a finite conjugate, while the rest are at infinite conjugates. One thing to note is that these are still only using a single lens. By using two achromatic doublets, near diffraction limited performance can be achieved when using a symmetric design. We will use a mix of achromatic triplets where we can, and achromatic doublets where different focal length options are needed.
In our final design, we elected to use just achromatic doublets because they have a greater variety of focal lengths. A total of five doublet lenses were used, four of them being 1 inch or 25.4 mm optics, with one half-inch or 12.7 mm optic. The design required more flexible focal lengths to choose from, as well as more compact (not as thick) lenses. We ended up purchasing mounted lenses to simplify the mounting process.

3.2.xii MCU Part Comparison

For our Crab Pulsar Polarimeter and Pulse Timer project, we need a microcontroller that can handle an ADC sample rate of 1 MSPS, manage control inputs from potentiometers, buttons, and switches, support flash memory, and interface with USB for data transfer, all while being compatible with a 32 kHz crystal. Here we evaluate four microcontroller boards: MSP430FR6989, ESP32C, STM32F407, and ATSAMD51, each with different capabilities and limitations. Ultimately, we aim to select the MCU that best meets our project's stringent requirements.

3.2.xii.a MSP430FR6989

The MSP430FR6989 from Texas Instruments is known for its ultra-low power consumption, which makes it suitable for battery-operated applications. It features a 16-bit RISC architecture CPU with a clock speed of up to 16 MHz, 128 KB Flash memory, and 2 KB SRAM. This MCU includes a high-speed ADC capable of sampling rates up to 1 MSPS, meeting our project's data acquisition needs. It also supports various peripherals, including ADC, UART, SPI, and I2C, and operates within a voltage range of 1.8V to 3.6V. Additionally, it is compatible with a 32 kHz crystal, ensuring accurate timing for our application.

Despite its low power consumption and compatibility with the required crystal, the MSP430FR6989's limited processing power and memory may not be adequate for the extensive data processing and real-time control needed in our project. The absence of built-in USB support further complicates data transfer, requiring additional components and increasing complexity.

3.2.xii.b ESP32C

The ESP32C by Espressif is a robust microcontroller known for its high performance. It features a dual-core 32-bit Xtensa LX6 CPU with a clock speed of up to 240 MHz, 520 KB SRAM, and 4 MB Flash memory. The ESP32C includes a high-speed ADC with a sample rate of up to 2 MSPS, surpassing our project's requirement. It also offers extensive peripheral support, including ADC, DAC, UART, SPI, I2C, and I2S, and operates within a voltage range of 2.2V to 3.6V. Moreover, it is compatible with a 32 kHz crystal and supports USB interfaces for efficient data transfer.

The ESP32C stands out due to its high processing power, ample memory, and integrated features, making it suitable for real-time data processing and remote operations. While it consumes more power than ultra-low-power MCUs, its deep sleep mode helps mitigate this issue, ensuring efficient power management when the system is inactive.

3.2.xii.c STM32F407

The STM32F407 from STMicroelectronics is a high-performance MCU widely used in embedded applications. It features a 32-bit ARM Cortex-M4 CPU with a clock speed of up to 168 MHz, 192 KB SRAM, and 1 MB Flash memory. It includes a high-speed ADC capable of sampling rates up to 2.4 MSPS, making it well-suited for high-resolution data capturing. It offers 140 I/O pins and a rich set of peripherals, including ADC, DAC, UART, SPI, I2C, USB, and CAN, operating within a voltage range of 1.8V to 3.6V. The MCU is also compatible with a 32 kHz crystal, ensuring precise timing.

The STM32F407 provides robust performance and extensive peripheral support, which are beneficial for complex applications. However, its higher cost and larger footprint may pose constraints for our project, where cost-effectiveness and compactness are critical. Despite its powerful capabilities, the need for a more cost-effective solution makes it less ideal for our specific requirements.

3.2.xii.d ATSAMD51

The ATSAMD51 from Microchip Technology is a powerful MCU that balances performance and power efficiency. It features a 32-bit ARM Cortex-M4 CPU with a clock speed of up to 120 MHz, 256 KB SRAM, and 1 MB Flash memory. It includes a high-speed ADC with a sampling rate of up to 1 MSPS, meeting our project's requirements. The MCU offers 52 I/O pins and supports various peripherals, including ADC, DAC, UART, SPI, I2C, and CAN, operating within a voltage range of 1.62V to 3.63V. It is also compatible with a 32 kHz crystal and supports USB interfaces for data transfer.

While the ATSAMD51 provides efficient processing capabilities and adequate memory for handling complex tasks, it falls short in several key areas for our project. Despite its cost-effectiveness, the ATSAMD51's lower maximum clock speed compared to the ESP32C may impact the performance of real-time data processing and the execution of complex algorithms. Additionally, the ATSAMD51's relatively lower number of I/O pins and peripherals compared to the STM32F407 limits its versatility in interfacing with multiple sensors and components. Furthermore, the power efficiency and performance trade-off might not align perfectly with the high processing demands of our project, making it a less attractive choice for our needs despite its affordability.

3.2.xii.e Conclusion

After evaluating the four candidates, the ESP32C stands out as the most suitable MCU for the Crab Pulsar Polarimeter and Pulse Timer project. The dual-core 32-bit Xtensa LX6 CPU with up to 240 MHz clock speed offers ample processing power to handle real-time data processing and complex algorithms required for pulsar data analysis. With 520 KB SRAM and 4 MB Flash, the ESP32C provides sufficient memory for both data processing and long-term storage, ensuring that high-resolution data is efficiently managed.

The extensive peripheral set, including ADC, DAC, UART, SPI, I2C, and I2S, ensures compatibility with various sensors and components, facilitating seamless integration and communication within the system. While the ESP32C has higher power consumption compared to ultra-low-power MCUs, its deep sleep mode at 10µA mitigates this issue, allowing for power-saving when the system is not actively processing data. Despite its advanced features, the ESP32C is competitively priced, providing a high-performance solution without significantly increasing the project's budget.

Table 3-28 *- Comparison of MCUs*

Specification	ESP32C	MSP430FR6989	STM32F407	ATSAMD51
CPU	Dual-core 32-bit Xtensa LX6	16-bit RISC	32-bit ARM Cortex-M4	32-bit ARM Cortex-M4
ADC Sample Rate	Up to 2 MSPS	Up to 1 MSPS	Up to 2.4 MSPS	Up to 1 MSPS
USB Support	Yes	No	Yes	Yes
Power Consumption	Active: 240 mA LPM: 10 µA	Active: 1.8 mA LPM: 2 µA	Active: 120 mA LPM: 1.7 µA	Active: 60 mA LPM: 20 µA
32kHz Crystal Compatibility	Yes	Yes	Yes	Yes
Peripheral Support	ADC, DAC, UART, SPI, I2C, I2S	ADC, UART, SPI, I2C	ADC, DAC, UART, SPI, I2C, USB, CAN	ADC, DAC, UART, SPI, I2C, CAN
Cost	$10	$19	$16	$9

The ESP32C's combination of high performance, robust memory capacity, comprehensive peripheral support, and efficient power management makes it the optimal choice for ensuring the success of our Crab Pulsar Polarimeter and Pulse Timer project. It aligns well with our requirements for efficient data processing, reliable long-term storage, and seamless integration with various components. By leveraging the ESP32C, we can meet our performance, cost, and reliability goals, ultimately contributing to the project's success.

3.2.xiii Memory Component Comparison

Selecting the appropriate memory technology for the Crab Pulsar Polarimeter and Pulse Timer project is crucial given the high-resolution data capturing requirements and the need for reliable long-term storage. We will evaluate four types of memory technologies: NOR Flash Memory, UFS (Universal Flash Storage), and NAND Flash Memory (including its various types: SLC, MLC, TLC, QLC). Each type has distinct advantages and disadvantages that must be carefully considered to ensure the optimal performance of our instrument.

3.2.xiii.a NOR Flash Memory

NOR Flash Memory offers several advantages, including fast read speeds and better random-access capabilities, allowing for efficient code execution directly from the memory. It is also highly reliable for read-intensive operations, which is beneficial for applications requiring frequent data access without modification. However, NOR flash is more expensive per gigabyte compared to NAND flash, making it less cost-effective for large storage capacities. Additionally, NOR flash has a lower storage density, meaning it occupies more physical space for the same amount of data compared to NAND flash. Furthermore, its write and erase operations are slower, which can be a limitation for data logging applications requiring frequent updates. While NOR flash's fast read speeds and random-access capabilities are advantageous, its high cost and lower storage density make it impractical for storing the extensive amounts of data generated by our pulsar observations. Additionally, the slower write and erase speeds are not suitable for our real-time data logging needs.

3.2.xiii.b UFS (Universal Flash Storage)

UFS (Universal Flash Storage) is another high-performance memory technology that offers significant benefits, including high data transfer rates and low latency, making it suitable for high-performance applications. It is designed for efficient power consumption, which is beneficial for battery-powered devices, and provides scalability in terms of storage capacity, accommodating various data storage needs. However, UFS is generally more expensive compared to traditional NAND flash solutions, and its integration may be more complex, requiring specific controllers and interfaces. As a relatively newer technology, UFS may also have less long-term reliability data compared to more established technologies like NAND flash. While UFS's high performance and efficient power consumption are beneficial, the higher cost and complexity of integration may not justify its use for our project. The primary need for large, reliable storage at a reasonable cost is better served by other technologies.

3.2.xiii.c NAND Flash Memory

NAND Flash Memory is available in several types, each with different characteristics. SLC (Single-Level Cell) NAND flash offers the highest endurance, best performance, and most reliability. However, it is the most expensive per gigabyte and has a lower storage density compared to MLC, TLC, and QLC. SLC NAND flash provides superior performance and reliability but is prohibitively expensive for the large storage requirements of our project. Its lower storage density also means it is not as space efficient. MLC (Multi-Level Cell) NAND flash, on the other hand, offers a good balance between performance, cost, and endurance. It has higher storage density than SLC, making it more suitable for our project's needs. MLC NAND flash provides a suitable balance of cost, performance, and endurance, making it an ideal choice for our project. It offers enough storage capacity at a reasonable cost, and its endurance is adequate for our data logging needs.

TLC (Triple-Level Cell) NAND flash provides higher storage density and lower cost per gigabyte. However, it has lower performance and endurance compared to SLC and MLC, with slower write speeds that could impact real-time data capture. While TLC NAND flash is more cost-effective and offers higher storage density, its lower performance and endurance may not meet the demands of our high-resolution data capturing requirements. QLC (Quad-Level Cell) NAND flash offers the highest storage density and lowest cost per gigabyte, but it has the lowest performance and endurance. Its slower write speeds and lower durability make it unsuitable for our project's needs. QLC NAND flash is very affordable and offers high storage density, but its low performance and endurance make it unsuitable for our project's needs.

3.2.xiii.d Summary

After evaluating the different types of memory technologies, MLC NAND flash emerges as the best choice for our Crab Pulsar Polarimeter and Pulse Timer project. MLC NAND flash offers a good compromise between cost, performance, and endurance. It is more affordable than SLC and provides better performance and endurance than TLC and QLC, making it a cost-effective solution for our project. The moderate write/erase cycles of MLC NAND flash are adequate for our data logging needs. MLC NAND flash offers higher storage density compared to SLC, allowing us to store extensive data within a reasonable physical footprint and budget. This is crucial for capturing and storing the large volumes of data generated by our pulsar observations. Additionally, MLC NAND flash is non-volatile, retaining data even when power is turned off, ensuring data integrity over extended periods, which is essential for our project's long-term data storage needs.

Table 3-29 *Memory Component Technology Comparison*

Specification	NOR	UFS	SLC NAND	MLC NAND	TLC NAND	QLC NAND
Read Speed (MB/s)	70-100	300-1000	100-200	70-150	50-100	30-70
Write Speed (MB/s)	2-10	150-600	50-100	20-50	10-30	5-20
$ per GB (USD)	1-3	0.5-2	1-5	0.2-1	0.1-0.5	.05-0.2
Power Consumption (mW)	10-20	50-100	10-30	20-40	30-60	40-80

Storage density (GB/cm²)	0.2-0.5	1-2	0.5-1	1-2	2-4	4-8

To ensure optimal performance and durability, we can implement strategies such as buffering, wear leveling, and error correction. Using faster memory (such as SRAM) to buffer real-time data before writing it to the MLC NAND flash can mitigate the slower write speeds and ensure efficient data capture. Employing wear leveling algorithms to distribute write and erase cycles evenly across the NAND flash memory can extend its lifespan. In summary, each memory technology has its own set of advantages and limitations relative to our project requirements. SRAM provides high speed and low latency but is costly and occupies more space. DRAM offers very high speed and storage density but is volatile and consumes a lot of power. FRAM provides non-volatility, fast speeds, and high endurance but comes with a higher cost and lower storage density. Flash Memory, specifically MLC NAND flash, balances capacity, cost, and non-volatility, making it the optimal choice for our Crab Pulsar Polarimeter and Pulse Timer project. Its capability to store large amounts of data reliably over long periods, despite slower write speeds, fits well with our project's requirements. This choice lets us meet our performance, cost, and reliability goals, ultimately contributing to our project's success.

With the analysis above, we did not consider how much flash or RAM the ESP32 microcontroller (MCU) supports. As such, we opted to go for an SD card. SD card readers are cheap, making it a cost-effective solution. An SD card is also capable of fast speeds, and they have high capacity. An SD card also comes with the advantage of easily being replaced. We found that our microcontroller does not have support for very much capacity of external RAM or flash. Since there is already an SD card protocol peripheral on our microcontroller, we ended up using an SD card as our memory solution.

Chapter 4 – Standards and Design Constraints

In this chapter, we look at engineering standards, and other design constraints that should be considered when designing our project. Following standards is important, as it allows for interoperability with other products and devices that are readily available.

4.1 Standards

Standards are an important aspect of the engineering world, as they allow for different products to be interoperable with each other. Standards for communication are especially important, otherwise the internet would not work if every country used different protocols! We will be looking at 2 specific standards and how they apply to our project's design. Afterwards, we will be discussing the different design constraints and how we handle them for our project.

4.1.i IPC Standards (PCB)

IPC is a non-profit organization trade association which develops industry standards for electronics manufacturing. IPC is accredited by the American National Standards institute (ASNI). IPC standards are accepted and are practiced globally in electronics manufacturing. Primarily IPC is focused on standardizing PCB, EMS, and OEM products. These standards focus but are not limited to environmental protection, safety and health, and pertinent government relations. Additionally, these standards are practiced ensuring proper functionality and correct design specifications for applications. For example, PCB trace width must be considered and proper PCB insulating material must be used to prevent a malfunction and/or possible danger to the consumer, IPC-2221 General Standard o Printed Board design details the correct trace width for a designated current maximum. IPC standards can be categorized in the following order; Design specifications, Material specifications, Performance and inspection, and lastly flex assembly and materials standards. We must consider what standards are used by the PCB manufacturer and we are currently looking at using the services of PCBWay or Microfab to produce our PCB for the power supply unit as well as our MCU/control board [33].

4.1.i.a Design Specifications

IPC-221 details the most general printed circuit board design specifications but is not the only design standard created. IPC has created many standards regarding Packaging of circuits and many requirements to generalize surface mounting for components. Many high-speed applications have additional standards as well. Lastly, the IPC also has Standardization requirements for electronic diagramming documentation. A few of these standards can be examined in IPC-2612 (documentation), IPC-2142A (high-speed design guide), IPC2251(Packaging of circuits), IPC-7351B (Surface mounting).

4.1.i.b Material Specifications

When manufacturing printed electronic circuit boards materials used in production must meet health, safety, and environmental standards. This means using materials that provide the proper protection, help improve product functionality, and extend the product's lifetime. The standards include Adhesive assembly guidelines, laminate material standards, and many dielectric film standards. These standards include IPC-FC-234 (Adhesives), IPC-4140 (laminate prepreg), and lastly IPC-4202, IPC-4203, IPC-4204 (Dielectric materials).

4.1.i.c Performance and Inspection Standards

These IPC standards put into place acceptability requirements for printed circuit board assembly. The products also must have performance guidelines to ensure the proper functionality of the circuit board. IPC-6011 contains the most generalized performance specifications of printed circuit boards, but addition standards such as IPC-6018 handles performance requirements of high frequency (microwave) circuit boards. Other standards which apply to this label include the wiring requirements for the circuits for both single and double-sided boards (IPC-FA-251, IPC-6202 IPC/JPCA, and PAS-62123).

It is crucial we keep these printed circuit board specifications in mind for the final board construction of this project to ensure proper functionality and safety practices. Following the IPC standards will help us to achieve a quality product that is able to be produced with professional quality design in mind.

4.1.ii IEEE Standards

The Institute of Electrical and Electronics Engineers (IEEE) have their own set list of standards produced by their very own standards association IEEE SA. The IEEE organization develops and creates standards independently from government organizations and bodies. IEEE also has many other departments which handle standards regarding registries, industry connections, conformity assessments, and alliance management services. IEEE SA creates global standards for electronics across the industry including but not restricted to power & energy, internet of things (IoT), biomedical, information technology, and many more emerging technology fields. Mainly the IEEE standards we are largely concerned with are standards relating to information exchange (IEEE 802.6), harmonic control in power systems (IEEE 519), proper component and units (IEEE P80 and 255). Many of the IEEE standards concern themselves with the operation and standardization of networking between devices, i.e., IEEE 802 which contains many subsections regarding the standards utilized for large area networks (LANs) and many IoT specifications for wireless communication (e.g. Wi-Fi and Bluetooth) between devices. In addition to handling many aspects of communication, IEEE standards also have criteria standardizing software. Standards such as IEEE 1471, IEEE 1016, IEEE 1028, IEEE 1044.1 and IEEE 1059 all handle software specifications such as software architecture, design description, reviews and audits, software anomaly classification, and program life cycle. Applying the IEEE standards to our design specifications will help to ensure our development meets regulatory requirements, keeping innovation and best practices at the forefront of the development process, and allow consumers to have trust in the product being developed. If these standards are not followed, there will be some issues in system communication and performance. Following the IEEE standards helps eliminate confusion and keep all segments of the product working together, which is crucial to our goal of an operational prototype and eventually a final product. Overall, IEEE standards are followed to a great length when discussing the design specifications and constraints criteria and must be followed to create a professional end product.

4.1.iii Software Standards

4.1.iii.a Date and Time Standards

Collecting data is an important part of the scientific process, but only gathering information is not enough. Good data handling practices ensure that raw data is collected and stored in a format that is easily readable and usable by any interested parties who wish to make use of it. This is broadly specified by ISO 8601, which provides an international standard for the exchange and communication of data that is contains time and date related information. It provides a system for digital representations of dates and times such that there is no ambiguity in the relevant information. This is particularly important when considering the different formats that countries use for calendar dates.

ISO 8601 states that calendar dates should be stored using four-digit years and two-digit months and days in that order, so that the year is always listed first. It uses the 24-hour time system, provides hours, minutes and seconds in that order. Leading zeroes are always included to avoid ambiguous cases, and separating characters are typically hyphens or colons, though these may be omitted. An example would be: `2024-07-05 15:27:05` for July 5th, 2024, at 3 hours, 27 minutes and 5 seconds after noon (pm). Relevant US standards complying with these rules are ANSI INCITS 30-1997, NIST FIPS PUB 4-2.

It is especially important that we follow this standard given that our instrument will collect time-stamped data to be shared with a larger community and is not meant for solely personal use. Adherence to this standard enables our product to be useful to others, with minimum unnecessary work to be done on their part.

4.1.iii.b Communication standards

A common means of communication between devices is the Universal Serial Bus or USB. It is an industry developed standard, that has become a de-facto standard. Preliminary research showed that there are no ANSI or ISO standards for the USB protocols themselves. The standards are overseen by the USB Implementers Forum, Inc. (USB-IF) which supports the advancement and adoption of USB technology by providing organization for a group of companies [34]. The typical USB connector will have 4 pins, 2 for power, and 2 for data. Type-A is the most popular, with other types having different shapes and sizes. Type-C is one of the newest connectors and was designed for high transmission rates, and high-power transfer. USB is meant to enable high interoperability for I/O devices, such as keyboards, mice, printers, and so on. It is also designed to be ‘plug-n-play’ meaning that a device can be connected at any time and removed at any time without requiring the host/computer to restart. If data is being transferred, it would be wise to wait until it is done before removing the device, otherwise corruption may occur. USB has different standards which specify the speeds, cable length, and power capabilities. The most basic is USB 2.0 capable of up to 480Mbps and 15W of charging power [35].

A bit more common nowadays is the USB 3.2 Standard. Like other USB standards, it allows for fast bidirectional data flow, and is low-cost to make. For USB 3.2, it allows for two lanes of 10Gbps, allowing up to 20Gbps overall without reducing cable length. What is also nice about the standard, is it is backwards compatible with older USB standards. In those cases, it will operate at the lowest common speed between them [36].

4.2 Design Constraints

Design constraints are limitations on how we can design our project. Constraints can take many forms, from environmental and economic, to political and ethical. These constraints act as considerations as we carry out our design. The project as a whole requires that our design adheres as much as possible to the constraints in order to be successful. We will look at a few constraints in detail, and then give an overview of the other constraints.

4.2.i Time

Due to the nature of astronomy final product testing can only be done at night. Otherwise, the sun would outshine our intended target and damage both the telescope and our instrumentation. Working for extended hours overnight will therefore be a requirement, but problematically so. Outside commitments such as work or classes require our team members to be awake and available during the day, which is complicated by additional requirements to be awake and available late at night.

A unique concern of ours is the time of year when we will do our product testing. The Crab Pulsar is not visible in the night sky during summers in the northern hemisphere. It can only be seen from around August to April and is too close to the sun for observation at other times of year. Peak visibility occurs during January. This limitation works well with our development schedule. Summer will be spent doing research, planning, and building a prototype, none of which will require field testing. The middle of Fall is when we plan to have a product ready for sky testing and calibration, at which point the visibility will be suitable to do so.

Similarly, the weather places a potentially severe constraint on us. We cannot do any sky testing if the sky is blocked by clouds. This is especially true during summer months in Central Florida which often have rainstorms several days a week. Again, our schedule works well despite this, and the weather improves as the year progresses. Even with reduced rain, final testing will still be limited by cloud cover. Weather is unpredictable and can change quickly, so it is important that we are able to perform testing even with short notice. Because of this it is exceedingly important that we are ready to make use of any openings as they come up.

We must also consider how the lack of time can impact the timetables for debugging software and hardware connections. Most projects that include programming at any level will have some kind of bug. There are two main types of bugs to be aware of: logical bugs and syntax errors.

Logical bugs occur when the code does not perform as intended, often due to incorrect logic or flawed algorithms. These can be particularly challenging to identify because the code may run without producing any errors, but it will yield incorrect results. Logical bugs often stem from misunderstandings of the problem requirements, incorrect assumptions, or overlooked edge cases. For example, in our project, if the data processing algorithm for our pulse timer has an incorrect calculation, it could result in inaccurate measurements of the pulsar's signals. Such inaccuracies would undermine the integrity of our entire project, leading to faulty data that could mislead subsequent analysis and findings. Logical bugs require thorough testing and a deep understanding of the expected outcomes to diagnose and correct.

Syntax errors, on the other hand, are issues with the code structure that prevent the program from compiling or running. These are usually easier to fix as they are often flagged by the compiler or development environment. However, they can still consume valuable time, especially if they are not immediately obvious or if they arise from complex interactions between different parts of the codebase.

Working with an embedded system also means that the pins must be connected to the correct pins on components. For example, for a 16x2 LCD module, there can be 8 bits for data transfer, or only 4 pins for data transfer. If using only 4 pins, then it must be the D4-D8 pins, and not the D0-D3 pins that are used on the LCD. Making sure we allocate enough time for debugging our connections during the prototyping phase must be a consideration.

By implementing thorough testing, utilizing appropriate tools, maintaining clear documentation, and managing time efficiently, we can mitigate the risks associated with debugging and ensure a robust and reliable system. Recognizing the complexity and potential for issues in embedded systems, our approach must be methodical and well-planned to achieve our project goals within the given constraints.

There is also the concern of how long a custom lens can be manufactured and shipped to us, and as such poses a constraint on time. We would have to have the design fully fleshed out quickly for us to have time to order a lens and sufficient time to prototype with it. This is particularly relevant to our Wedged Double Wollaston Prism, which the polarimeter relies on. This is not a product that is sold by any supplier and is not commercially available in any capacity as an off-the-shelf part. We will need to produce a design of our own to be built by a custom optics manufacturer. But the manufacturing process may take several weeks.

Regarding constructing the demonstrable prototype, we must keep the time aspect of ordering the components as well as the general construction time required to get the prototype in a functional state. Most importantly the bulk of this project is going to be sourced from only a handful of select vendors for electronic components, mainly Thorlabs, DigiKey, and Mouser Electronics. We must keep in mind that it will take at most a few weeks to get components ordered after the initial designs have been drawn up and properly inspected. When ordering components for assembly, we are concerned with using what components are available in stock to ensure a short shipping time. This is mainly being done rather than waiting on a few specific types of components because we are limited to getting this prototype constructed within a month's time due to the shortened length of our given semester. Furthermore, once the components that have been ordered have all arrived, we must construct and take the proper testing measurements to ensure our prototype design is functional and able to be used for demonstration purposes. This allocated construction time requires proper soldering and board assembly to ensure functionality and safety of our product. We must also consider during the ordering of components that we are stocked with enough to build a few protypes, this is to prevent any failures if only one component was faulty. So, what must be considered heavily is the time to construct multiple prototypes and execute procedural testing. With all this time in consideration we must work diligently to achieve our goal.

Another portion of the project that is impacted by the time constraint is prototyping the hardware and optical systems. With only a couple of weeks to build a prototype with the components, we must be sure that our design is solid as we don’t have the time to go back to the drawing board. We also must be good at integrating the different aspects of the project together, as there is still the crunch for time. Concurrently with all this, we still have to write around 16 pages a week as a group to stay on track. As such, the margin for error is small if we are to remain on schedule with the deadlines.

4.2.ii Health and Safety

It is important that no part of the design compromises the health and safety of any individuals working with the instrument, or bystanders. As such, we will make sure no dangerous forms of radiation are emitted, nor any fires started. We will make sure the power supply doesn’t pose an explosion risk due to overheating, or by going over its ratings. Any battery backup source will also be designed to not pose a fire/explosion risk from improper use. The optical components will also be careful not to focus any high energy sources, like the sun or a laser, which could start a fire when focused to a point. Since our design is laser free, the main concern would be having intense light entering the system and getting focused by the strong lenses. As such, we will ensure that the instrument does not point towards high intensity light sources by having a warning label and a cover for the entrance aperture.

Dangerous forms of radiation include X-rays, ultraviolet light, and high-power light from the rest of the spectrum (visible, infrared, microwaves). X-rays are commonly used in medical applications to see through the skin and image bones. They are also the most dangerous due to their energy which can cause cancer or other health ailments. Ultraviolet light poses more of a threat to the skin, which can cause sunburn and cancer. The good news is that there are no sources of this dangerous radiation that will be emitting from our instrument. The only emissions might be radio waves or microwaves (2.4GHz) that are used for wireless communications. While wireless communication is a stretch goal, it is important to consider its effects.

We also want to avoid using any components that have poisonous elements in them, such as lead or arsenic, that are not properly contained. This also includes any acids that may exist in a battery.

We also want to be mindful of the health and safety of everyone when in a laboratory environment. In a lab, there is risk of electrocution, tripping, eye and skin damage from high energy lasers, and if in a machining lab, contusions and loss of limbs. To remedy any problems, we will ensure proper usage of equipment is followed, and if lasers are involved, we will place beam blocks so that the light does not reflect off any surfaces unintentionally. If we also test at the observatory, there will also be the possibility of tripping or falling from stairs or a raised platform.

Part of ensuring the health of everyone is maintained is to ensure that noise levels are kept below safe levels so that hearing damage does not occur. Hearing damage is permanent, and so it is important to provide hearing protection as needed if loud noise is expected. As part of fire prevention, is to design measures to avoid overheating. Simple mechanisms like a heatsink can help remove excess heat by increasing the surface area for air to exchange energy (heat). This can be done passively, or actively by adding a simple fan that blows the air over the heatsink. Ensuring that the heat is dissipated properly will ensure that the components are in their safe operating temperature range, which will reduce the risk of combustion, and the possibility of an explosion.

If a failure were to occur, then it might be prudent to have fail-safe mechanisms that ensure that the device does not snowball into more serious issues. An automatic power shut-off in case of a fault could be one such solution, while a fire shut-off system could be another (in a different use case). In critical applications, building redundancy into the design will help keep the product functioning even after a component fails. In our case, the instrument can be maintained and does not require the redundancy that inaccessible systems need. An example of an inaccessible system are the ones in satellites, as it is costly to attempt a repair in orbit. It is also expensive to even launch a satellite and so reliability and robustness is of great importance.

4.2.iii Equipment Constraints

Final product testing will need to be done using a suitable telescope. For the case of our product, we will need access to a telescope capable of seeing very faint objects since we are focusing on observing a class of objects which emit dramatically less optical power than even a dim star. This requires a large aperture telescope, which itself needs an associated observatory system. Product testing in this case is not something that can be done with amateur astronomy equipment. For this, we will need access to the telescope at the University of Central Florida’s Robinson Observatory, which has a 20-inch diameter telescope and a high precision tracking system that will allow it to detect the Crab Pulsar and maintain its alignment over time. Access to this equipment is limited by the telescope's availability, as others may have to use it for unrelated purposes.

Before the product is ready for on sky testing at the observatory, we will need to put it through extensive in-lab testing. The laboratory is where most of the development process will occur, but this requires some specialized equipment to simulate the needed environment. We will need access to a broad spectrum, pulsed light source to simulate the Crab Pulsar. Dr. Eikenberry will give us access to a supercontinuum laser source, which we can adjust to suit our testing parameters. Others will need access to the supercontinuum laser as well, so we need to ensure that our equipment use does not conflict with other's plans.

Due to the system's high precision, we require some specific parameters for many components. The high sensitivity detectors, variable waveplates, and Wollaston polarization optics are all accessible components that find common use in a wide variety of instruments. The specific parameters that we need make these products difficult to source though. We are unable to use electrooptically variable waveplates since these have unacceptably high retardance variations with wavelength. As such, we conducted more research then adjusted our design to use a mechanically rotating waveplate instead.

4.2.iv Manufacturability

In terms of manufacturability and our design, we want our design to be realizable or producible. This means ensuring that the hardware components exist and can be integrated into the design. In terms of optical components, it puts restrictions on how the lenses are made. Using Zemax to design a lens can result in an unmanufacturable lens if it is not constrained enough or properly. These lenses typically have a small radius of curvature, or not thick enough, so that the edge thickness is a 'negative' distance. Such lenses cannot be made. As such, we will prefer off-the-shelf lenses over custom lenses due to both the potential cost of manufacturing, and the additional time that comes with manufacturing.

Manufacturability constraints apply to the construction of both our prototype module and the final product. We must concern ourselves with how each iteration of the design is going to be constructed and implemented. Firstly, we must construct a prototype of both the power supply unit and the MCU/control unit. Regarding this first iteration, we must have all the correct components sourced and available to begin prototype construction This stage of development will all be handled by our group, and we have no work commissioned out for soldering, connecting, and programming the module. It is key to note that all components used are outsourced by large electronics manufacturers and that we are not developing any individual components ourselves. This module's construction will require components with extremely niche applications and is only provided by a few manufacturers. This is a concern with the optics portion of the scientific module and limits the possibility of large commercial production due to components which may be only developed by only one or two manufacturers. As far as the basic power unit and MCU circuits are concerned, these sections of the module will be easily manufactured because the components required for their construction are in large availability and can possibly be all constructed at a single time by the PCB manufacture in a best-case scenario. The construction of these units is limited by the design constraints we have in place such as the IPC PCB standards to ensure our product is assembled correctly and follows the proper safety requirements for the product's intended application. Additionally, if the PCB manufacturer doesn't allow for our submitted design to be assembled and pre-soldered, the senior design lab will allow us to use commercial grade equipment to properly assemble the circuits. In summary, the manufacturability of our product is heavily dependent on the stock of the component manufacturers and the technologies available.

4.2.v Sustainability

While constructing our project we must be presently aware of how we can develop a product which can be used for many years and provides a long product lifespan. This means that during development and construction of the module we must make sure the design is robust and of solid composition, whilst using materials that are safe and do not pose potential harm to the environment. Furthermore, engineers must seek ways to improve the technology to consume less power or to find new ways to source power from renewable alternatives. To achieve these benefits, selection of components such as the voltage regulators and batteries, must be carefully looked at to minimize power loss. Using RoHS compliant and properly rated components we can ensure the device can last for many sampling sessions. Overall, the sustainability constraints of our project largely deal with power consumption, as the power supply is going to handle many high-current functions. Focus on power loss minimization and proper heat management cannot be ignored when designing the module.

4.2.vi Environmental Constraints

In terms of using components that are environmentally friendly, we will avoid products made with hazardous materials, including our lenses. Regular BK7 glass is made with lead and other toxic materials, but N-BK7 is made without these, and so is a more environmentally friendly choice. Our choice of backup battery will also be made to ensure minimal environmental impact by

Since we are planning on directly observing the Crab Nebula at some point during testing, it is important to consider the environment for when we will view it. A cloudy day or inclement weather would prevent us from performing a real test of the instrument. The intended location for the instrument is to be mounted to a telescope, which usually is in a protective dome. This means our instrument will be protected from the environment when the dome is closed but is still not temperature controlled. This will then constrain the power supply design to ensure that it can operate in such conditions. Furthermore, being mounted to the telescope also requires a certain form-factor for our design to fit into. As such, there is a size constraint, which gave us our goal to minimize the size of the instrument as best we could.

During testing, we will also be constrained by what we have available to us in the labs. It is not feasible or practical to develop and test our system using the telescope in the Robinson Observatory. The reasons for this are that we do not have access to components at the observatory to modify the design if necessary, and as mentioned above, we do not have control over the sky to permit viewing of the Crab Pulsar. Luckily, we will have access to a supercontinuum laser which has the broad spectral characteristics of stars and can be pulsed to simulate a pulsar. This would allow us to test in a laboratory setting.

4.2.vii Economic

It is important to consider the costs associated with the development of any product, whether it is intended for sale to a wider consumer market or meant solely for personal use. Our product is in something of a niche and is meant only for astronomers. As such we should consider keeping the price low enough that a researcher with funding may put it to use, but high enough that we do not sacrifice the overall quality.

This project is planned, designed, and constructed by four college students, and as such personal funding sources are limited. Due to the high cost associated with optics components, the development of optical systems has a high price tag attached. Furthermore, astronomy projects often face significant economic constraints from the cost of equipment that is niche or specialized. This project would not be possible without the support from our sponsor Dr. Stephen Eikenberry, who has provided the required funding for us to build and complete this project.

High sensitivity photodetectors will be one of the primary expenses. The ability to detect exceedingly weak optical signals often comes with a very high price tag of at least one thousand dollars, and frequently several times that. The photodetector technology we originally intended to use would have been cost prohibitive even with sponsored support, and as such we conducted further research to find a product that both our technical and financial needs.

4.2.viii Ethical

Ethical concerns can also play a role in how a project is constrained. How a project's work is developed and used could pose ethical concerns. Some may find weaponization as being unethical, regardless of the circumstance. Others may not like developments that involve testing on animals or humans (as is more common in the medical sense). In our case, our instrument is not designed with the purpose of harming anyone/anything, and so there are no ethical qualms of potential weaponization of our work. Our project's goal is to build an instrument to enable further research on optical pulsars, such as the Crab Pulsar. There are no real classic ethical concerns that we can think of for such a project.

In terms of other the other constraints, we feel that having an instrument that doesn't strain the environment, or harm others is an ethical responsibility. We believe that our work should have integrity to stand the test of time as both a product and design. We want the design to be as robust and correct as possible, so that the product can last as long as it can. We also want our written work to fall under the notion of integrity. This means avoiding plagiarism by citing all our sources, including if that source was AI generated by ChatGPT or something similar. This shows that we investigated the topic beforehand, and it shows how creditable that information is.

4.2.ix Social & Political

Developing and deploying a polarimeter instrument is not limited by political support. The project is funded locally by a university professor who already has the available funding ready to be committed to this project. The goals for this instrument are purely to collect data for future scientific research in physics and astronomy, which aligns perfectly with the University of Central Florida and CREOL's aims as educational and research institutions. Some related technologies, namely infrared optics and detectors, fall under ITAR restrictions. That is, certain components have notable applications in weapons and the defense industry, and their use is strictly controlled as a result. Fortunately, we will not require any technology that is restricted in such a way, and we are free to use the necessary components as needed. All components we are using are publicly available for anybody to purchase.

Social constraints are similarly not an issue. This project has minimal direct relevance to the public as a whole and is only of interest to astronomers or physicists. Among this community though we hope that its application will be useful, interesting, and exciting. As previously stated, funding is already pledged and is not affected by maintaining further interest.

Chapter 5 – Comparison of ChatGPT with other Similar Platforms

In this chapter, we look at how large language models (LLMs), such as ChatGPT, have affected our experience with senior design. We will first look at the pros and cons of these types of platforms, as well as their limitations. Then we will provide a few examples of how using these models has helped us or harmed us.

5.1 ChatGPT

OpenAI's ChatGPT is one of the first large language models (LLM) that have made it to the open market. As a kind of artificial intelligence (AI), an LLM is geared towards being a more conversational program, capable of interpreting text prompts, and responding to them with text of its own. The GPT stands for 'generative pre-trained transformer' and so as a transformer, it operates like a giant linear equation, taking a text as an input and transforming it into a different text as output. This is done using immensely large matrices and performing multiplications with them to get the output. With enough hardware (typically GPUs) for computing, the output doesn't take very long to be generated. Transformers are of course more complicated than suggested above. They mainly address the shortcomings of other AI architectures, like Recurrent Neural Networks and Long Short-Term Memory systems by implementing a self-attention mechanism.

5.1.i Limitations

The main limitation of these LLMs is that they require to be trained with new data before they can be fully utilized. Training requires that the data is labeled, in this case, for input text, there should be a specified output text. This brings up another limitation, which is how recent it's knowledge base is. Without direct access to the internet, these models may not have the must updated knowledge available to it. While this may change over time, it can still be a limitation of their ability.

Another limitation is that LLMs are limited to text-based information. While there is research into making AI that can deal with image and/or audio generation, they have not made it into the public's hands just yet (for free).

5.1.ii Pros and Cons

With the limitations of LLMs in mind, we look at some of the general pros and cons of their use for engineering projects. Later we look at more specific examples of our experiences with using them.

5.1.ii.a Pros

There can be many pros for using a generative AI like ChatGPT, as it can potentially answer any question or prompt that it is given. Specifically, as a research starter, ChatGPT does a decent job. For example, while doing our parts comparisons, it is rather easy to start the research by identifying viable technologies, which can be done quickly with one prompt. We can then follow up with other prompts for more information. While this can be done with a search engine, we would have to have multiple searches to have the same breadth of information and go to multiple websites to ensure reliable information. Of course, ChatGPT is not always reliable, and so that is why it is good to start preliminary research, where the intent is to go and search for creditable sources after the fact. An example as a research starter is given by the prompt in [GPT-A].

Some other benefits are the increase to efficiency and productivity that comes with using an AI to generate large volumes of text very quickly. This text is generated based on the inputs given to it, and due to its speed, reduces the time and effort by the engineer required to complete documentation. The time that is saved allows the engineer to spent more of their time on actual design tasks, which an AI cannot do (at least not reliably). Another benefit is that generative AI can be taught to use specific terminology and formatting throughout the documentation, increasing the consistency of the written work. This is especially useful if it (AI) is used for multiple different documents, as it may be hard for a human to maintain the same styles from one document to the next. AI is also better at identifying errors in the text and correcting them which would reduce misinforming the reader. [paraphrasing from GPTB]

Additional benefits include being able to use the AI to tailor the content for different audiences. Being able to simplify a technical document for stakeholders or consumers helps save the engineer even more time as it takes more thought (and time) to come up with simpler ways of explaining a concept. By using the AI in this way, it makes the document more accessible to a broader range of readers. And with multiple documents and sources, AI can more easily integrate and cross-reference them to produce a more comprehensive and cohesive overview for the entire engineering project. [GPTB]

As to our specific experiences with using generative AI, such as ChatGPT, if it is used in proper scenarios then it is a very beneficial tool to have at our disposal. It does a good job at getting us motivated by providing a good starting point for research and can help save us time when writing about tedious topics.

5.1.ii.b Cons

On the other side, there are some cons to using generative AI. The main drawback is not knowing the exact source of the content/response of the AI. Even if all the source material is tracked, generative AI works by predicting characters or words in a sequence based on previous words in the sentence. As such, we can never know the true source of the generated content despite the predictions coming from training data. If the data is flawed by being biased or by not being enough, the generated content can produce incorrect or misleading information. As such, for critical written content, a thorough human review should double check any AI generated content, which would reduce the benefit of using the AI by taking up time [GPTC].

One example is when trying to think of some constraints for engineering projects. While we had a broad overview, we also need to have more details. Using ChatGPT for some examples of health and safety constraints for an electrical engineering project resulted in constraints that relate more to the construction of buildings than the design of a project. For example, it referred to following OSHA guidelines, insulating cables, installing fuses or breakers, using fire suppression systems, fall protection, and so on. Similarly, it took considerable prompting for ChatGPT to provide optics related standards that are relevant to optical design. Most responses were focused on ophthalmology, human vision, and eyeglass lens standards.

Some other issues with using generative AI for engineering documentation, is that the AI lacks deep contextual understanding, despite the recent advances in the technology. Engineering topics and concepts can be very complex, intricate and nuanced, which makes it hard for an AI to pick up on the underlying meanings. High-quality documentation requires depth and specificity, as engineers need to convey their methodologies, troubleshooting, and technical specifications. AI does not yet have the level of expertise or contextual awareness to produce such documentation, instead producing generic or superficial documentation. [GPTC]

Of more concern to academia, is the effect of over-relying on generative AI for writing. If engineers (or anyone) use AI extensively, they are no longer committed to critically thinking about what is being written. This can result in a loss of expertise for communicating technical information, which is a big part of engineering. There are a lot of complex technical problems that engineers must solve to produce a product, and being able to communicate effectively with a team is a must. Therefore, a balance must be struck with using AI to boost efficiency and save time, and with preserving human expertise for effective communication of technical ideas [GPTC].

There is also an ethical aspect to the use of generative AI. Since AI requires specific inputs, it will require data on the project, and if it is sensitive data, then there are concerns for the security of this data. Ethical handling of this information is important, perhaps not so much for a senior design project, but would be imperative when working for a company in the future. Part of the ethical concern is how biased AI data can be, as it is important to remain objective in our writing [GPTC].

5.1.iii Effects on Senior Design

As a newly developed and still actively developing technology, the status of LLMs as productivity tools is not yet solidified. In this section we will look at some of the major benefits that come from using LLMs along with any associated downsides to their use.

5.1.iii.a Benefits and Downsides of Research Using LLMs

LLMs have access to immense quantities of data which they use to generate their responses. This makes them potentially valuable research tools.

Outside of data they were initially trained on, modern LLM products have direct access to the internet, allowing them to search for specific information that the training data may not be equipped to handle. This is useful in that it outsources much of the research work to an automated tool since the AI model can dig through the internet for information relevant to the search query. This can save a lot of time for us as Senior Design students, since research and searching for relevant information is a major portion of the work that needs to be done. Automating this process would give us more time to focus our efforts on other, non-automatable tasks, such as engineering design. Theoretically, by being able to spend more time on planning, design, and implementation work would boost the overall quality of the final product.

Using LLMs for research comes with risks, however. As we have experienced personally and will see examples of in the following section, information given by LLMs may be somewhat or entirely inaccurate. The generated response can contain information that is not true but is still provided with confidence as if it were. This poses a serious problem for using AI tools in any stage of the Senior Design Process. To add to this, models such as ChatGPT have recently added a feature where citations for information are given along with the response. Unfortunately, these citations suffer from the same issue where the source is of limited or no relevance to the desired information. We cannot use any information from an LLM response without doing further research independently to confirm its validity. Ultimately, this solidifies LLMs of any model as a supplementary source, rather than a primary research tool. Their primary usefulness would be for broad, initial summaries of topics that can direct us going forward.

Also, outsourcing the research process can harm our overall understanding of the field we are working in. As students and engineers, it is important that we continuously maintain and grow our knowledge in our field. Part of that involves doing research on our own, and familiarizing ourselves with the field as a whole, and not just the specific pieces that are immediately relevant to our work. Using AI to filter through and provide only the most directly relevant information denies us the opportunity to learn about potential alternatives, broaden our understating, and make connections between distinct technologies.

5.1.iii.b Benefits and Downsides of Image and Graphic Generation

A less utilized function of new AI tools is generating images and graphics. LLM chatbots like ChatGPT are not capable of producing graphics on their own. A recent development in AI products is the integration of AI image generating tools with existing LLMs. Some popular models are DALLE-3 and Stable Diffusion, which can produce a huge variety of images from a user's prompt.

Image generating AI, in spite of advancements, faces several practical limitations that affect output quality. A major constraint is the dependency on input training data. This is less of an issue for LLMs, as the quantity of text-based training data available on the internet is many orders of magnitude larger than training data for images. The variety of images that exist to be trained on is simply more limited. In images, the overall structure in addition to the specific content is entirely dependent on the information supplied with the prompt. This can lead to issues where image generating AI is incapable of providing the user with a desirable product as a result of it being unfamiliar with the subject. As such, the use of image generating AI models is going to be of limited use for us as engineering students engaging in a complex and specific design process. Technical diagrams, schematics, or even prototype mockups are outside the capabilities of current technology. The use of image generating AI in Senior Design would ultimately be detrimental to the quality of our work.

5.1.iv LLM Comparisons

Part of our research in writing this paper and designing our product includes using LLMs, which has been simultaneously useful and problematic. In this section we will provide specific examples of some previously discussed issues, in the form of a prompt given to different LLM models, their responses, and our comments on its validity.

5.1.iv.a LLMs in Part Selection

In this section we assess the quality of ChatGPT responses regarding specific components. We prompt the model to provide us with a general overview of a specific product, along with detailed specifications.

- **Prompt:** *Write about the Edmund Optics 39-033 half wave plate. Provide specific Information as well as a general overview.*

- **ChatGPT Response:** *The Edmund Optics 39-033 half wave plate is a high-performance optical component designed for precision applications within the 600 nm to 800 nm spectral range. This waveplate is constructed from high-quality crystal quartz, which ensures its durability and stable performance under various conditions. The clear aperture of this waveplate is 0.5 inches (12.7 mm), making it suitable for accommodating beams with diameters up to 12.7 mm. This feature is essential for many optical systems requiring precise control of polarization states.*

  One of the key specifications of the 39-033 half wave plate is its retardance accuracy, which is crucial for ensuring that the phase shift induced by the waveplate closely matches the desired half wavelength (180 degrees) for the specified operating wavelength. The waveplate exhibits a high transmission rate, with a minimum transmission of approximately 95% and a maximum transmission close to 98%, making it ideal for applications that require maintaining high transmission efficiency. Priced at around $332.00, this waveplate offers a cost-effective solution without compromising on quality, making it a valuable addition to various optical setups (Edmund Optics) (Edmund Optics).

Comments:

- The information it provides is not accurate. The waveplate in question has a spectral range of 450 nm to 650 nm, but the response provides 600 – 800 nm. Other key details are also wrong, such as the price and clear aperture.

- The citations provided are at best tangentially relevant to the product mentioned in the prompt.
- The overall structure of the response is well written, and clearly conveys information, even if it is inaccurate.

This response is a prime example of a major issue with LLMs. They cannot verify the information that they provide in their responses, resulting in them possibly providing users with objectively false information. The price, clear aperture, and wavelength specifications are all completely incorrect. The product price is three times higher, the clear aperture is nearly twice as large, and the spectral ranges barely even overlap. This indicates that ChatGPT is not a reliable source for product information, and that any given information should be personally confirmed by the user before using it in technical documentation. However, this may be somewhat difficult, as even citations provided are links to the wrong product pages, and overly general background information, neither of which can be used to double-check information.

- **Gemini Response:**
  The Edmund Optics 39-033 is a specific model of a half wave plate, a type of optical component used to manipulate the polarization of light. Here's a breakdown of its key features:

  General Overview

  - *A waveplate introduces a specific phase delay between two orthogonal polarization states of light. In the case of a half wave plate, the delay introduced is half the wavelength of light traveling through it. This results in a specific rotation of the polarization ellipse.*

  - *Half wave plates are used in various applications including:*
  - *Linear polarization generation: By placing a half wave plate behind a polarizer, light emerges linearly polarized.*
  - *Polarization modulation: By rotating the waveplate, the polarization state of light can be continuously varied.*
  - *Polarization analysis: Certain optical setups can analyze the polarization state of light by observing its interaction with a waveplate.*

  Specifics of Edmund Optics 39-033 Half Wave Plate

  - *Material: Crystal Quartz*
  - *Waveplate Type: Zero-Order Half Wave Plate (designed for minimal wavefront distortion)*
  - *Wavelength Range: 450 nm - 650 nm (achromatic - works well over this broad wavelength range)*
  - *Clear Aperture: 1 inch (25.4 mm) diameter*
  - *Surface Quality: Excellent surface flatness - less than λ/10 at 633 nm over 80% of the diameter (λ refers to the wavelength of light)*

- *Wavefront Distortion: Minimal wavefront distortion - less than λ/20 (peak-to-valley) at 633 nm over 80% of the diameter*
- *Thickness: 3.1 mm ± 0.1 mm*

Additional Notes

- *The Edmund Optics 39-033 is a high-quality waveplate suited for demanding applications requiring precise control of light polarization.*
- *Its achromatic design makes it particularly useful for applications where a wide range of wavelengths is used.*
- *The price of Edmund Optics 39-033 is around $980 (single unit).*

I hope this information is helpful! If you'd like to learn more about waveplates or their applications, feel free to ask.

Comments:

- The provided information is mostly accurate.
- The citations are relevant in general. Many pieces of information are not cited properly or at all.
- The response is not structured as a written paragraph and is instead a bulleted list of product information with pieces of supporting text.

This response from Google's Gemini LLM is significantly better than the response from ChatGPT. Primarily this is because the information is mostly correct. For most of the crucial performance specifications the LLM response matches with the product information given by the supplier. The citations are better than ChatGPT as well, but not by much. The in-text hyperlinks it provides link to overall product landing pages rather than the specific location where information can be found for double-checking purposes. Additionally, some information is not cited at all. For example, the response's Wavefront Distortion number is not a listed product specification, and no citation is given for where the data came from. This makes it very difficult to trust the validity of information provided by this LLM, despite it being something of an improvement over other models.

Chapter 6 – Hardware Design

In this chapter, we will look at the physical designs for the project. This includes the optical components and their design process, as well as the electrical hardware, like the power supply regulator circuits. We also include the physical aspects of the microcontroller, like which pins are connected to the various components for control.

6.1 Optical Design

Our optical design can be broken down into two areas: the polarimeter, and the image acquisition system. The image acquisition system involves taking the light from the telescope, splitting it into two paths, one for imaging and the other for the polarimeter. The imaging path itself is broken into two paths, one for tracking and the other for imaging the telescope's pupil/aperture for alignment. The polarimeter splits light into two pairs of orthogonal polarization components, each with its own beam path. Additionally, we tabulate the losses of optical components along each beam path in the system.

6.1.i Image Acquisition System

The responsibility for the image acquisition system is to couple the light from the telescope, image it, and collimate it for the polarimeter, all while minimizing optical power loss, and maintaining low aberrations. To lower power loss on reflections, anti-reflective coatings will be used on the lens's surfaces. The target range is in the visible spectrum, so 400-700nm ideally. Some manufacturers have broader coatings running from 400-1000nm which may also be used. The design process begins by using paraxial approximations to work out the general location of components and their desired focal lengths. One of our goals is to keep the size down as well. To minimize variables, we look at using lenses of ½" and 1" diameters (12.7mm and 25.4mm, respectively), and using standard focal lengths, such as 20mm, 25mm, 50mm, etc. This will make it easier to design and order the lenses.

6.1.i.a Paraxial Design

In this first iteration of the design, paraxial approximations and equations are used for working the design out. Some of these equations are listed below. The first one is the Gaussian Imaging equation for thin lenses, which relates the focal length to the object and image distances. The second one is the thick lens' makers equation. The 3rd one is Gullstrand's Equation, which works for a thick lens with surface powers K_1 and K_2 separated by distance *d*, or with two thin lenses of powers K_1 and K_2 separated by distance *d*. Additionally, the equation for f/# (f-number) also helped design for the diameter, or height of light rays.

$$Eq.\,6\text{-}1\!: \frac{1}{f} = \frac{1}{u} + \frac{1}{v}$$

$$Eq.\,6\text{-}2\!: \frac{1}{f} = (n-1)\left[\frac{1}{R_1} - \frac{1}{R_2} + \frac{(n-1)d}{nR_1R_2}\right]$$

$$Eq. 6\text{-}3: K = K_1 + K_2 - K_1 K_2 d$$

$$Eq. 6\text{-}4: f/_{\#} = \frac{f}{D}$$

These equations help with finding the appropriate focal length or lens to use. There are a lot of initial variables for the design. These are mainly the location of components, as well as their focal lengths. To aid in the paraxial design, some distances are fixed for convenience. The main consideration for this phase of the design is keeping the overall footprint of the components as small as we can without compromising imaging quality. The fixed distances are mainly mirror placements that would allow enough room for optical components to fit between them. There are four-fold mirrors involved, two of which will be on flip mounts that allow light to continue past them.

One of the initial design ideas was to instead use a lens that would change the focal point of the first coupling lens, so that only one component would need to be flipped into the optical path. The lens by itself would image the output of the telescope, while the combination of the additional lens made it so that it would image the telescope's aperture, which is farther away when compared to the telescope's output image. While this design held promise, using a singlet plano-concave lens would add too much chromatic aberration to the pupil imaging, as well as spherical aberration. To correct for chromatic aberration, a negative achromatic doublet could be used but was not explored.

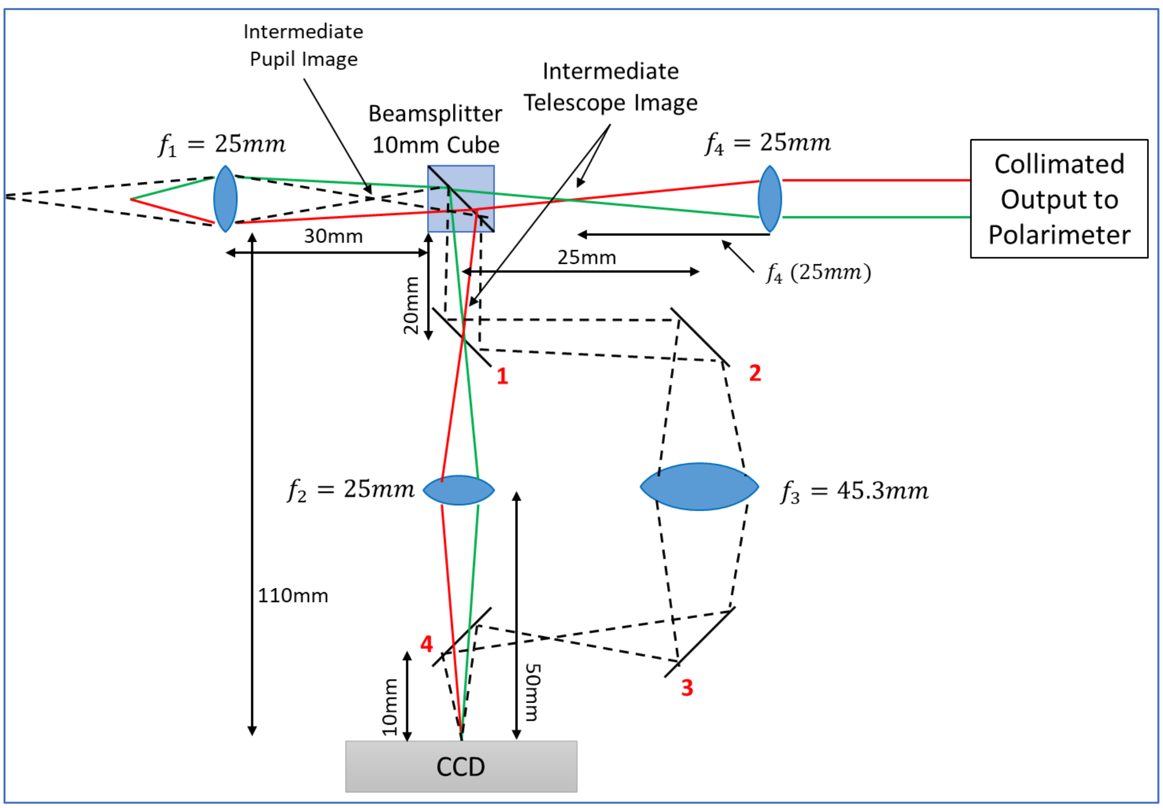

Figure 6-1 – Intermediate paraxial design for the image acquisition system. Red numbers denote the mirror number for reference in the text.

The main design using fold mirrors to have a second imaging path is initially sketched in Figure 6-1. Since we want to use ∅1/2" optics where possible, the only achromatic triplets available were from Thorlabs, which had only one focal length of 20.4mm. Since these offer the best performance in one lens for chromatic aberration, and are nearly diffraction limited by themselves, they are chosen for the coupling optic, and the tracking image path. They make two kinds, one for finite conjugates called a Steinheil triplet, and one for infinite conjugates called a Hastings triplet. The exact Steinheil lens is TRS127-020-A, which has Thorlabs' A-coating for 400-700nm (visible) operation. With these selected, along with the size of the beamsplitter being 10mm, we can find the distances for the tracking image path. The working distance for the Steinheil is 37.3mm from the back of the lens, and so for 1:1 imaging, we want lens 2 (from figure 6.1) to be 37.3mm from the intermediate image and 37.3mm from the camera/CCD. This gives us an initial constraint for the position of the CCD from the beamsplitter to be 95.46mm, given that the intermediate image is 10.83mm from the beamsplitter cube. This is found because the distance from lens 1 to the beamsplitter is fixed at 20mm. The effects of the beamsplitter on focused light would be to add a transverse shift to the light's position at the end of the beamsplitter cube. Zemax is used to get the intermediate image position, as the paraxial calculations disagreed due to not accounting for the shift mentioned. To get the shift amount, ray tracing is required to get the angle of incidence onto the beamsplitter, and then using the following equation: $L = \frac{d \sin\theta_i}{\sqrt{n^2 - \sin^2\theta_i}}$. This is derived from using Snell's law and using geometry (or trigonometry) for a parallel plate of thickness d.

With all the distances initially constrained, we can calculate using the Gaussian imaging formula (eq. 6-1), the approximate focal length required of lens 3. For this, we start with placing the mirrors in a way so that they do not interfere with other components. We also find the image location for an object that is farther away from the first lens. Initially we use 500mm, but later it is increased to 1000mm in Zemax. When the actual distance is known, updating it in Zemax and then optimizing will update the distances/placement of the optics. The image location is then 21.27mm from the principal plane, which is roughly 3.3mm from the edge. The distance from the beamsplitter is then $20\text{mm} - 17.92\text{mm}$ or 2.482mm. For a lens placed roughly in the middle of the 2nd and 3rd fold mirrors, we can add up the distance before the lens to the intermediate image, and the distance after the lens to the CCD to find the focal length. This gives $u = 2.482 + 10 + 20 + 25 + 25 = 82.482\text{mm}$, and $v = 25 + 25 + 12.3 = 62.3\text{mm}$. Thus, the approximate focal length for lens 3 is $f = \left(\frac{1}{u} + \frac{1}{v}\right)^{-1} = 35.45\text{mm}$. A singlet lens with a focal length of 35mm is then used and analyzed in Zemax.

For lens 4, we want the output light to be collimated, so we match the focal length, or working distance for a thick lens to be the distance from the intermediate image. For the best achromatic performance, a Hastings triplet is used, which has a working distance of 15.9mm.

For the final design, the approach remained the same, but more time was spent in the paraxial design phase. The main purpose of the redesign was to account for using a pinhole mirror and to avoid adding optics before the waveplate. The pinhole mirror requires the light from the telescope to be placed at the telescopes focus, which changes the placement of the lenses. Having optics in front of the waveplate would add additional polarization defects to the data we want to collect. Minimizing the effects in the first place is good practice. The redesign itself even went into a few iterations to explore different ideas.

The first step of the redesign was to recreate a paraxial version of the telescope in the Robinson Observatory. From equations on the manufacturer's website, the radius of curvature and conic constants of the primary and secondary mirrors can be found. This allowed us to more accurately determine performance characteristics of our design when optimizing it in Zemax. Having the prescription also meant having a more accurate way of finding the exit pupil of the telescope. In the paraxial redesign phase, the design was constrained based on fitting the images onto the camera's detector, which was around 4.3 mm by 7 mm. Images are circular, and so an image size of 4 mm was designed for. From the first iterations of design, it was planned ahead of time to incorporate multiple lenses, as splitting optical power between multiple lenses reduces aberrations.

6.1.i.b Zemax Design and Optimizations

Once the general layout was designed, it was put into Zemax to analyze the performance. The initial design is plagued mostly by spherical aberration and defocusing between the two imaging paths. The defocus is caused by forcing the two paths to have the same image plane. This is fixed by properly constraining the different configurations of the design. Getting the proper constraints took the most time in designing, as well as the trial-and-error of selecting various focal lengths for lenses before the system was properly constrained.

From the desired focal length for lens 3, a system is designed with an effective focal length of 36mm that has better spherical aberration. Initially, this was to use meniscus lenses to help split the light bending power needed, which would decrease the spherical aberration. Eventually, aberrations were near diffraction limited, but chromatic aberration was a problem, despite using an achromat with two meniscus lenses on either side (Figure 6-2). Taking this subsystem and incorporating it into the main design resulted in worse spherical aberration, due to the light hitting more of the lens. It was also hard to optimize it as it needed to take up a certain amount of space/distance between the 2nd and 3rd fold mirrors. The savior was a constraint known as TTHI, which sums all the thickness between two surfaces, and forces it to be equal to a specified value. This allowed for improvements to spherical aberration, but the solution still had too much chromatic aberration.

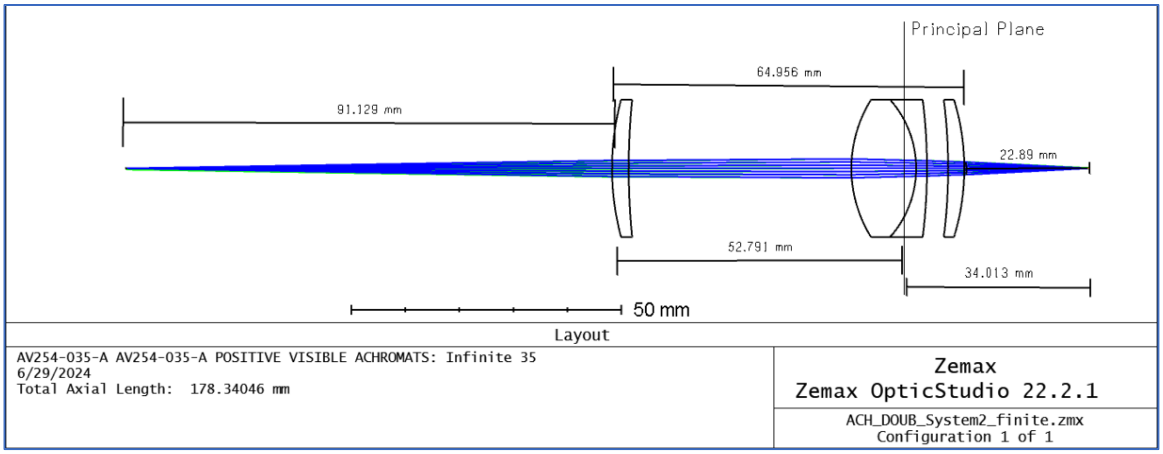

Figure 6-2 *- Zemax layout of optimizing 35mm effective focal length system.*

The next major revelation to the design was allowing the distance between the 1st and 2nd fold mirrors to be variable, with a pickup for the distance between the 3rd and 4th fold mirrors. This helped to get the two paths to have the same image plane without defocusing one or the other. The final revelation was to use two achromatic doublets in a symmetric design so that aberrations would cancel. Using the two achromats made chromatic aberration less of a concern, and the symmetric design brought the spherical aberration down to around 2.5λ (wavelengths).

The initial final design is shown in Figure 6-3 below. The final aberrations are tabulated in Table 6-1 below for the different paths. In the first design iteration, spherical aberration was minimized to near diffraction-limited spot size. For the tracking imaging path, spherical aberration was 1.304λ (wavelengths), giving an RMS spot size of 6.001µm or a GEO size of 17.142µm where the airy disk (diffraction-limit) is 3.851µm. The focal shift from chromatic aberration is defined as the focal point difference between the F- and C-emission lines of hydrogen (486.1327nm to 656.2725nm). The diffraction limited spot size is determined by the focal length and diameter of the lens (the f/#). For the polarimeter path, since it is an afocal system (collimated light) the spot size looks at the angular spot in milliradians (mr). The focal shift is then described using units of optical power (diopters or m^{-1}).

Table 6-1 *- Aberration Summary of 1st image acquisition system design.*

	Polarimeter Path	**Tracking Image Path**	**Pupil Image Path**
Spherical Aberration	0.531λ	1.304λ	3.605λ
RMS/GEO spot size (Airy disk size)	0.199mr / 0.388mr (0.2627mr)	6.001µm / 17.142µm (3.851µm)	6.64µm / 13.48µm (2.85µm)
Focal shift (diff. limit)	0.1803 diopters	61.03µm (67.85µm)	176µm (37.1µm)

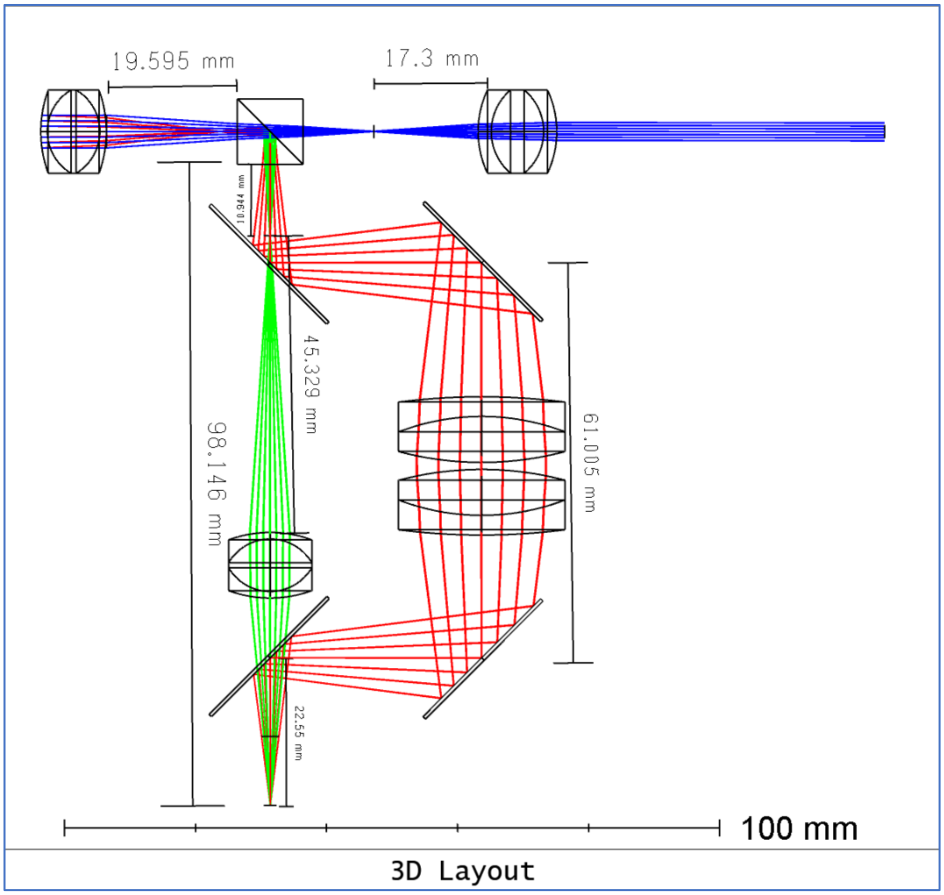

__Figure 6-3__ – 1st iteration of the image acquisition system, with a pupil imaging path to ensure alignment with the telescope.

For the final redesign of the image acquisition system, we took our paraxial pre-design and put it into Zemax. Before we could begin optimizing, many constraints had to be added to ensure that the design remained valid. Among these would be the magnification of the two imaging paths and the total distance between the two imaging paths (to ensure both image to the same plane). These were accomplished using the DMVA and TTHI merit function constraints. The final design uses the 4-fold mirrors from the previous design to implement the alternate pupil path. The main imaging path used for tracking is denoted as the star imaging path, while the other path is called the pupil imaging path. The final design is shown in Figure 6-4 below. A summary of the performance of the system is given in Table 6-2. The lenses chosen were Thorlabs AC127-050-A-ML (∅0.5” f = 50 mm), AC254-050-A-ML (1” 50 mm), AC254-0750-A-ML (x2 1” 75 mm), and AC254-100-A-ML (1” 100 mm). All are ‘A’ coated for 400-700 nm operation and mounted in SM1 or SM05 adapters.

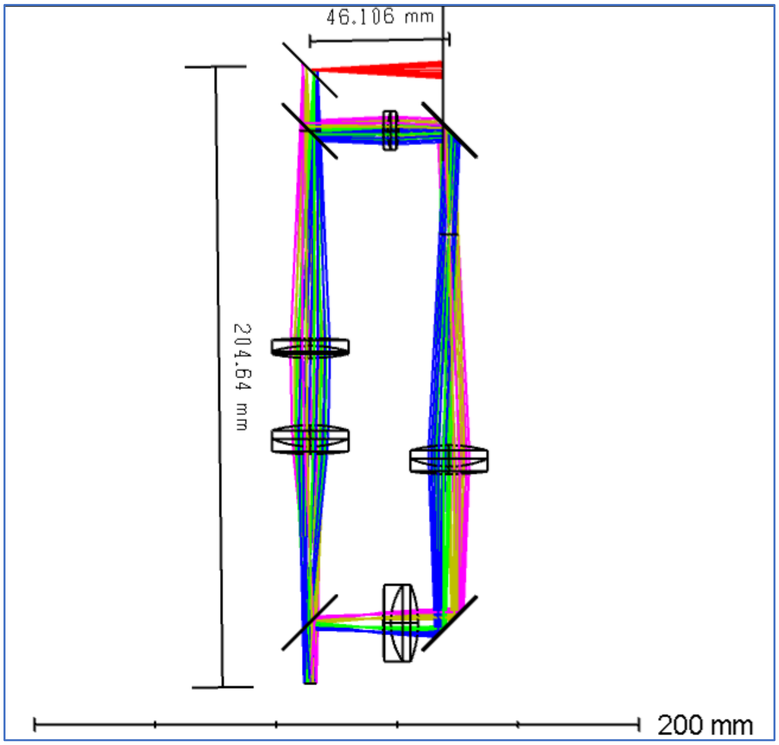

Figure 6-4 – Final image acquisition system design. The full field is shown, where each color is a different field angle. The maximum field angle is ±2 arcminutes shown in blue and magenta.

Compared with the original design, the final design has much better performance. Both fields have lower spot sizes near the diffraction-limit, and less spherical aberration. Despite using achromatic lenses, there ended up being more chromatic focal shift. This is likely caused by using achromats with similar materials, and so the small amount of chromatic aberration for each lens would stack up.

Table 6-2 – Performance metrics for the final imaging system design. The metrics are for the star (tracking) imaging path. The primary wavelength is at 588 nm.

Metric	1' field	2' field
RMS Spot Size	4.408 μm	6.3 μm
Diff-Limit Spot Size	5.043 μm	5.043 μm
Chromatic Focal Shift	214.95 μm (Diff-Limit: 116 μm)	
Spherical Aberration	0.377 λ	
Coma	-0.367 λ	
Astigmatism	0.457 λ	

6.1.ii Polarimeter Design

The polarimeter is the primary data collecting subsystem. As a linear Stokes Polarimeter it can measure the three Stokes parameters needed to quantify the linear polarization state of light. All components are designed for consistent performance over the 400 to 700 nm spectral range of our observation target. The first step taken in designing the polarimeter is determining mechanical and geometric constraints to know where components can be positioned. This concern originates primarily from the large size of our photodetectors relative to the other optics, and the divergence angle of Wollaston prisms. Additionally, we consider the active detector area since this creates limits on beam diameters. Using this information, we can then calculate the beam divergence requirements of our wedged double Wollaston prism.

The initial polarimeter design made use of four photodetectors, a Wedged Double Wollaston prism (WeDoWo), and a rotating half wave plate to collect high resolution polarimetry data. The key component in this design is the WeDoWo, which, like the typical Wollaston prism, splits light into ordinary and extraordinary polarization components. The WeDoWo is special in that there is a second prism with differently aligned crystal axes, producing four output polarization states. Additionally, the front face is cut at an angle to further separate outgoing beams. This produces four distinct beam paths with unique polarization states (0°, 45°, 90°, and 135°). Each beam path ends upon a detector, and the differences between the measured signal from each detector can be used to calculate the three linear Stokes parameters.

A critical issue in polarimetry is the polarization inherent to optical systems, and in astronomy, the atmosphere itself. This is an issue that cannot be solved through simple calibration as the environmental and instrumental polarization change over time. By rotating a half wave plate at a rate faster than this polarization shift, we can effectively negate the effect this has on our measurements. The ideal location for the HWP is early in the optical system, before any other optics

6.1.ii.a Pre-Design Considerations

The first step in the design of this polarimeter is to consider the overall limitations, and how they influence each other. The overall geometry of the system will be our starting point. The Thorlabs PDA44 SiPM Photodetectors have a length and width of 53.3mm by 52.9mm, respectively. The active detector area for each of these components is a 1.3mm square.

One issue with our choice of detector technology is that the responsivity is not constant across the active area, due to unavoidable imperfections in the manufacturing process. If the entire optical system was motionless this would not be an issue since the focused spot would never move along the detector. As an astronomy instrument, our device will be mounted onto a telescope that is constantly moving to stay pointed at the Crab Pulsar. Star tracking with any telescope is never exact, and there will be constant adjustments and atmospheric turbulence, shifting the position of the light source over time. Imaging the pupil onto the detector mitigates this issue, since the pupil position will be constant, only the incident ray angle will vary as the telescope moves.

Despite the presence of the pinhole mirror which deflects most captured light away from the polarimeter, the relevant system aperture is still that of the telescope. This is because the entirety of the signal meant for the polarimeter will pass through the pinhole mirror unaffected. Additionally, we must consider the defocus introduced by planar elements. These are the half waveplate and Wedged Double Wollaston prism itself.

Table 6-3 *– Overall Polarimeter Design Constraints and Considerations*

Parameter	Value
Prism Internal Interface Angle	3.5°
Wedge Angle	3.05°
Prism Absorption Loss	$\alpha = 0.004\text{cm}^{-1}$
Photodetector Dimensions	2.08" Width

6.1.ii.b Collimating Lens and Half Wave Plate Design

The first design decision made was to place the achromatic half wave plate before any other polarimeter optics, including any telescope coupling optics. Otherwise, it would be unable to correct for instrumental polarization originating from earlier optics. Immediately after is the EFL 60mm collimating lens. This focal length was chosen as a tradeoff between beam diameter and system length. When considering the F/8.2 input beam, a 60mm lens creates a beam diameter of approximately 7.3mm. This is sufficiently large for quality pupil splitting, without excessively large mechanical requirements.

Positioning this lens required us to account for lateral defocus introduced by the half wave plate. The AHWP10M-580 is 6.1mm thick and constructed from crystalline quartz and UV sapphire.

6.1.ii.c Wedged Double Wollaston Prism Design

The Wedged Double Wollaston Prim consists of Wollaston prism with its front face cut into a wedge. This is then mirrored across the optical axis. The key parameters of each half of the WeDoWo are its beam separation and ordinary divergence angle. The ordinary divergence angle is the angle of solely the ordinary ray from the optical axis. This must be positive to avoid overlap with outgoing rays from the other half of the prism and is determined mainly by the wedge angle. Separation angle is the angle between the outgoing ordinary and extraordinary rays, determined by the material birefringence, and interface angle.

Maximizing divergence angle necessarily increases chromatic dispersion as well. Due to the overall geometry of the WeDoWo, it is not possible for the chromatism introduced by the front wedge to be corrected by other parts of the prism geometry. As such, we designed a minimally angled front interface that is still able to provide an adequate divergence angle that outgoing rays remain separate.

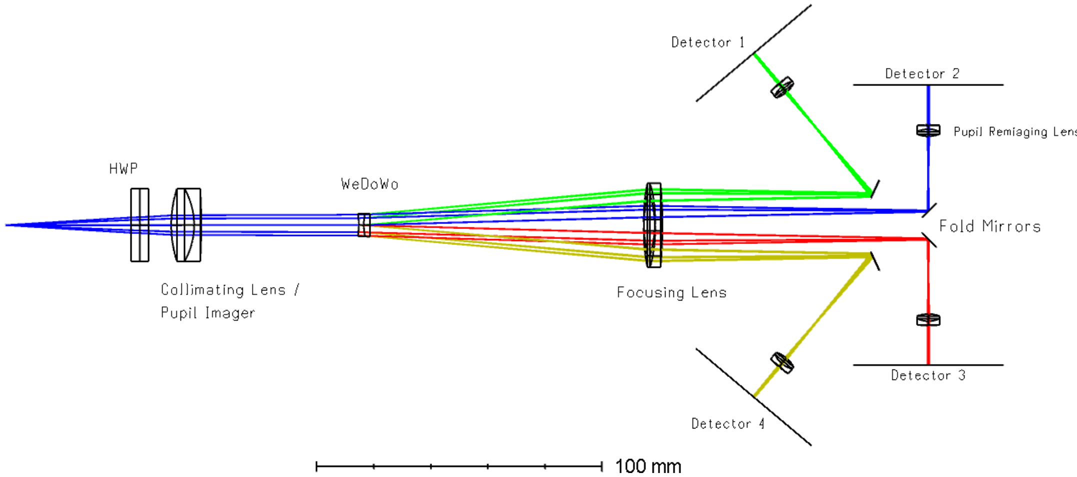

Figure 6-5 *– Initial Polarimeter Design, light enters the system from the left. Different colors represent distinct polarizations. The final polarimeter design is discussed and shown below.*

6.1.iii Polarimeter Redesign

Due to significant delays on the supplier's end, we would have been unable to receive our custom WeDoWo in time for Senior Design 2. After some months of delays in discussions with the manufacturer, we received a quote and an estimated delivery date in mid-December, several weeks after the product was needed. This forced us to redesign the polarimeter such that it no longer relied on any custom optical components.

The primary functions of a WeDoWo are to split light at the pupil and separate it into 0°, 45°, 90°, and 135° polarized rays. The replacement components must do the same. In our redesign, we determined that the best way to pupil split was using a mirror angled at 45°, intersecting with only half of the incoming beam. This deflects half of all incoming light, while the other half passes through unaffected. We accomplished polarization splitting using two regular Wollaston prisms. One prism oriented horizontally produces the 0° and 90° beams, while another, rotated by 45°, produces the 45° and 135° beams. Because of a completely unrelated, but similarly stressful and infuriating, series of supply issues, the polarimeter uses both a ThorLabs WP10-A and a Newport 10WLP08AR.14 Wollaston. Despite being different products, these two components are effectively identical.

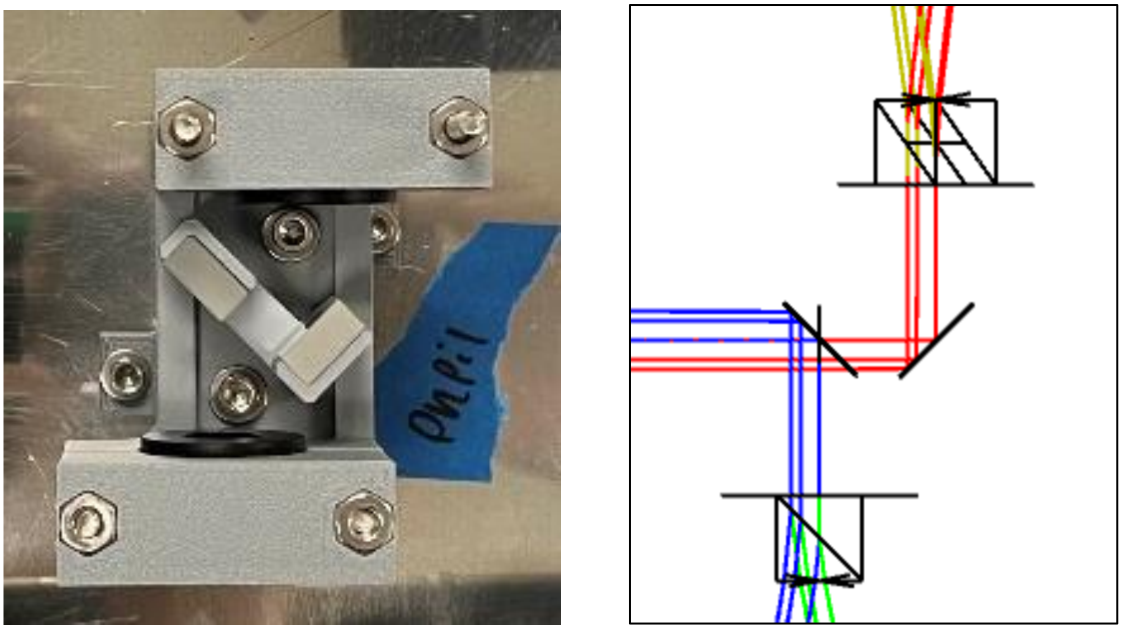

Figure 6-6 - *WeDoWo replacement assembly (left), and the equivalent Zemax drawing (right). The horizontal Wollaston is at the bottom of each image, and the 45 degree Wollaston is at the top.*

6.1.iii.a Pupil Reimaging Lens Design

Replacing the WeDoWo has continued effects on all optics further down the line. The separated geometry no longer allows for a single focusing lens to be used for all four polarizations. Instead, each path has its own lens tube assembly consisting of a 60 mm EFL focusing lens, then a 7.5 mm EFL lens for reimaging the pupil. The focal lengths in this system were chosen based on two criteria. Most important is that the input beam is reduced from 7.3 mm in diameter, to a size that is compatible with the 1.3 mm detector size. Secondly, that the total length of the lens assembly is minimized. The 7.5 mm lens is located approximately 7.5 mm after the intermediate image from the first lens. Combined, these two lenses create a Keplerian beam expander operating in reverse to shrink the output beam diameter to approximately 0.9 mm in diameter. This dimension was chosen to allow for maximum coverage of the detector area, while also allowing buffer space for minor alignment errors. The distances were then optimized in Zemax to simultaneously reposition the pupil image at the detector surface while maintaining its diameter.

The lenses themselves are mounted into a 1 inch lens tube that can attach directly to the front face of our PDA44 photodetectors. We used a series of 3D printed spacing rings to ensure each lens is correctly positioned within the assembly.

6.1.iii.b Fold Mirror Design

For compactness, the polarimeter uses a set of three fold mirrors to redirect polarimeter arms, while the fourth remains undeflected to allow the Acquisition and Guide system to fit. The mirrors we used are Thorlabs BB03-E02 broadband dielectric mirrors. These AR coated fused silica mirrors have a reflectivity >99% for all wavelengths between 400 and 700 nm. We chose ½ inch mirrors in order to accommodate the relatively narrow 20 degree divergence angle of O and E rays outgoing from the Wollastons. They are located as close as mechanically possible to the prism itself to minimize footprint.

6.1.iii.c Zemax Design and Optimizations

Once the new design parameters were decided on, the polarimeter was assembled and tested in Zemax. We began by implementing the F/8.2 input beam, and optimizing the HWP and pupil imaging lens positions to collimate the beam. All components were initially placed at distances pre-determined by calculations, and were then more finely adjusted by optimzation. This allowed us to move on and determine the exact location of the pupil and position the pupil splitting mirrors there. Unlike the WeDoWo, there is nothing that we can do to affect the performance of our Wollaston prisms, but we were careful to ensure that this design was created using an accurate representation of the real product. Separate configurations were created to allow for each of the system's different beam paths. To implement the fold mirrors, the mirror angle was made variable and the system optimized for outgoing ray angles at zero degrees.

Finally, we added the two pupil reimaging lenses to each configuration. Each detector-lens combination was optimized separately, since none of the polarimeter arms are identical. The position of each detector and 7.5 mm EFL lens was made variable, and the system optimized to position the paraxial pupil at the same location as the image (detector) plane, and simultaneously maintain an approximately 0.9 mm pupil diameter.

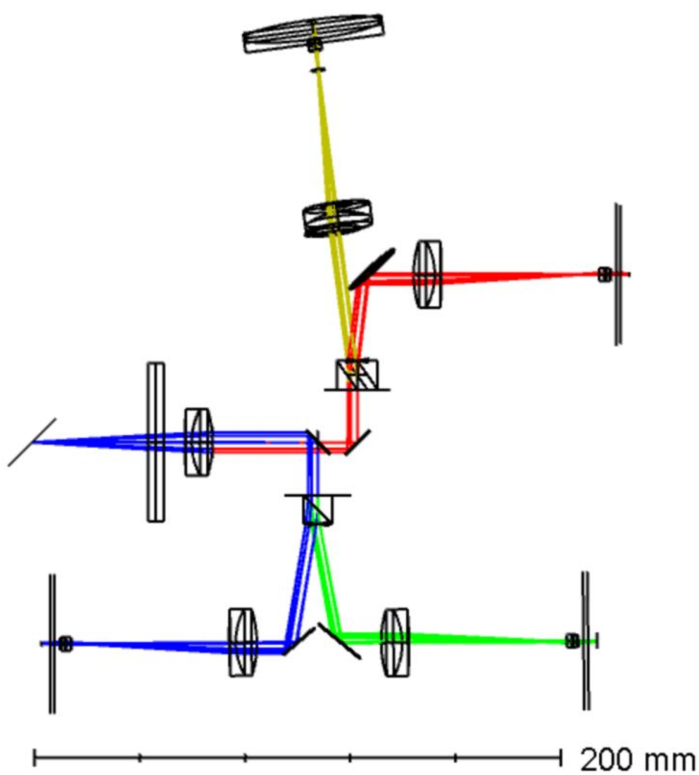

Figure 6-7 *– Full Polarimeter design. Shown with the intended 3 arcsec input field and all wavelengths. Different colors represent the distinct polarization states in each arm.*

Analysis of the pupil image is our primary means of quantifying system performance. Pupil position is quantified by measuring the image location and how it varies across the range of input field angles. The result is listed as the pupil image position variation. Initially, these positions varied by up to 100 µm. The optimization process brought this down to an average of 3 µm. We also account for chromatic aberrations by measuring the pupil diameter variation as a function of wavelength, since this description is more directly relevant than measuring chromatic focal shift in a collimated or nearly collimated beam. When considering these parameters, the F, d, and C wavelengths were analyzed simultaneously for coverage over the visible spectrum.

Table 6-4 *- Polarimeter Pupil Imaging Metrics*

Metric	Value
Pupil Image Diameter	935 µm
Detector Area Coverage	71.9%
Wavelength Dependent Area Variation	12.1 µm
Pupil Image Position Variation	3 µm

6.1.iv Light Losses

To ensure that we minimize the optical power loss, we use the absorption coefficients, and indices of refraction for the different materials to find reflection and absorption losses. With AR coatings, the air-glass reflections are minimized to <0.5%, but we also consider internal reflection losses from the different glass materials used in the achromatic doublets/triplets. The equation for the transmitted light after absorption is:

$$Eq.\,6\text{-}5\text{: } \frac{I}{I_0} = 1 - e^{-\alpha d}$$

Where α is the absorption coefficient of the material, and d is the thickness of that material. I is the intensity of the light, and so I/I_0 is the relative intensity after absorption. The equation for reflection from one material to another at normal incidence (0° AOI):

$$Eq.\,6\text{-}6\text{: } R = \left(\frac{n_1 - n_2}{n_1 + n_2}\right)^2$$

With these two equations we find the theoretical power that is lost through the different optical paths. There are 3 different lenses being used and so we begin by finding the power loss of each so that we can sum these losses up for the different paths. To get the index of refraction and absorption coefficient, we use RefractiveIndex.info which is a database of the many different optical materials and their characteristics [37].

Table 6-5 – Total theoretical power loss per optical component

	Air Reflection	Internal Reflection	Absorption	Total
Steinheil Triplet	1%	0.1186%	0.4452%	1.5638%
Hastings Triplet	1%	0.4420%	0.3274%	1.7694%
Achromatic Doublets	1%	0.2389%	0.2616%	1.5005%
Beamsplitter cube*	1%	-	0.2084%	1.2084%
"WeDoWo"	No Coat: 8.43% AR coat: 1%	NA	0.3992%	1.3992%

* Beamsplitter has >85% transmission of both polarizations, so <15% is lost. We plan to replace the beamsplitter with a pinhole mirror (fabricated in CREOL) in SDII.

To find the power loss per path, we simply count the number of components along the path and sum each component's loss. For the first path – the one to the polarimeter – there is a Steinheil triplet, beamsplitter cube, hastings triplet, and the wedged double Wollaston (WeDoWo) prism. From the table the total loss is 5.9408% for path 1. For path 2 – which images the telescopes object of interest – it has 2 Steinheil triplets, and the beamsplitter. The total loss is then 4.336% for path 2. The last path – the pupil imaging path – has 1 Steinheil triplet, the beamsplitter, and then 2 achromatic doublets. This results in a loss of 5.7732%. These are under our basic goal of less than 10% power loss through the system.

For the final design, a similar process of finding the power loss for each component is performed. There are 3 different material combinations used between the 4 different achromatic doublets in the design. For the lenses chosen, the power loss for the star imaging path (2 lenses) is 2.791%, and for the pupil path (3 lenses) 4.246%.

6.2 Hardware Design

In this section, we look at the design of electrical hardware for our project. The bulk of hardware design is in the power supply unit (PSU), as the detectors and op amps will both require ±12V voltage outputs. There is also an additional 3.3V output for the MCU and 5V output which will be used for the mirror servo motors and the rotating wave plate. The detectors also require a decent amount of current (250mA each), and with 4 of them, the PSU will need to handle this current without a decrease to any output voltages. The MCU also needs connections for the peripherals to work correctly, such as the LCD display.

6.2.i PSU and MCU/Control modules

To begin the hardware design, we decided to begin the prototyping in two phases, PSU construction and discrete component construction. Firstly, the power supply design must be created to service all components needing power. Within this portion of the design, we have decided to take a 12V 7A wall wart to supply DC power into the board. Using this 12V 7A wall wart source, we will construct our own power supply which will provide sufficient voltage and currents required by the many devices utilized within our module. The plan is to have a 5V 1A output, 3.3V 1.2A output, ±12V 1A output. To achieve these voltage outputs, we will be using switching regulators in buck configuration to achieve a lower stable output voltage. When constructing the prototype, we must keep in mind the dropout voltage and output current capabilities of the voltage regulators, this is key for power management. We need to make sure our system can handle the high current and power dissipation properly to avoid a potentially dangerous failure. Additionally, we must consider what voltages are required for operation of the MCU and how much current will be demanded/ handled by the MCU these factors mainly concern the 3.3V output which is what is required by the ESP32. The 5V 1A output is primarily going to be in use for supplying the rotating wave plate mount with the proper operating voltage and supply the necessary current, in this case 800 mA at use and 50 mA in idle. We possibly want to design a circuit that will open the connection during the idle, if possible; this is to minimize power consumption. Additionally, the servos will use the 5V output for positioning adjustment before sampling begins. The ESP32 MCU will at most draw 1.2A of current so our 3.3V regulated output must be able to have this current output available. Lastly, the ±12V output is required for the photo detectors which will consume 250 mA of current. Additionally, the ±12V output will be utilized by the op amps used for the sensor input signal, this will require negligible current as we are just passing the signal to the ADC.

6.2.i.a Voltage Regulator design schemes

Starting the design for the PSU, we utilized the Texas Instruments' WEBENCH to help create a scheme for the 3.3V and 5V regulated outputs. Detailed in this WEBENCH design report is the topology of the regulator circuit and the recommended components for a desired output. For the 5V and 3.3V regulated outputs will be constructed using a LM2576 adjustable version. I chose this regulator because it is a relatively cheap switching regulator that can handle the output currents required by each of the loads. For the +12V the plan is to run this either through an LDO regulator just to maintain the output or just be a trace open to connect to. As for getting the –12V output we must somehow find a way to flip in the input signal phase by 180 degrees. Rather than using an inverting op-amp to flip the signal, the use of a switching regulator with an inverting scheme can provide a sufficient way to invert the 12V signal whilst still maintaining the output current requirements of the load devices attached to the regulated output. For the inversion regulator we chose to go with using the LM2576 adjustable to achieve the –12V output with 0.7A available.

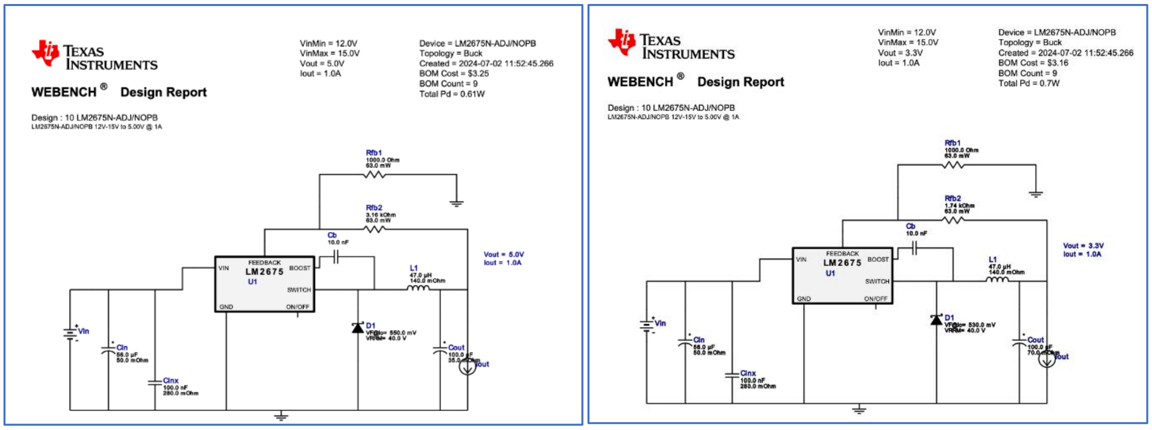

Figure 6-8 - *5V Regulator (Left) and 3.3V regulator (right).*

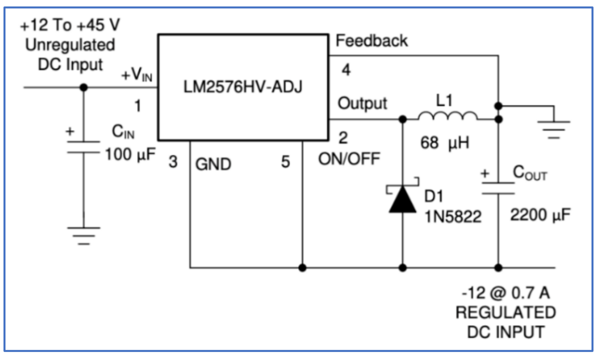

Figure 6-9 - *Negative 12V DC regulator*

The current testing plan is to construct a breadboard version of each voltage regulator and input a low amperage input of 12V. This first test is to confirm we have the correct voltage outputs at each regulator for all terminals. The circuit must be carefully constructed with the proper rated components to assure safety standards are abided. Additionally, we must have proper housing for the unit to ensure user safety and protection of the components. To implement the case, we will use 3D printers to construct a base for the board and a matching cover for the top of the unit.

After the initial circuit testing, both the 3.3V and 5V regulators were successfully constructed and lab tested for proper functionality. Below are the schematics created using the imported library files for fusion 360 for each component. It is needed to import the proper components to ensure the PCB is compatible with the selected components and make the layout of the board easier to design. This design uses the same rated components but utilizes a surface design for PCB construction. The surface mounted components also offer reduction in the instrument’s overall dimensions.

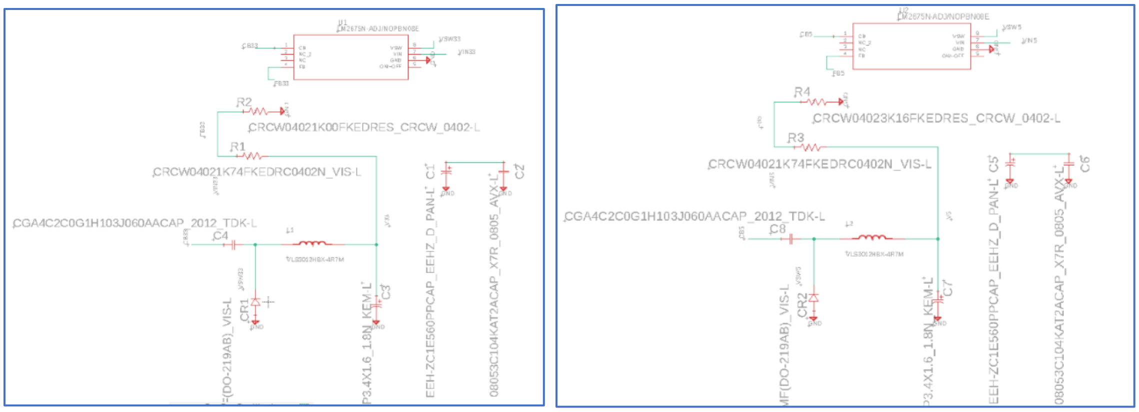

Figure 6-10 - 3.3V Regulator Schematic (left), 5V regulator schematic (right).

There was an issue during the testing of the inverting regulator circuit. Following the datasheet's recommendations for component values and ratings for implementing an inverting 12V output, no success was achieved. The circuit was tested and constructed multiple times each with new LM2576-ADJ regulators, NEB and KTT packaging of the regulator. After this drawback it was necessary to begin a redesign of the new inverting regulator. Following an almost identical scheme as the previous regulators, a 12V regulator was designed with an inverting charge pump taking a PWM input from the VSW pin of the regulator. Using the datasheet, we calculated the proper resistor values required for a 12V output. The design resulted in using a 1kΩ feedback resistor to ground, and a 9kΩ feedback resistor connected to the output. We can take the 12V PWM/ switching output of the regulator to create an inverting charge pump. The inverting charge pump is created using two Schottky diodes (1N5818; 1A) and two capacitors, the scheme allows for the inversion of the PWM input signal. The current output of the charge pump should be the same as the max output current of the regulator, if the diode current rating is properly selected. Furthermore, the currently chosen capacitors are 1µF. However, it may be a better alternative to choose larger capacitor values to provide a "boost" of current. The next capacitors we will test will be 10 µF and should provide sufficient charge to maintain an output current of 250 mA. To improve design, capacitors chosen should have a low ESR rating to reduce the output ripple current.

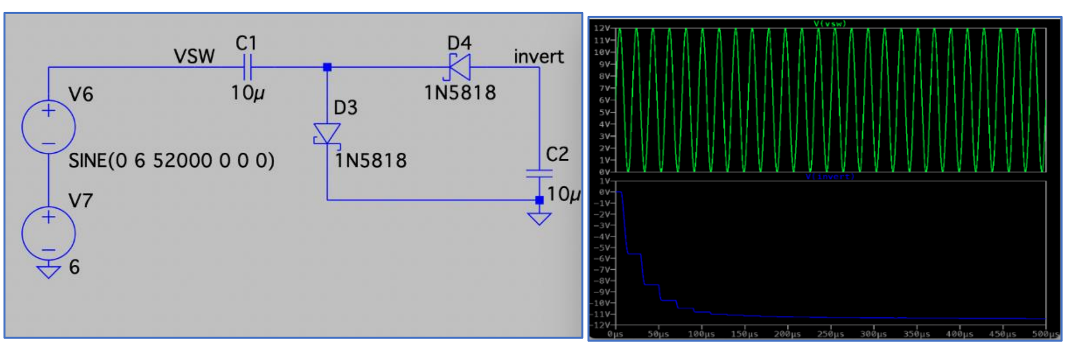

Figure 6-11 - Charge pump LTSpice schematic (left). Output of the charge plot (right).

The next plan to solve the inverting output issue is to use a MAX17577 4.5V to 60V, 1A Inverting Output DC-DC Converter. This voltage regulator is only available in a surface mount package, which means testing must be done on a PCB layout which isn't ideal. However, the component is rated to take the 12V input and successfully output –12V that will see no loading effect.

6.2.i.b Battery Design

Considering the implementation of a battery within the design, we must create a circuit which will allow for the battery to be used in the state that the module is not connected through a wall wart. The idea is to use a depletion mode MOSFET to act as a voltage sensing switch which will read if the 12V input is present in the system or not. The MOSFET will have the following connections: the source will be connected to the positive end of the 3.7V Li-ion battery, the gate will be connected to the 12V wall wart trace connection, and lastly the drain will attach to the 3.3V regulator output. The battery is intended to only power the MCU for data transfer/reprogramming. Additionally, a charge controller circuit will provide the battery with recharge capabilities while the device is connected with the main power source. This will ensure the battery can be used for extended periods of time and has a long lifespan before needing to recharge.

6.2.i.c MCU/Controls and ADC Front-End

In conjunction with the power supply unit design, our team also met together to discuss and decide what controls we would want implemented in the device. To begin with, it was necessary to include an LCD attached to our ESP32 MCU to have a display that would allow the user to navigate adjustable settings. Next, we included 4 buttons which are fed into the GPIO pins on the ESP32. Here, we can configure the buttons and debounce them as well. The use of the buttons will be to select menu page and controls to increase or decrease the displayed control value. We have been discussing the introduction of a rotary knob for the increase/decrease value and using the buttons to alter adjusted digit. Lastly, we began configuring the ADC module to 1 MSPS however using the internal 8 MHz clock rather than a crystal oscillator. The crystal will be implemented into the final PCB but is currently unable to be implemented due to the ESP32 dev kit grounding the external crystal for up to 40MHz. Simply using a 32kHz crystal for our stable clock source wouldn't meet the system requirements.

Furthermore, on handling the ADC module we must create a front end to the ADC to ensure our photodetector signal can be properly sampled and interpreted by the MCU. The ADC requires an input signal between 0V-1V, so we must DC offset and attenuate our photodetector signal. The photodetector signal is specified as a ±2V signal which will have various pulses depending on photon intensity. The front-end design is to DC offset the detector signal by 500mV and then attenuate the signal to 13.33% of the original waveform. This will ensure the signal can be properly read by the ADC module. To begin the design, we had to find a way to bring in a DC offset. This was achieved by using an inverting op amp scheme with a unity gain, using feedback and input resistors of the same 10kΩ value. This op-amp's output will provide an inverted 5V signal which will then be connected to a voltage divider of two resistors. The resistors chosen were a 9kΩ and 1kΩ resistor, with the 9kΩ connected to the output of the inverting amp and the 1kΩ connected to ground. The output was taken at the top of the 1kΩ resistor, providing an inverted 500mV. Next was to bring the photodetector signal into the scheme. While creating a connection for this signal we will utilize another inverting op amp, once again with matching resistors to achieve a unity gain on the output. It is important to ensure the input impedance of this inverting amp matches the recommended BNC cable termination of 50Ω, therefore the resistors used were both 50Ω. Once the –500mV and inverted sensor signal have been successfully created we must use a summing amplifier to achieve the desired output for the ADC. The summing amplifier must keep the 500mV DC offset signal the same magnitude which will require the input resistor and feedback resistor to have matched resistances. However, unlike the offset, the photodetector signal must be attenuated. To achieve a reduction of magnitude we must use a larger input resistance as compared to the feedback. After circuit simulation testing in LTSpice, 10kΩ resistors were used for the feedback and offset signal resistors, and a 75kΩ resistor was used for the inverted sensor signal. Using this ADC front-end scheme, we achieve an ADC input signal which has matched phase to the original input signal, along with keeping the signal between 0V-1V. More specifically the signal will sit nicely between 750mV and 250mV when the signal is at a maximum of 4Vp-p. It is important to consider though that a smaller inverted sensor signal resistor may be implemented in the future after testing to ensure fidelity of a signal that is weaker than the 4Vp-p sine wave input. This design tested the absolute maximum of the photodetector's output signal and ensured it would remain within the sampleable range of the ESP32's ADC module.

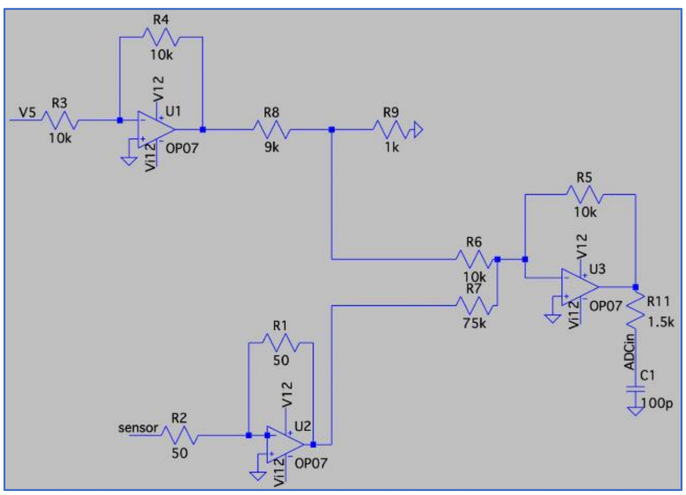

__Figure 6-12__ - ADC front-end schematic in LTSpice.

6.2.i.d Hardware Design Update: Analog Front End (AFE)

AFE purpose and design: The analog front end (AFE) amplifies the photodetector's small signal (50–100 mV, 4 ns duration) using a 3.9 GHz GBW op-amps, ensuring compatibility with the ESP32. Next, the signal is fed into a high-speed Comparator which will limit any dark count noise. Proceeding, A Schmitt trigger lengthens the amplified pulse for a clean square wave output, while a comparator removes unwanted noise. This processed signal enables the ESP32 to accurately count pulses which represent incident photons. Using small resistance on the op amps was crucial to getting the correct output, use of large resistors would eliminate the signal output. **Figure 6-13** provides a block diagram of the processing steps, followed by the gain stage scheme. **Figure 6-14** gives the schematic for the Schmitt trigger.

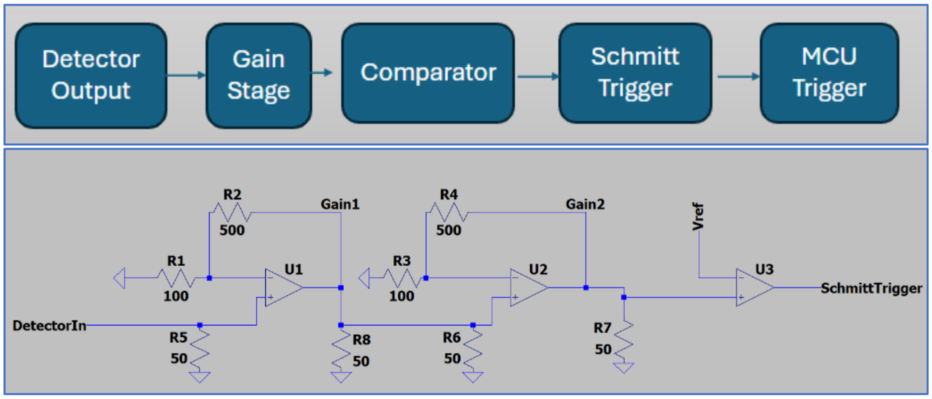

Figure 6-13 *– High-speed analog front end. Two gain stages are shown, sent into a comparator and then a Schmitt trigger. This provides pulses that can be sent to and read by the MCU.*

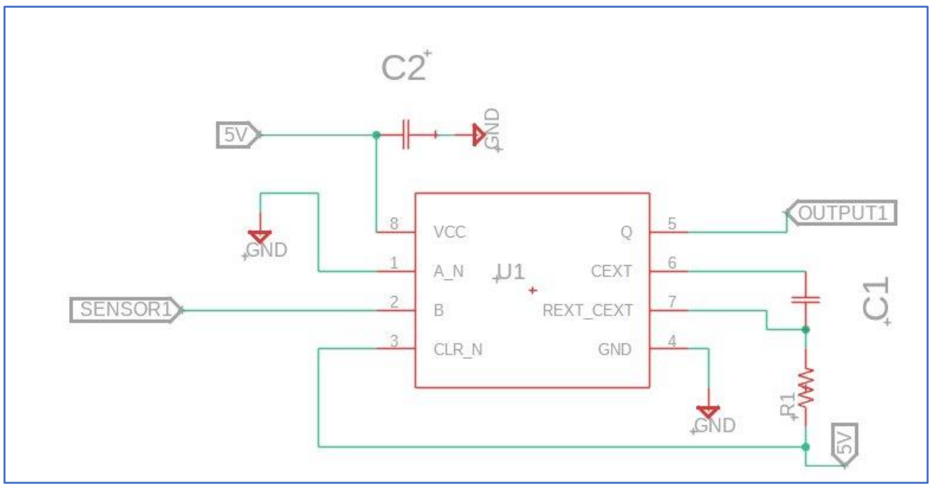

Figure 6-14 *–Schematic for the Schmitt trigger.*

Chapter 7 – Software Design

There are a few different areas for the software component of the project. The main part is embedded systems programming, which includes handling user inputs (via buttons), displaying parameters to the user with an LCD, and sampling the detectors. Sampling the detectors will require that the ADC be set up with the parameters given by the user, such as sampling frequency and duration. The second half of the sampling is storing the data in a proper format so that it can be off-loaded to the connected PC via a UART to USB bridge.

The other portion of the software design is to write a Python application that can process the raw data and provide us with the pulse timing and polarization of the pulsar (or other source). Finding the polarization is done by finding the Stoke's parameters, as we are using a Stoke's polarimeter which gives enough information to calculate the linear polarization parameters. The pulse timing can be found in a couple of ways, the primary way is using derivatives to find extrema, and then finding the time difference between them. It is also possible to calculate it using non-analytical methods, as computers are sufficiently fast in today's age.

7.1 ESP32 Embedded Programming

As mentioned above, extensive programming of the ESP32 microcontroller is required. There are a couple of IDEs that can be used to accomplish this, which are discussed in the software technology section of chapter 3 (3.1.xv.g). In order to have the most control over the hardware, we program using the native framework for ESP32 chips, which is the ESP-IDF framework. Originally, we used the Arduino framework for its simplicity but would not be able to run the ADC in continuous mode which allows for higher sampling rates. The move to the native framework took some additional time as we had to familiarize ourselves with the structure. The ESP32 has two processors, and so synchronization and mutual exclusion become concerns. Luckily, ESP32 comes with the freeRTOS (real-time operating system) kernel that provides mutexes, semaphores, and other synchronization tools, including a task scheduler. Once understood, this makes the programming more abstracted, as we can set up individual tasks to be run.

For running the ADC, the code follows the following flow chart. The process begins by initializing the ADC by providing buffer sizes and the DIG controller. Once the ADC has been configured, the interrupt service routines (ISRs) can be registered as callback functions when certain events take place, such as a completed conversion frame, or the overflow of the ADC buffer. When the start button is pressed, a timer starts the conversion for the sample duration specified by the user. Data is printed one conversion frame at a time. Our future goal is to store the data internally in flash storage that we can then access and send the full sample to the Python script at once, as opposed to sending only single conversion frames at a time. Luckily, there are a few storage APIs with examples available from Espressif that will make this task feasible. These API allow for a FAT file system to be mounted and formatted onto external flash memory. This would allow us to create files that contain the ADC data, which can then be read and sent to the connected PC at the most convenient time (when sampling is finished).

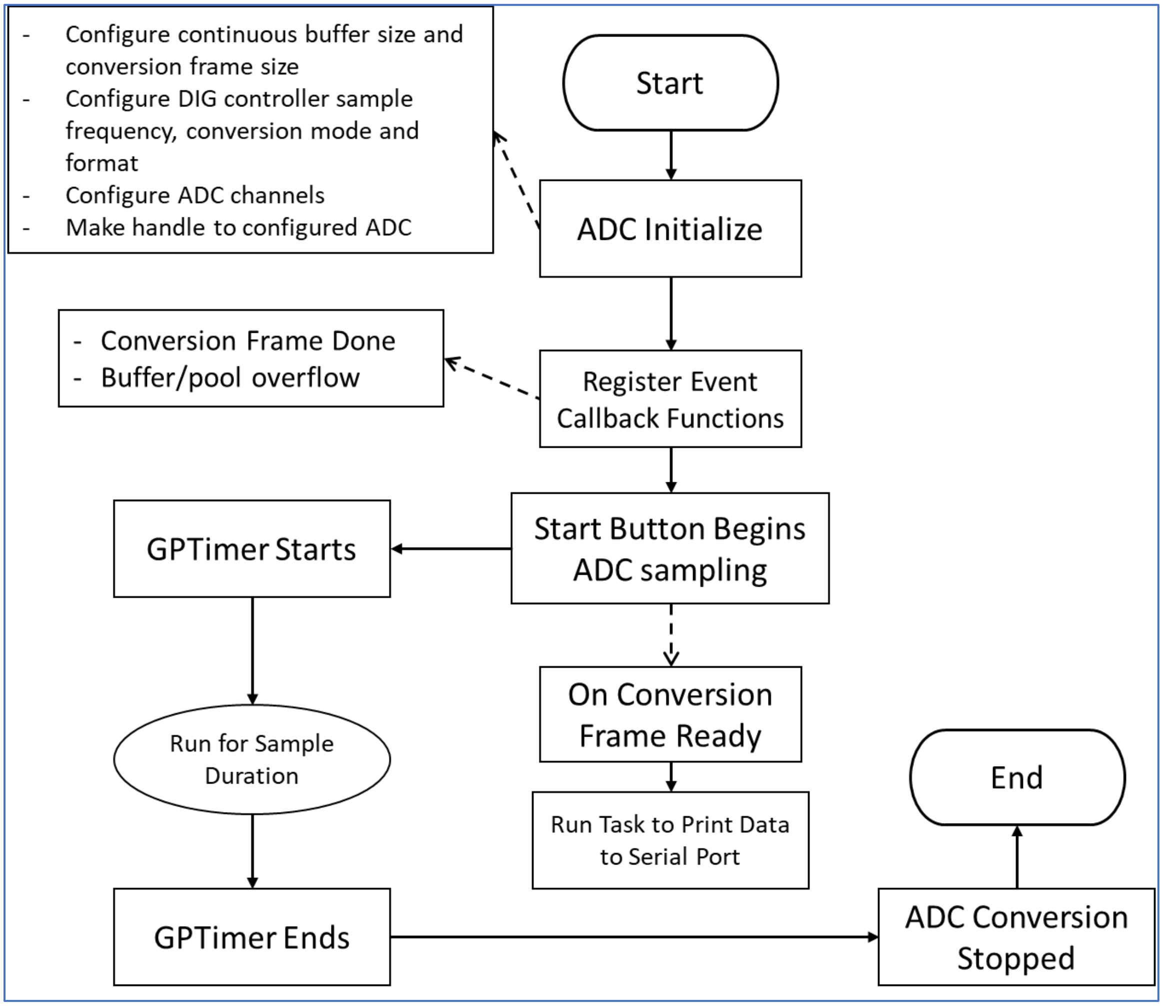

Figure 7-1 *- ADC sampling flowchart (initial process)*

Additionally, the MCU also needs to accept user input and display parameters to the user via the LCD display. User input is taken in via a rotary dial for incrementing or decrementing the displayed value; via buttons for switching the displayed parameter, or for starting the ADC conversion; and via a switch for changing the optical path of the light. The MCU will use the inputs to either update the ADC configuration or send output signals to the LCD via an I2C bus, or to one of the status LEDs. The servos that flip the mirrors into the imaging path to change to the pupil imager would also be controlled by the MCU, as they require a PWM signal to control the angular position. A generalized state diagram is shown in Figure 7-5 below, in the Python package section.

In Figure 7-2 (below), the process of sampling the ADC is shown in a state diagram. The ADC sampling involves three main states: ADC start, ADC running, and ADC done, as well as idle. This diagram shows how the program flows from one process to another as different triggers occur. The diagram also provides the steps taken at the different states to store the ADC data efficiently for retrieval by a connected computer. In this case, the method is to calculate the number of bytes needed for the given sample duration. Using the timer to run the ADC resulted in only 1 buffer's worth of data to be sent during the sample duration, since after the ADC is finished, `adc_continuous_read` fails to read data from the buffer anymore.

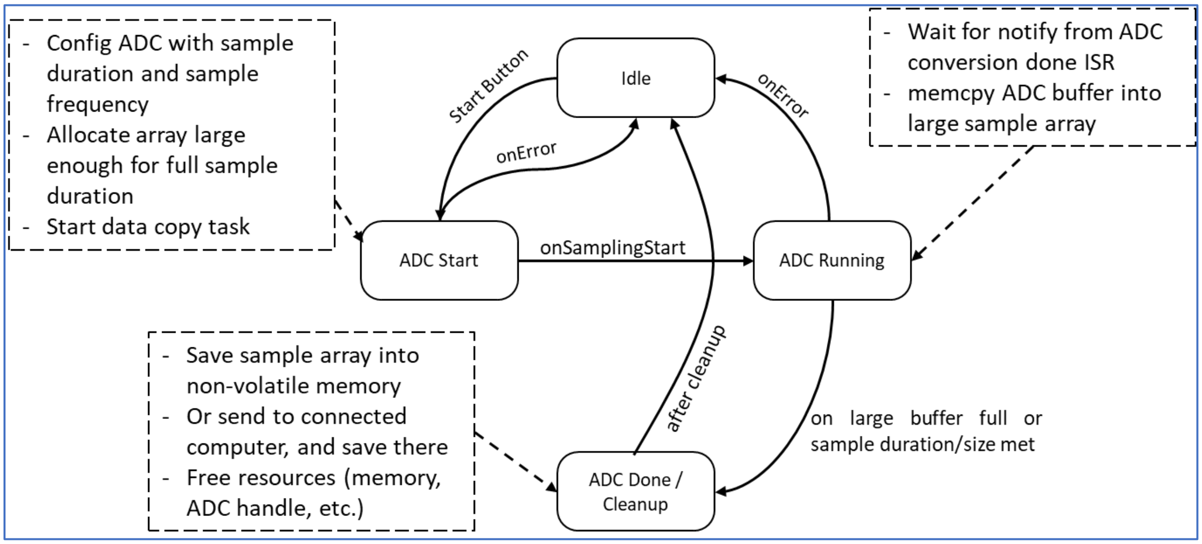

Figure 7-2 *- State diagram showing the temporal flow of the ADC sampling process.*

In the final implementation, we needed to pivot to using the pulse counter (PCNT) peripheral to count digital pulses that correspond to single photon events. This rework required more manual buffer management as there was no built-in buffer system as there was in the continuous ADC driver. For speed reasons, we had to use raw writes and reads with the SD card to hit the maximum sampling rates that we desired. The updated flow chart is shown below in Figure 7-3. Timers are used to define the sample period, the inverse of sample frequency which is called segment in the code, and the sample duration. A custom structure is defined to store the counts of the 4 input channels, as well as the current count of the duration timer, which gives us the time when the data is collected. The built-in flash memory of the ESP32 is used to save metadata files on each sample, including information on the sample frequency, duration, number, starting memory address (on SD card), and number of sectors (size) on the SD card. An updated state machine is included underneath the flowchart, in Figure 7-4. Tasks and task notifications are used to facilitate the control flow of program execution.

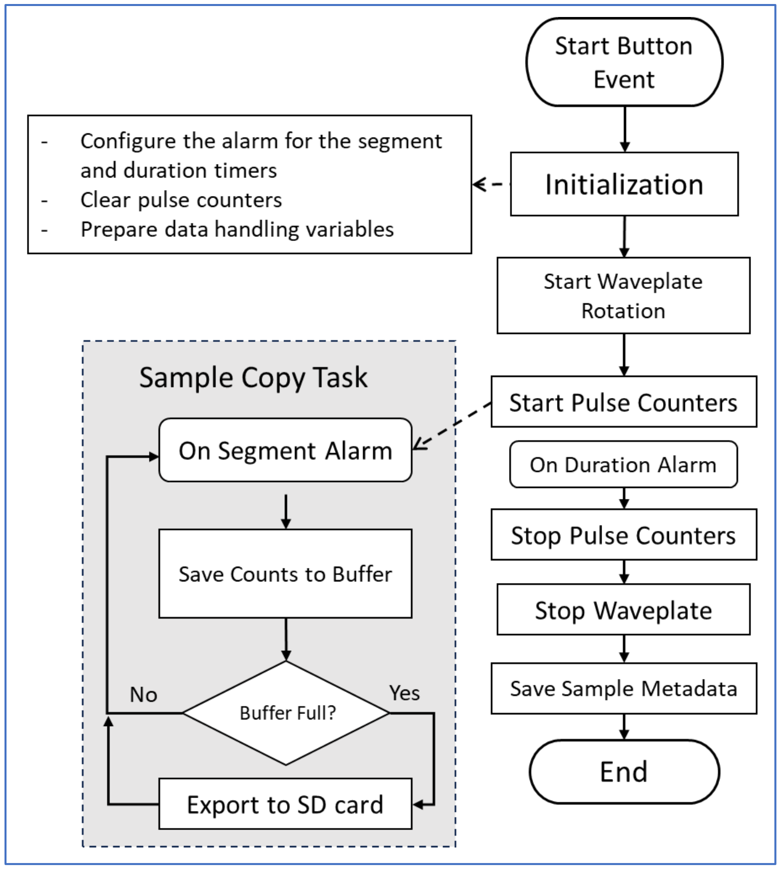

Figure 7-3 *– Flowchart of the PCNT sampling program. Data buffer is offloaded to the SD card when it fills up. At end, the data is read off of the SD card and sent to the waiting Python program through UART.*

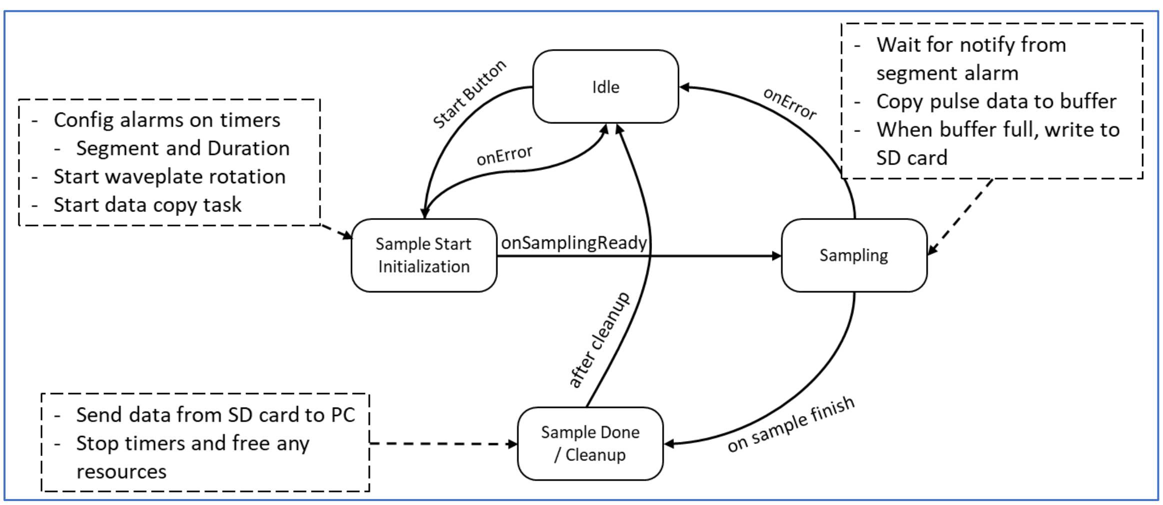

Figure 7-4 *– State machine outline the process of sampling. Tasks are used to facilitate program flow control using task notifications available in the microcontroller's freeRTOS implementation.*

7.2 Python Package

Another portion of our software design is to design a Python application that can calculate the polarization and pulse timing from the data that we collect. This will allow us to see what data we are collecting and allow us to compare it with predictions to ensure our project operates as expected. We also use Python to get data from the chip via the UART-USB bridge. This is accomplished by opening a serial port in Python using the *pyserial* package.

The serial input parser has the flowchart shown in Figure 7-6 below. It runs in an infinite loop, reading data off the serial connection to the MCU. When a certain tag appears, it runs a function to get the raw ADC data from the serial connection. This tag is important so that the program knows when to parse the input as ADC data. The formatting must follow from the embedded programming side as well as the Python side. The data that is read is as bytes, and so it must be appropriately converted into strings and integers. For strings we use the UTF-8 encoding, and for integers we convert using base-10 or base-16 based on the formatting. An array data type is used to store the ADC data, which we can convert into a numpy array later. The array is stored into a dictionary, where the key is the channel number of the data, and the value is the array. This gives an easy way to access the data when many channels are sent at once. Plotting of the data is done with *matplotlib*, and our goal is to asynchronously show the plot so that the terminal doesn't freeze while waiting for the plot to be closed. After the data is plotted, the data is stored into a text file marked with the channel number, and a time stamp that includes the year, month, day, followed by the hour, minute, and second. Figure 7-5 below shows how the serial Python program changes states based on events. When the ESP32 is done converting a sample, the data is piped over to the Python program that monitors the connection, waiting for a tag to appear. After the data is read, it is saved into a file, which can then be read by a separate Python program to process the data.

Part of our data processing will include calibrating the data. The main calibration would be the ADC, as it measures the signal based on a reference voltage that changes based on the chip manufacturing. Included in the ESP-IDF framework API, is a means for calibrating the ADC using two known points. The other calibrations that we can perform are related to the optical components. For example, differences in the paths of the split light out of the Wollaston prims could result in some slight, but known, errors. By also characterizing the detectors themselves, we can fine tune the calibration of each data source based on the dark counts of the detectors. Performing these calibrations will enable us to reach even higher levels of precision for our measured data.

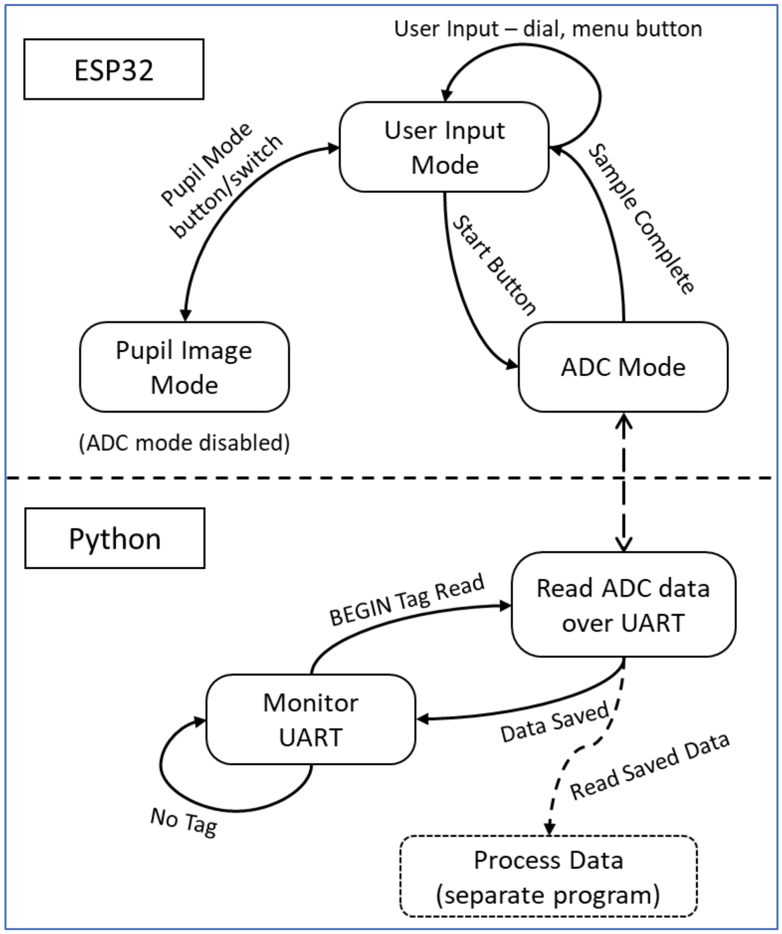

Figure 7-5 *- General state diagram for the embedded programming, and the Python code, including their connection.*

The next Python program is the pulse time calculator. Calculating the pulse timing is essential for understanding the periodicity and behavior of the pulsar. One method to achieve this is through a calculus-based technique. In this method for pulse timing calculation, we start by processing the raw ADC data to reduce noise and smooth out any irregularities. We use the Savitzky-Golay filter, a popular smoothing technique, which fits successive subsets of adjacent data points with a low-degree polynomial by the method of linear least squares. This filter helps in maintaining the shape and features of the signal while reducing noise. After smoothing the data, we compute the first derivative of the smoothed signal. The first derivative helps in identifying the rate of change in the signal, which is crucial for locating the extrema (i.e., maxima and minima). These points represent the peaks and troughs of the pulsar's signal, which correspond to the pulsar's periodic pulses.

By examining the points where the derivative changes sign (from positive to negative for maxima, and from negative to positive for minima), we can accurately identify the positions of the extrema. We use the positions of these extrema to calculate the time intervals between successive pulses. These time intervals, or pulse intervals, give us a direct measurement of the pulsar's pulse timing. This method leverages the precision of calculus to determine pulse timing, making it highly accurate for clean and well-sampled data.

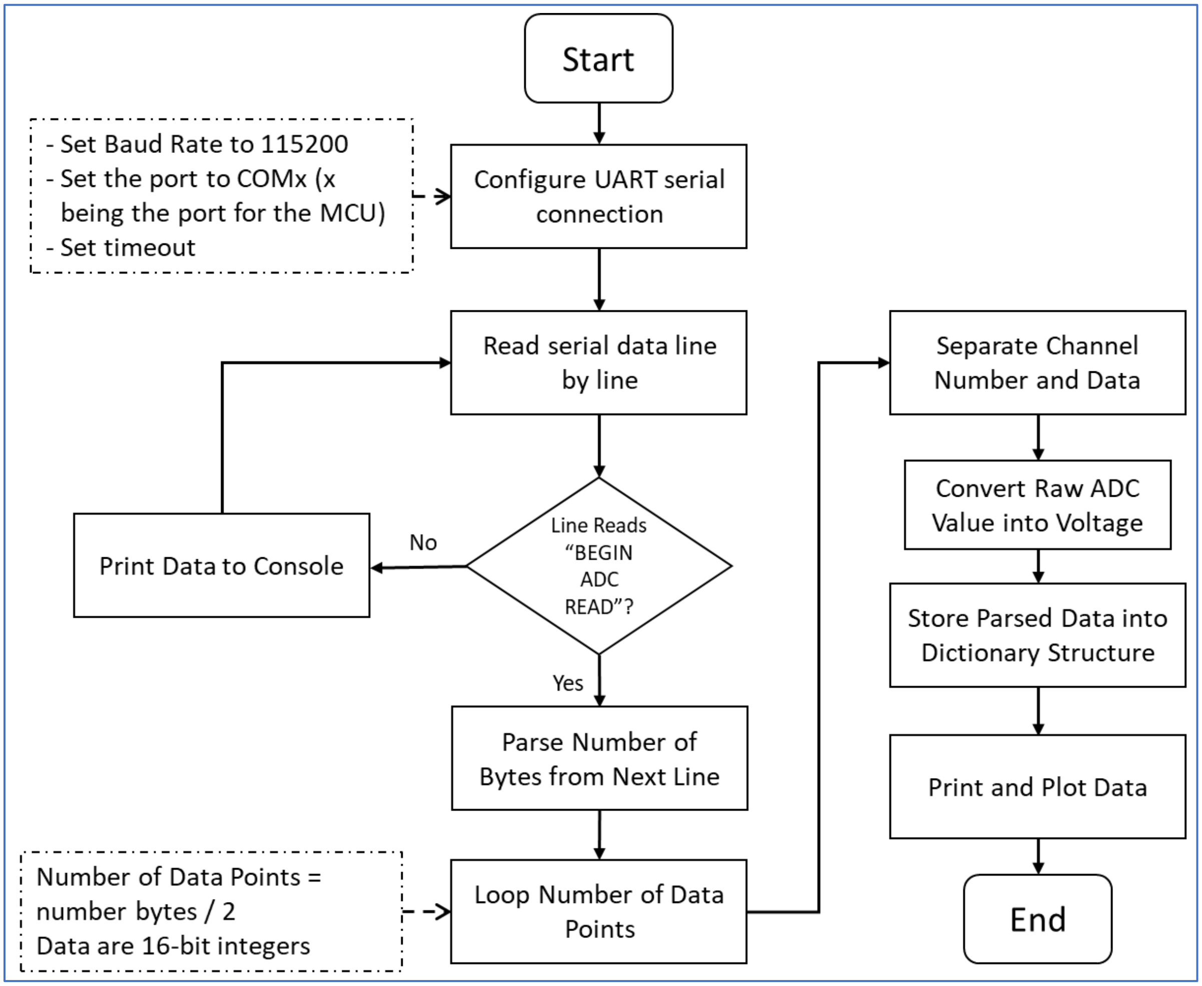

Figure 7-6 *- Flowchart for reading in the ADC data from the UART-USB bridge.*

Another method to calculate pulse timing is by performing a Fast Fourier Transform (FFT). The FFT transforms the time-domain signal into the frequency domain, allowing us to identify the dominant frequencies in the pulsar's signal. This method is particularly useful when dealing with noisy data or when the signal has multiple frequency components. By using these methods, we can accurately calculate the pulse timing and ensure that our system operates as expected. Both approaches have their advantages: the calculus-based method is straightforward and highly accurate for clean data, while the FFT-based method is robust against noise and can reveal additional frequency components. Implementing these methods in our Python package will provide us with reliable pulse timing measurements and allow us to validate our data against predictions.

The polarization is found by following the flow chart in Figure 7-7 (below). In addition to finding the linear Stokes's parameters, we can convert the intensity into the proper unit of watts per area (W/m^2 in SI). This can be done by assuming the average photon energy incident on the detector and using the measured flux to convert photons per second per unit area to optical power (watts) per unit area. We can also find the degree of linear polarization, which is how linear the light's polarization is, as compared to the other forms of polarization (elliptical, circular, and unpolarized). The data is then plotted with the pulse time to show how the polarization and pulse time can be correlated together.

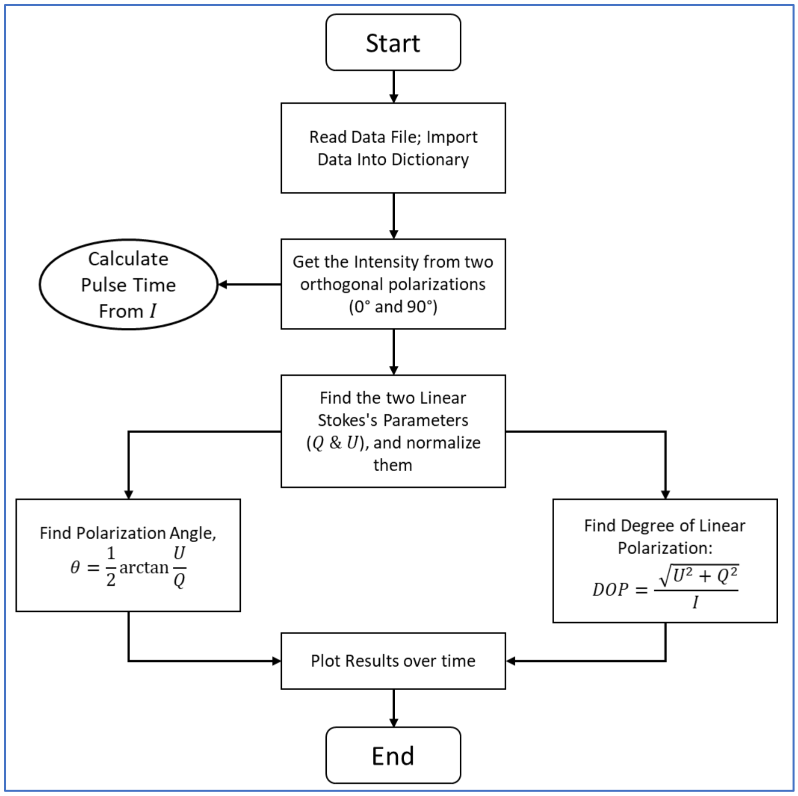

Figure 7-7 - Detailed flow chart for finding the angle and degree of linear polarization

The use case diagram for the polarimeter and pulse timer, depicted in Figure 7-8 (below), provides a comprehensive view of the interaction between the system's key components and the users, illustrating the workflow from configuration to data storage. The diagram features two primary actors: the researcher and the engineer, each playing distinct yet interconnected roles in ensuring the system's functionality.

The researcher is central to the operational aspects of the system. Their responsibilities begin with configuring the system to meet the specific requirements of the pulsar observations. This involves setting parameters such as sampling the frequency and duration, which are critical for data collection. Once the system is configured, the researcher initiates the data collection process, which involves starting the ADC to sample the detectors. This step is crucial as it captures the high-resolution data needed for the subsequent analysis. Throughout the data collection process, the researcher monitors the system to ensure it operates correctly by checking real-time data outputs. After data collection, the researcher transfers the collected data to a PC, enabling further processing and analysis.

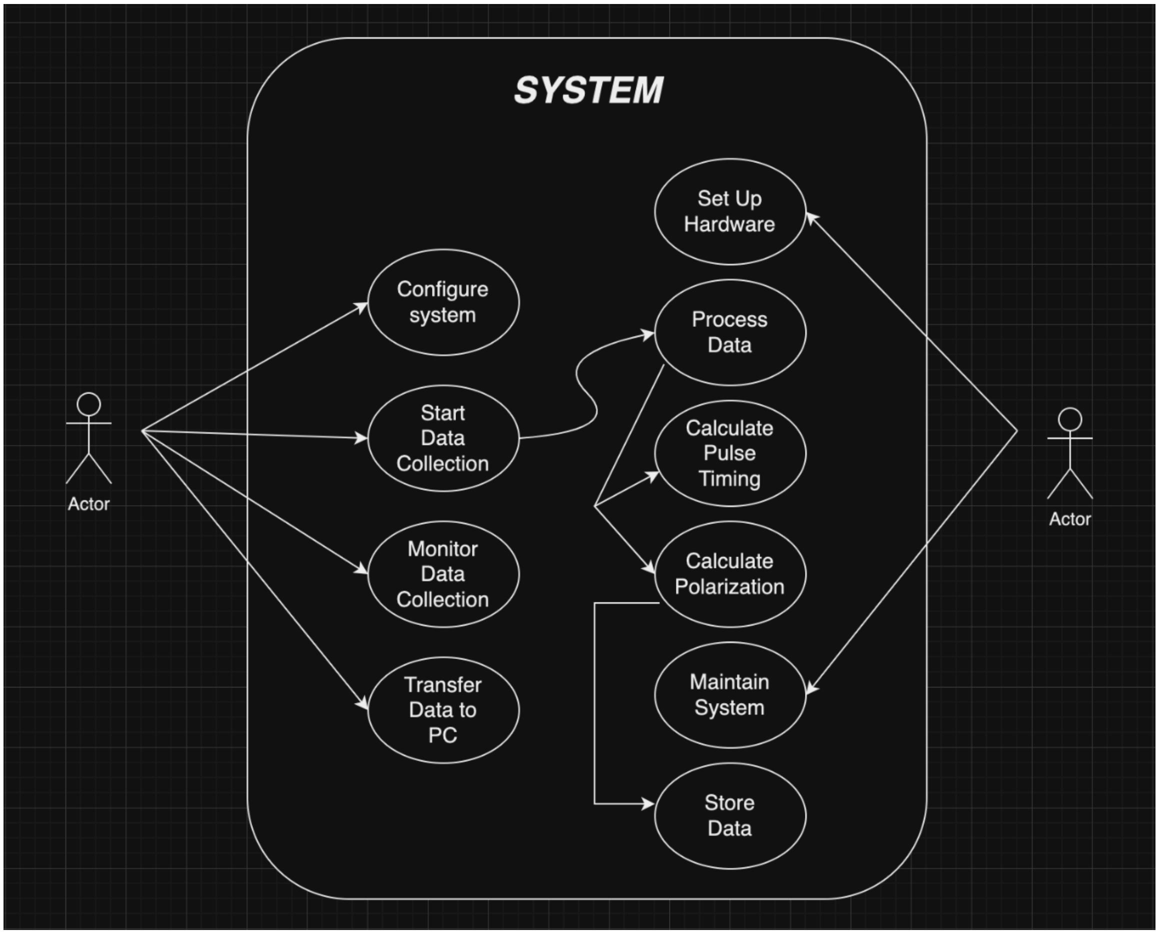

Figure 7-8 *- Use Case Diagram. Left actor is referred to as the researcher, and the right actor as the engineer.*

Data processing is a significant part of the system's functionality, as it involves analyzing raw data to derive meaningful insights. The processing includes calculating the pulse timing, which can be done by using calculus-based methods or Fast Fourier Transform (FFT) techniques. These methods provide critical information about the time intervals between successive pulses of the pulsar, which is essential for understanding its behavior. Additionally, the system calculates the polarization characteristics using the Stokes parameters, providing a comprehensive description of the polarization state. This information is vital for understanding the emission mechanisms of the pulsar. Finally, the processed data, including pulse timing and polarization information, is stored for future reference, ensuring that valuable data is archived securely.

The engineer, on the other hand, focuses on the technical maintenance and setup of the system. They are responsible for the initial setup and calibration of the hardware components, ensuring that everything is correctly assembled and ready for data collection. This includes configuring the ADC, detectors, LCD, and other peripherals to work together seamlessly. The engineer also performs ongoing maintenance, addressing any hardware or software issues that may arise, thus ensuring the system's reliability and accuracy. This role is crucial for the continuous and effective operation of the system, as any malfunction or inaccuracy can significantly impact data collection and analysis.

In our final design, the Python serial monitor reads a whole pulse counting sample from the MCU and accepts user input to be sent over to the MCU. The MCU processes the command and can perform a variety of tasks: start sampling, set frequency or duration, reduce logging, and restore logging. User input through the computer was a feature requested later in the design process, and it turned out to be very useful when testing and debugging the code by speeding up the setting of parameters. The updated interaction between the MCU and Python is given in the state diagram in Figure 7-9. The final iteration also includes a GUI that acts as a console, with additional buttons to the side for sending commands. The GUI connects to the serial monitor program under the hood.

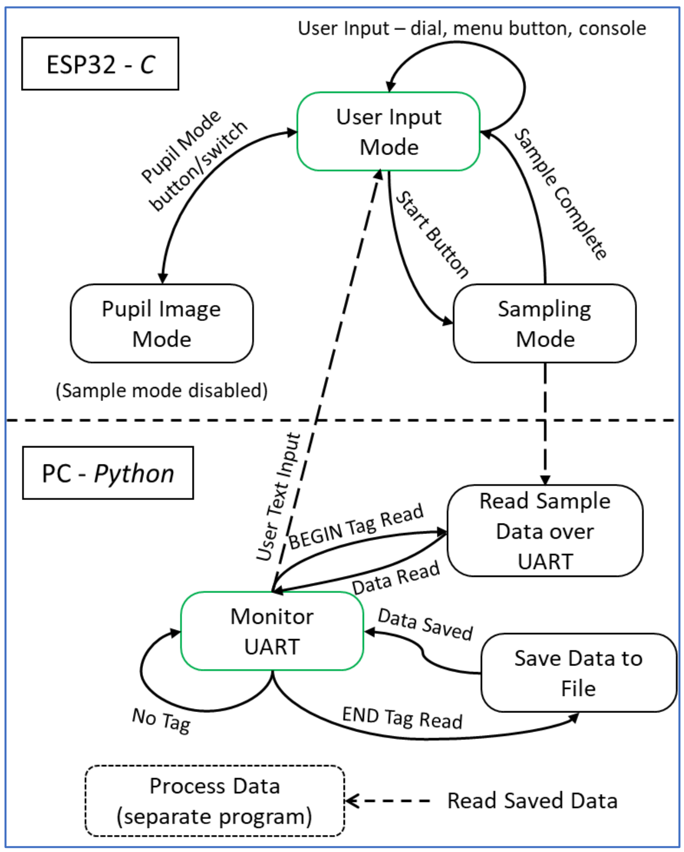

Figure 7-9 *– Joint state diagram showing how the MCU and Python programs operate and when they interact with each other.*

Chapter 8 – Prototype Fabrication

In this chapter, we look at how the prototype is constructed. This includes the specifics of wiring the MCU and all the peripherals. We also describe how we will mount the optical components and how we integrate it with the electronics. In the first section, we will look at the fabrication steps we have done so far in Senior Design I, and in the last section, we look forward to what we will do in Senior Design II.

8.1 Prototype Construction

In this section we will discuss how the prototype is constructed. We begin with the electrical connections that need to be made, and then how this couples with the optical parts of the system.

8.1.i ESP32 Dev Board Connections

The MCU is the heart of the project, as it will be what integrates the optical and electrical aspects of the project together. The MCU will use its analog-to-digital converter (ADC) to take the analog signal that the detectors produce and digitize it into a computer-friendly format. This is done continuously for the sample duration, so that the data is useful. Our goal is to sample at 1MHz, which is within specification for the MCU, but we also want to give the user the option of adjusting this frequency using a rotary encoder, which is a dial that can increment or decrement MCU variables. This is accomplished using the pulse counter (PCNT) peripheral of the MCU. The sample duration is also adjustable with the rotary dial and is implemented using the General Purpose Timer (GPTimer) peripheral of the MCU. To enable these adjustments, a 20 character by 4-line LCD display is used for relaying the configuration settings. This LCD uses the inter-integrated circuit (I2C) protocol, which utilizes another peripheral of the MCU.

In terms of which pins are used, we start by eliminating the strapping pins that are used for booting the chip. While not strictly necessary, there are enough General-Purpose Input-Output (GPIO) pins available, so we do not need to use the strapping pins for the prototype. For the ADC, we use unit 1, channels 0 to 3, which corresponds to pins 36, 37, 38, and 39. These pins will be connected to the detectors which output ±2V. A conversion circuit will then adjust this range to fit within the ADC input range, which is 150mV to 2450mV at max attenuation, or 100mV to 950mV at no attenuation. Our goal will be to not use attenuation, as the ADC error will be less, and the attenuator circuit adds additional noise to the signal. For the I2C LCD, pin 10 is used for the data line (SDA) and pin 9 is used for the clock pin (SCL). The LCD itself also takes VCC at 5V, and a ground (GND) connection. For the rotary encoder, there are two outputs that enable the detection of the rotation direction. For output 'A' we use pin 33, and for output 'B' pin 32. It also has a switch/button when the dial is pressed, which is hooked to pin 4. A start button is added to pin 35 and uses an internal pull-up resistor. We also have 2 LEDs as outputs for providing basic information, like if the power is on, and if the ADC is running. These are mainly useful for testing and debugging. They are connected to pins 13 and 0. For testing, the MCU uses

UART to communicate with the attached PC via a UART-to-USB bridge. In the final product, we will have a USB port for a computer to plug into for pulling data off the instrument. There are multiple UART ports available, but we will use GPIO1 and GPIO3 as the TX and RX. If RTS and CTS pins are needed, then GPIOs 22 and 19 would be relocated. The servo motors will require a PWM signal, which is accomplished by using the motor control PWM (MCPWM) peripheral that comes with the ESP32 chip. Each servo only needs 1 pin, we choose 25 and 26 for them. Table 8-1 below provides a quick reference to the pin assignments used for the demo.

Table 8-1 *- Pins used on the microcontroller for the various peripherals.*

Functionality	**GPIO Pin**
ADC Channels 0 to 3	36, 37, 38, 39
SPI Memory Chip	18 (CLK), 19 (MISO), 21 (HOLD), 22 (WP), 23 (MOSI), 5 (CS/CMD)
LCD I2C	SCL: 9, SDA: 10
Start Button	35
Menu/Auxiliary Button	34
Rotary Encoder/Dial	‘A’: 33, ‘B’:32, Switch: 4
Servo Motors	25 and 26
ADC Status LED	13
Debug LED	0

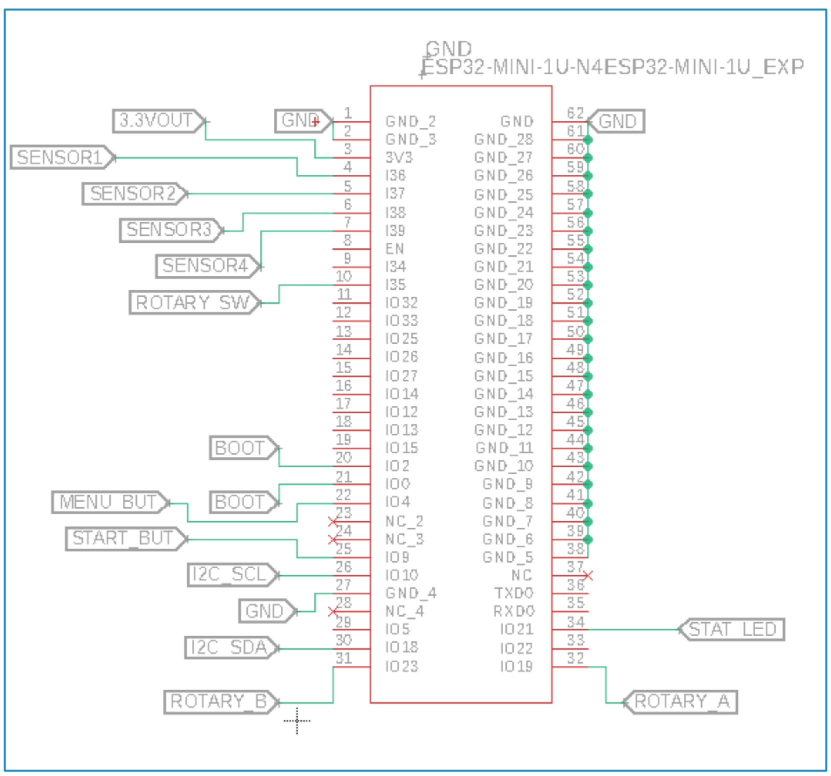

Figure 8-1 *- Pin assignment of the MCU, showing which components are connected to the MCU pins.*

As we changed how we are collecting and storing the data, the pinout had to change with it. We repurposed the ADC pins as pulse counter inputs. Using the SDMMC peripheral for communicating with the SD card, 6 pins must be used for this purpose. The updated pinout of the MCU schematic is shown in **Figure 8-2** below. We ended up using all but two GPIO pins, and considering how many peripherals were integrated, this makes sense.

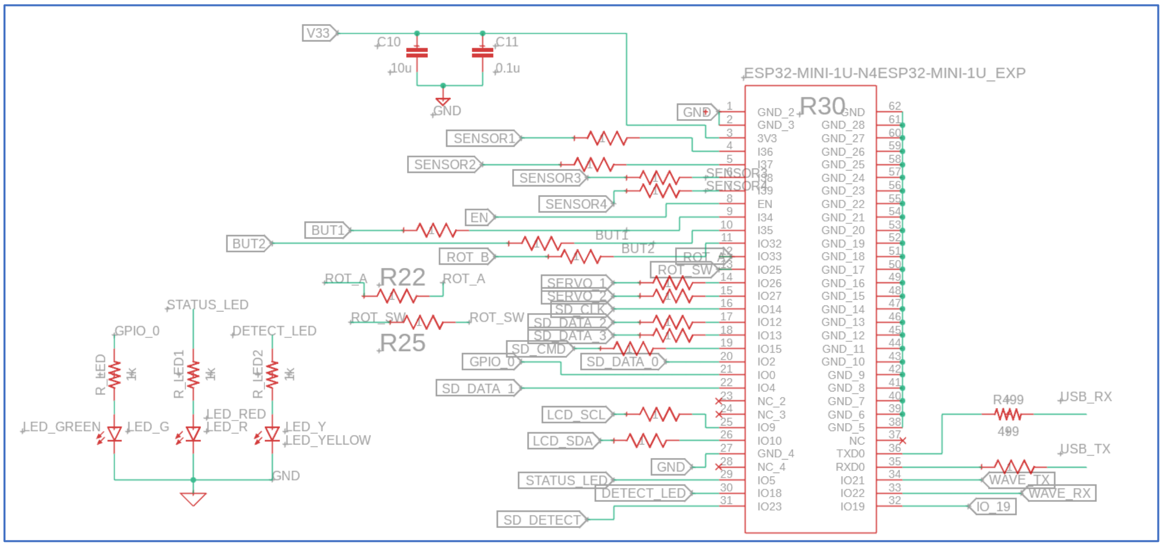

Figure 8-2 – *Updated schematic for the microcontroller's pinout. The resistors shown are 0Ω resistors used as jumpers.*

8.1.ii Power Supply

To construct the power supply, we must take into consideration how our design will be first tested and evaluated. When constructing a first prototype, the device will be comprised of "monolithic" through hole components assembled on a breadboard to see whether the design achieves the required specifications of 4 voltage outputs. During the testing phase, we can adjust or redesign the prototype if performance is unsatisfactory. However, it is important to consider that a redesign has a large impact on the project pacing and goals, therefore we must ensure we order the correct rated components. When presented with ordering the correct components for the prototype construction, we utilized TI WEBENCH which offers design with a parts list comprised of surface mount components. If we chose to order these parts individually, we would have no proper way to breadboard demo our circuit designs. A solution to this would be to order a PCB of the design however creating the proper tracings and component placement requires quite a bit of time, rather it is easier to order the discrete through hole components to use for ease of construction. It is of upmost importance to find alternative through hole components that are rated the exact same as the surface mount components to ensure proper functionality of entire circuit as recommended by the manufacturer of the voltage regulators. Also, when ordering parts for the prototype, multiple copies of each component are required if one unit used is defective, mainly with IC components. When taking the circuits into the lab for testing we must do one last inspection of the connections to ensure contacts is made precisely as the design requests, as the construction occurs, we ran into some issue with the discrete component's lead sizes, especially for the Schottky diode. To solve this issue, we sized down the leads using a wire stripper. For the placement of the capacitors, the manufacturer recommends making the leads for all capacitor components as small as possible for the best operation. results. After constructing and testing the 3.3V and 5V regulator, they were deemed a success. The inverting regulator did not have the same results. The inverting circuit was constructed using the recommended external components, and yet the design did not achieve the proper output. Multiple LM2576-ADJ ICs were interchanged yet still yielded the same underperformance. Clearly demonstrating that it wasn't a defect issue, but rather an external component selection issue. Redesign for the inverting output was needed following this test failure. To save on parts and project cost, a design using the same LM2675-ADJ regulators as the previous two circuits was implemented in conjunction with a simple inverting charge pump. All the resources were available to construct the inverting charge pump, and the circuit revealed to be successful with producing the inverted signal. However, once the inverting charge pump was connected to any load there was a severe drop in output voltage from this scheme. Greater value capacitors such as 100 µF and 470 µF were used in place of the 10 µF capacitors to attempt and provide more stabilization, but this plan did not go into effect. Additionally, use of a 2N2222 NPN transistor was implemented to see if we could buffer, and once again this plan did not work and a new design must be implemented.

8.2 Fabrication Steps

The first step in fabrication is finalizing our designs. PCB designs were finished early so we can send them for production as soon as possible. Early production gives us more time for testing and planning

To keep costs down, and for easy of manufacturing, we utilized the 3D printers available for producing various mounts and housings for our components. The main mounts that we needed were ½" and 1" lens and mirror mounts. The WeDoWo is not a standard optic and will likely require us to 3D print a mount that securely holds it in place from all sides. PCB electronics are manufactured with holes in them to allow for mounting into the housing. The exact location of these parts is subject to change, so before fabrication plans can be finalized, we needed the finalized PCB design. All components that we custom build are manufactured cheaply and quickly for the sake of rapid prototyping. Once we confirmed the design was valid, we began producing a final part that we are sure will meet our expectations.

Optical components were first tested using an optical breadboard setup. Once all testing and validation was complete in the prototyping stage, we recreated system design using custom manufactured mechanical components. The precise locations where we need to place optics will correspond to pre-drilled holes into the instrument casing, and standard or 3D printed optical mounts.

For building the housing, we used a sturdier material, aluminum, that can be shaped to form a rectangular housing for the instrument. This would make the end product look more professional.

8.3 Fabrication Results

We assembled the final product out of a mix of light balsa wood for the PCBs, and an aluminum base plate for the polarimeter. The acquisition and guide system, or image acquisition system, was 3D printed and then attached to the polarimeter's base after final testing. Multiple iterations went into designing 3D mounts for the different optical components. **Figure 8-3** shows the polarimeter and image acquisition system, while **Figure 8-4** shows the PCBs in their assembly.

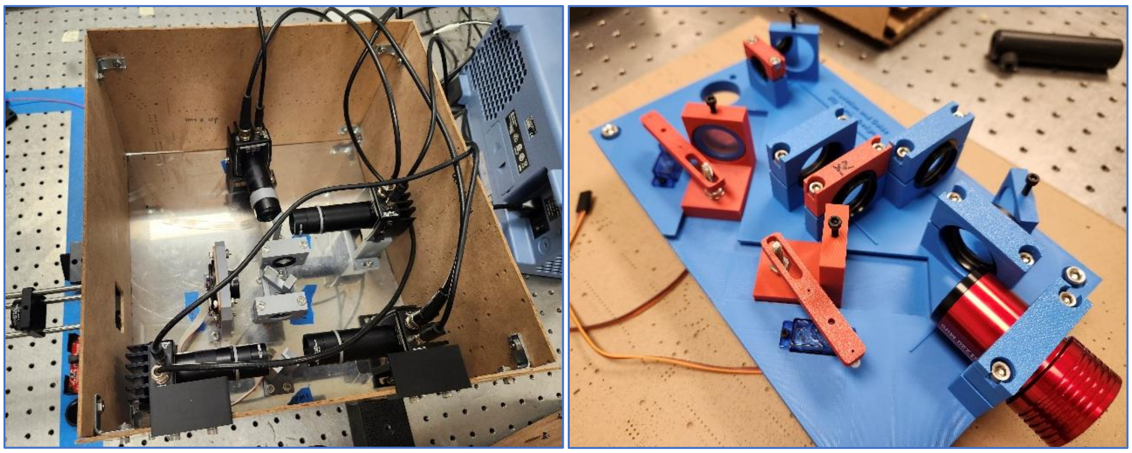

Figure 8-3 *– (Left) Polarimeter mounted to an aluminum baseplate, with a cardboard enclose to reduce ambient light from hitting the detectors during testing. (Right) Acquisition and guide system's 3D printed base and mounts.*

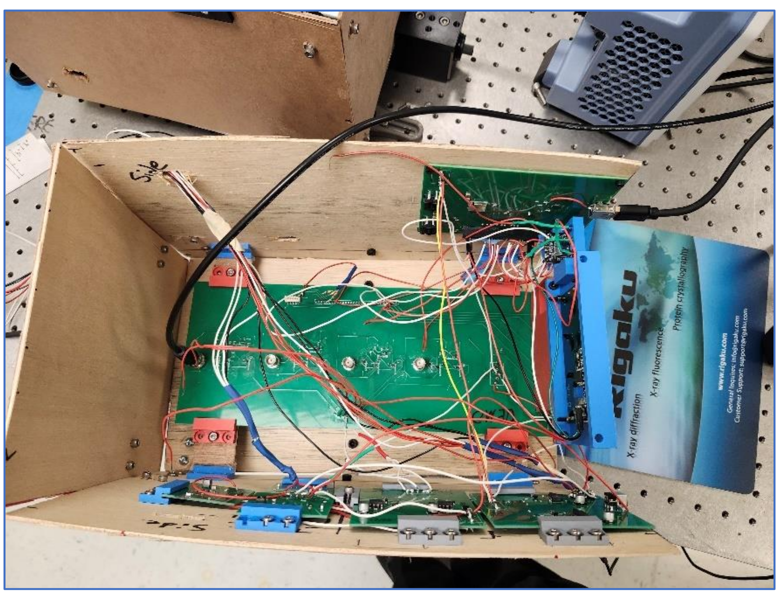

Figure 8-4 *– PCB housing assembly. The boards to the bottom of the image are the power supply units, the board to the top is the MCU board, and the board on the bottom of the housing is the peripheral board.*

Additionally, the latest design version of the AFE began development. We successfully created the amplifier and comparator, and as of current are waiting on the PCB which will host the Schmitt trigger. Below, in **Figure 8-5**, you can see the finished amplifier and its corresponding signal output from the photodetector. **Figure 8-6** shows the output out of the comparator.

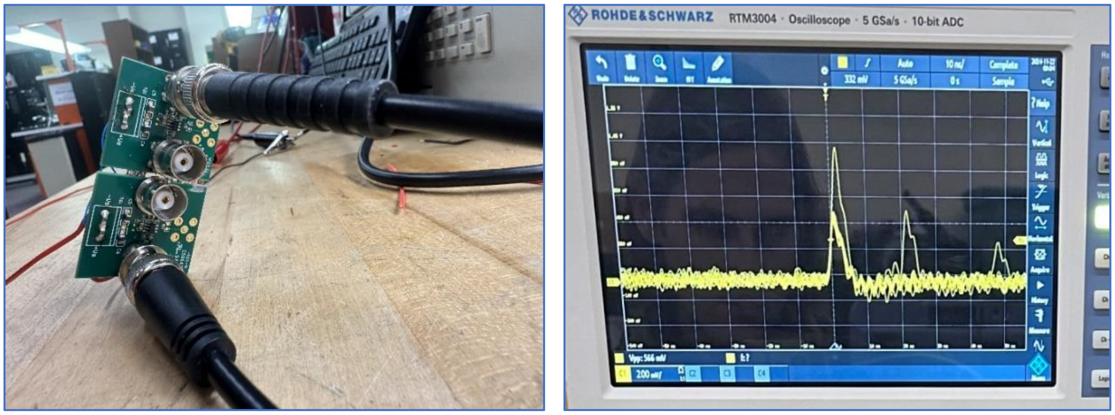

Figure 8-5 *– (Left) High-speed op-amps built on evaluation board. (Right) Amplified signal from the photodetector*

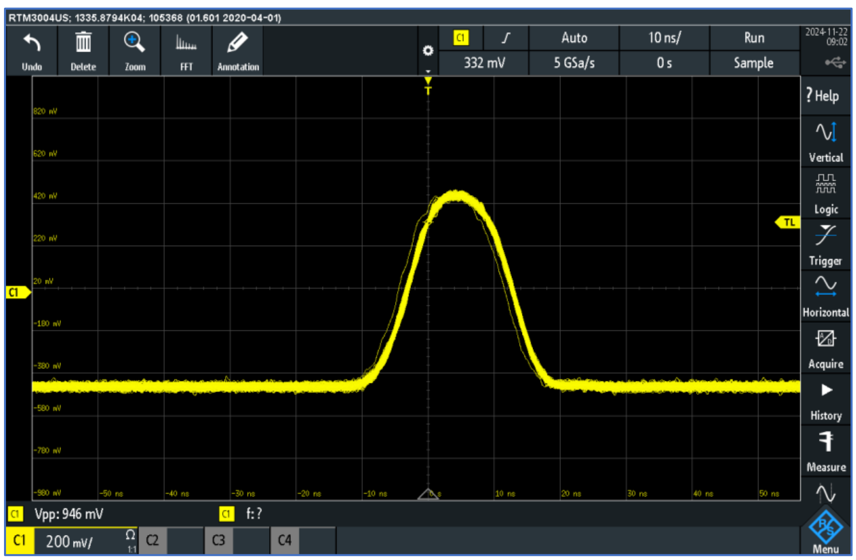

Figure 8-6 *– Photodetector signal coming out of the comparator.*

Chapter 9 – System Testing and Evaluation

In this chapter, we look at how we will test the different aspects of our design. We begin by looking at how we will test the hardware design of the project, which consists of multiple power supply regulators. We also test how the optics will measure the polarization of the input light. We then look at how we test the software code, both the embedded coding, and the Python helper code. Lastly, we look at how we will evaluate the performance of our final product in Senior Design II.

9.1 Hardware Testing

In this section, we describe the processes and results of testing our hardware circuits. The main circuitry is for the power supply, which must power our detectors, a piezoelectric rotation mount for the waveplate, and the embedded system itself. The MCU will require 3.3V with a maximum current draw of 1.2A, the rotating wave plate requires 5V with a current draw of 850mA to operate, and lastly the photodetectors require a ±12V input with a current requirement of 250mA.The circuits we test are a 12V regulator, 5V regulator, 3.3V regulator, and a 12V to -12V circuit. We also test a circuit that attenuates and offsets the detector input so that it fits into the voltage range of the MCU's ADC.

Testing the power supply we used the following equipment.

- Rohde and Shwartz RTM3004 oscilloscope
- Rohde and Shwartz NGE100 power supply
- Tektronix AFG3022B function generator
- Rohde and Schwartz HMC DMM

The initial set up was to first configure all the lab equipment. First, we set the power supply to allow for a 12V DC output of at least 0.7A. All regulator inputs were attached to this node as a common source to replicate the 12V 7A wall wart that will be included in the final design and made compatible with the PCB. The DMM was used to ensure proper resistor values and voltage values upon each regulator's output.

When creating the new circuit design for the inverting regulator, we had to confirm the signal produced by the VSW pin of the LM2675-ADJ was a high frequency PWM/ square wave signal. To do so, we used the oscilloscope to probe and show that in fact the output was a perfect signal for the inverting charge pump design. Lastly, on the inverting regulator we used the DMM to confirm the output voltages of both the noninverted and inverted 12V signals. The function generator was used to confirm the inverting charge pump design. We had the generator supply a 12V peak square wave at 52 kHz (Switching frequency of the LM2675-ADJ) to the simple capacitor and diode scheme. The scope waveform revealed that you could achieve an inverted output using the inverting charge pump with a PWM input. Following the construction of the 12V LM2675-ADJ regulator with an inverting charge pump, testing revealed a stable 11.9V output and a –12V output. However, after testing compatibility of this inverting regulator with other modules in our device, we observed a severe loading effect. The inverting output of the charge pump would drop voltage significantly, almost to ground when connected to any load. Capacitors used within the charge pump were adjusted to larger capacitance values to see if that would help stabilize the output but remained unsuccessful at maintaining a regulated inverted voltage. Another redesign is needed for the inverting voltage output.

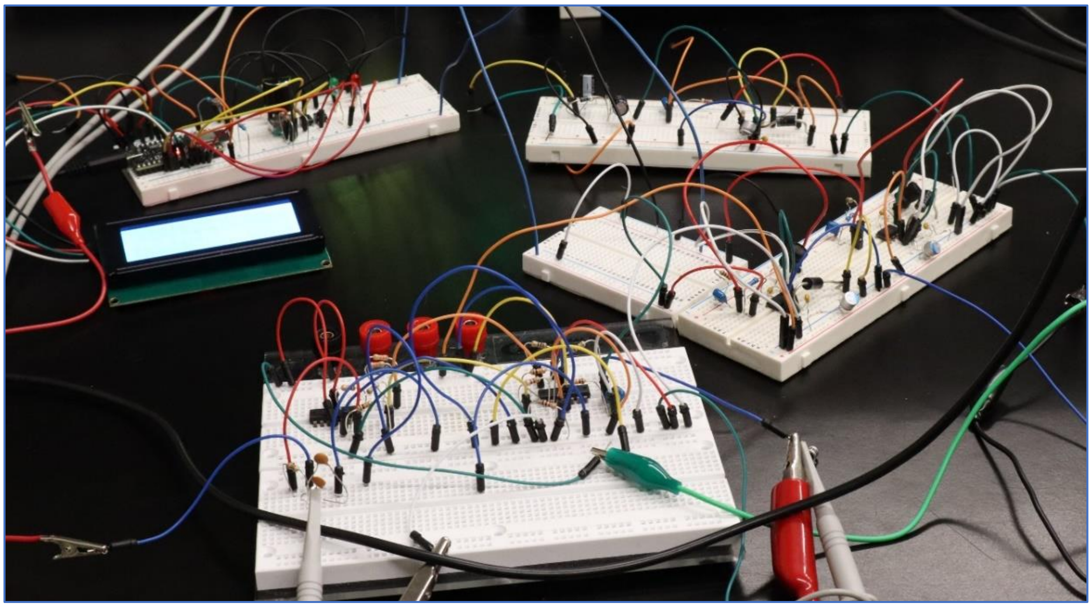

Figure 9-1 *- Breadboard testing setup for the power supply regulators, ADC attenuation circuit, and MCU setup. Top left is the MCU with the LCD screen beneath it; top right is the -12V regulator ; mid-right are the 3.3V and 5V regulators; and bottom center is the attenuator circuit for the ADC.*

Testing of the 3.3V and 5V regulators was a success. To test these circuits, we used the power supply to bring in 12V to act as our wall wart source. Using the DMM, we measured properly regulated outputs of the 3.3V and 5V regulators. Additionally, we tested the loading of the regulators to confirm stability. The load we connected was the MCU/controls prototype to test if the voltages were maintained once connected. After connection to the MCU/control module we observed stable output voltages from the regulators, and that the MCU could be powered by the two LM2675-ADJ regulator circuits. The 5V regulator was also connected to the input of the ADC front end module to be used in a voltage divider to provide a proper offset to the photodetector signal. Using the oscilloscope, we observed that the output of the 5V regulator was at 5V, but the signal did have some high frequency noise and replicated a minute triangle wave. A solution in lab to provide a “cleaner” 5V signal was to connect two 100 μF capacitors from the 5V output to ground. These capacitors helped filter the signal and provided an easy solution for a more stable output. This additional filtering is necessary for the most effective performance of the ADC front-end module. The same will be done with 3.3V output to help provide a more “clean” and stable power signal to all peripheral devices.

Proceeding the voltage regulator testing, we set up the ADC front-end alongside the MCU and voltage regulators (providing the 5V) to test if we could clearly receive a proper sample. The power supply was used to provide the ±12V needed for the op amp supply, this was only used as we did not have the input from the wall plug available as well as the inverting regulator was not functional along with the op amp circuit due to loading effect. The test was done utilizing a function generator outputting 4Vp-p at 10kHz, this tone replicates the PDA44 photodetector's voltage output maximums in terms of amplitude. Using the op-amp scheme, we successfully offset and attenuate the input signal as intended. The result was tested using an oscilloscope reading in conjunction with the ADC result which we had programmed to print on a PC terminal. Further steps were taken to alter the design of the front-end circuit during testing. Originally the output of the last op amp would connect to the ADC directly, instead we decided to attach a simple RC low pass filter (cutoff frequency = 1MHz) to the output which helped tremendously to remove any high frequency noise.

9.2 Optical Testing

For optical testing, we mainly look at the rotating waveplate, Wollaston prism, detectors, and beam geometry. Using lab equipment, we can manually find the polarization of the input light by using a polarizer and a photodetector. This is, however, a slow process, requiring that the polarizer be rotated until the power is at a maximum or at a minimum where the polarization is aligned to the polarizer or orthogonal to it, respectively. Since we want to know the polarization on a much faster time scale, a rotating waveplate is used along with a wedged double Wollaston prism that splits the light into 4 polarization components.

To test our optics, we recreate an f/8.2 beam to mimic the telescope in the Robinson Observatory at UCF. To make a suitably dim source of light, we use a series of neutral density (ND) filters after using crossed polarizers. The combination of these enables us to test using optical powers at or below a nanowatt, in combination with a polarization. An optical chopper is used to simulate a pulsing effect to add further realism to our testing. Measurements of dark count rate and photon count rate from sample light sources have been taken using a trigger counting mode on laboratory oscilloscopes. Using these methods, we created a 10 fW vertically polarized input beam. With this, we should be able to detect approximately 26,000 photons per second on corresponding detector (detector 1). Our measurements were closely in line with this expectation after accounting for the effects of background light.

Additionally, we take measurements of our detectors with the lenses covered and all lights in the room turned off. This is done to measure the dark count rate of each detector, which is stated to vary between 5k and 13k photons/sec per product. As shown in Table 9-1, our detectors mostly fall towards the high end of this range, with one of them being the exception. Dark counts are indistinguishable from real photon detection events, however they will always be present in measurements.

Table 9-1 - Measured dark count rates of each detector

Detector Number	Dark Count Rate (photons/sec)
1	10.1k
2	9.5k
3	6.1k
4	10.2k

Other testing that we will do is testing the performance of the camera and detectors. For the guide camera, we want to be sure that the camera can see the object we are trying to observe, by matching the angular field of view. To ensure that the images fit onto the guide camera, the proper magnification is calculated and used to design the image system. This magnification can then be measured experimentally to validate the design and tell us if the system is well-aligned. The test images used to find the magnification are shown in **Figure 9-2**. A ruler is used as a test image because the spacing between lines is known. By calculating the pixel width and by knowing the pixel size, the image size can be calculated. The profiles used to find the pixel widths are shown in **Figure 9-3**. The results of finding the magnification for multiple millimeter spacings is shown in Table 9-2.

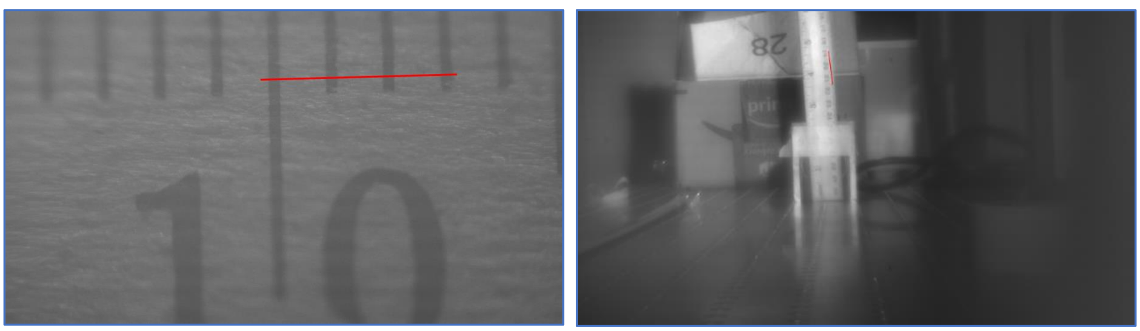

Figure 9-2 *– Test images from the image acquisition system. (Left) image of rule from the star imaging path. (Right) Image of ruler from pupil imaging path. The red lines are where profiles were taken in the process of finding the magnification.*

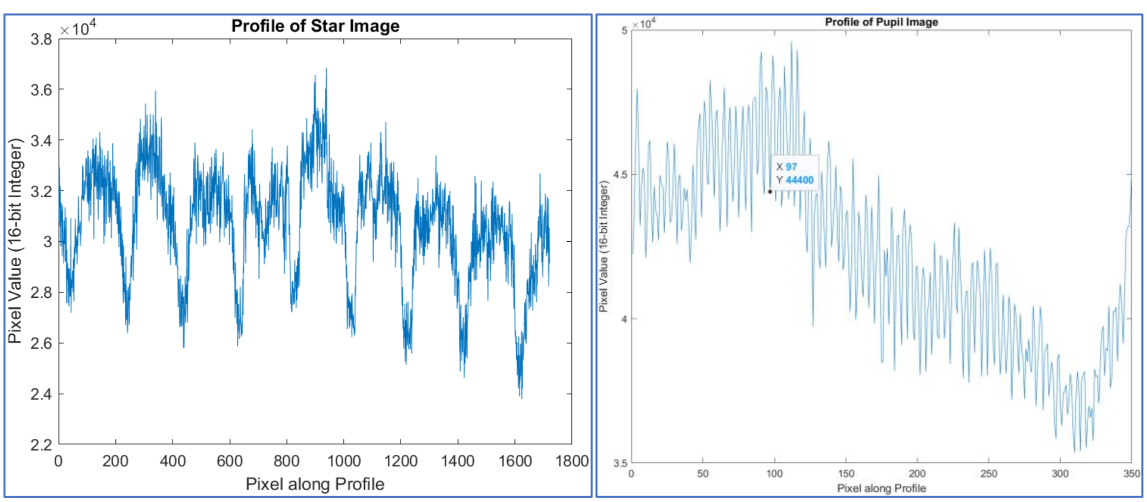

Figure 9-3 *– Profiles of the star imaging test image (left), and the profile of the pupil test image (right).*

Table 9-2 – Results from profiling the imaging system test images.

Metric	Pupil Image	Star Image
Sample Size	60 over 3 images	24 over 3 images
Avg Pixel Width	4.65	209.23
Avg Size (µm)	18.6	836.9
Avg Size (mm)	0.0186	0.8369
Magnification	0.0186	0.8369
Designed Mag.	0.0189	0.863
% - Error	1.59%	3.02%

As we can see from Table 9-2, the average magnifications agree closely with the desired/designed magnifications. The pupil imager expects a magnification close to 0.0189, while the star imager expects a magnification close to 0.863. The low percentage error means that the lenses are aligned very well, especially considering it was done by-hand and eye. Having the magnifications a little lower than the designed also ensures that the images will fit onto the detectors as expected.

9.3 Software Testing

In this section we describe the processes we used to test the embedded code. The main functions to test are the ADC sampling and then importing the data into Python. Other aspects to test, would be the operation of the LCD along with the buttons and rotary encoder dial that make up the user interface for the user. Our main priority is to ensure that the ADC is indeed sampling at 1MHz, and that we can transfer the data into Python for data processing.

9.3.i ADC Testing

To test that the ADC is functional, we hook up a function generator to one of the ADC channel pins on the ESP dev board. The ground of the ESP and function generator are connected, and the positive of the function generator goes to pin 35 for ADC1 channel 6 for the dev board. The function generator is set to high-impedance mode, and configured to produce a sinusoidal wave that is within the board's conversion range. Without using the on-board attenuation circuit, which adds noise to the signal, we are limited to voltages within 100mV and 950mV. When using the actual detectors, we will have an external attenuation circuit described in chapter 7: MCU/Control design. During our testing we noticed that the ADC would output a constant voltage after it samples the signal. Using a multimeter, we measured the voltage on the pin, and it remained constant at around 3.6V. This happens when either the function generator is plugged into that pin, or a simple photoconductor is plugged in. We determined that this occurs even when the board starts with no voltage applied to the pin. We tried the adjacent pin, and similar behavior occurred, and so we conclude that it is normal behavior.

To test the noisiness of the ADC, we first set the sample frequency to 100kHz, and pass it a 1kHz signal, and then a 50kHz signal. At 1kHz, there would be 100 points per cycle of the sinusoidal input, and at 50kHz only 2 points per cycle would be expected. The raw ADC value (integer with 12-bit resolution) is then plotted versus the index of that array. At 100kHz, each horizontal index would be 10µs (0.01ms). To convert the raw data into a voltage, a simple formula can be applied. Below is the plot of the raw data for the 1kHz signal at 100kHz sampling.

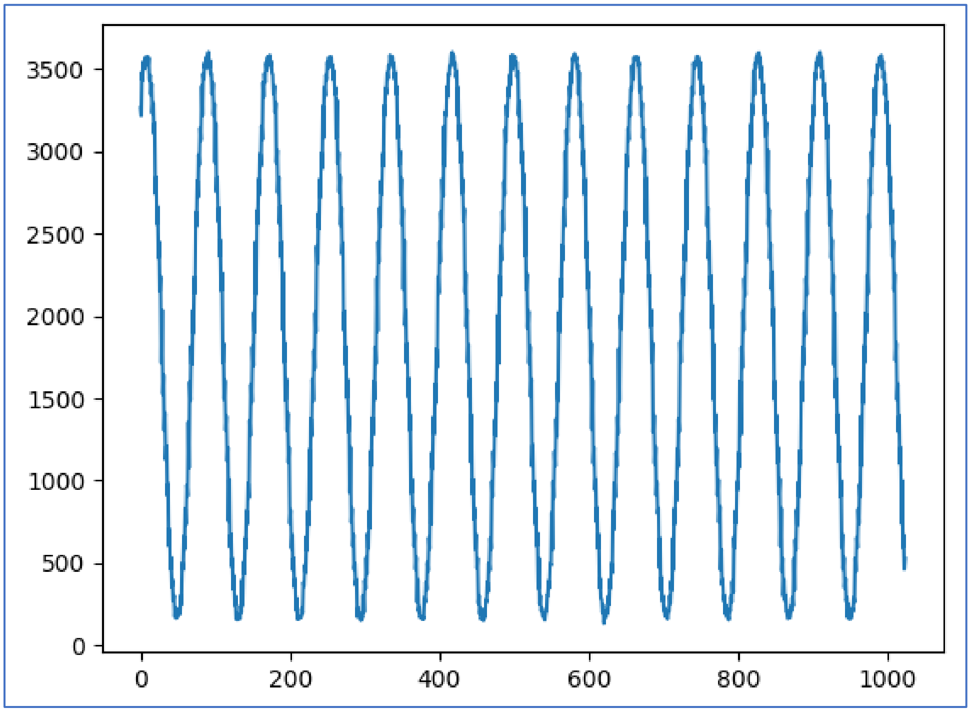

Figure 9-4 *- Plot of raw ADC data from a 1kHz signal sampled at 100kHz. Measured over 10.24ms.*

From Figure 9-4, we clearly see the sinusoidal shape of the input signal. Counting the peaks, there are 12 in this 10.24ms span, but at 1kHz there should be only 10 peaks in 10ms. As such, the ADC may not be sampling at the 100kHz specified. Now we look at sampling at 1MHz. Again, we looked at two different signal frequencies – 10kHz, and 500kHz. Now the horizontal divisions would be 1µs in length, so the whole sample covers 1.024ms.

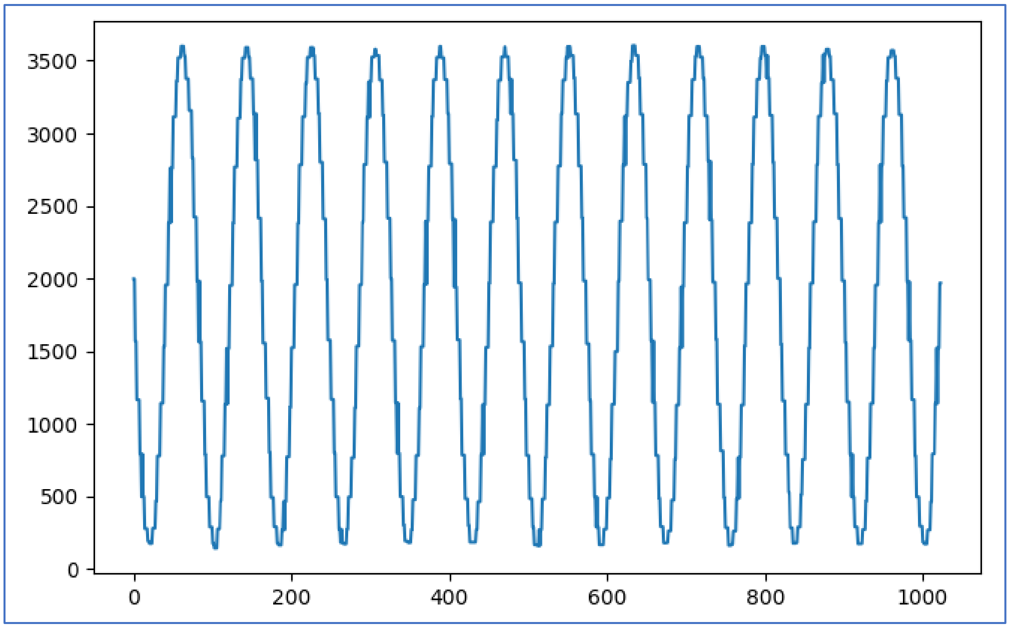

Figure 9-5 *- Plot of raw ADC values of a 10kHz signal at 1MHz. Measured over 1.024ms.*

From the plot, we see that the signal has some more noise than the previous plot. This time, there are 13 cycles of the 10kHz signal, when there should only be 10 cycles for 1ms of time. (1cycle per 100µs). Again, this suggests that the ADC sampling is off. Whether this is from the clock driving the ADC, or arises from the data buffer access, is unclear.

These plots were generated using the Python package *matplotlib*, which operates similarly to MATLAB. These plots show that the data was successfully sent over the UART-USB bridge to be read by the Python script, which then parsed the input and generated the plots above. As such, by testing the ADC setup, we also tested the Python code to get and plot the data from the MCU.

In the final design, we ended up switching to use the pulse counter peripheral to count digital pulses from the photodetectors. Since we could not get an analog frontend finished in time, we used the trigger out of an oscilloscope to read detector data and output a square pulse. This pulse is then detected by the pulse counter and is counted by the MCU.

9.3.ii User Interface Testing

Now we look at how we tested the user interface. The main user interface is a 20 character by 4-line LCD display that is driven by an I2C board. This makes it much easier to interface with the MCU and reduces the number of wires required as well. We used a component library for 1602/2004 LCD displays distributed by Zorxx free of charge under the MIT license. The other UI components are two buttons, and a rotary encoder, which acts as a digital potentiometer and has a switch (button) built in. An LED for testing interrupts and an LED for showing when the ADC is on is also included. The buttons were easily tested by toggling the LED on press. The rotary encoder was implemented with the pulse counter peripheral of the ESP32 chip, following an example by Espressif. The value of the counter is checked when the dial rotates.

For testing the LCD, we attempt to write a string to each line of the LCD, but only two lines were showing at any one time. Initially we thought there might be a configuration to change in the library, but there wasn't one. Eventually, we tried to write more than 20 characters to a single line, and it went to either line 3 or line 4 based on which line it was originally from. From our research, we found that the memory addresses for the 3rd and 4th line were just extensions from the 1st and 2nd line, respectively. For example, line one starts at 0x00, while line 2 starts at 0x40. The 1st line would end at 0x13 (19 in decimal), and the 3rd line would start at 0x14 and end at 0x27 [38].

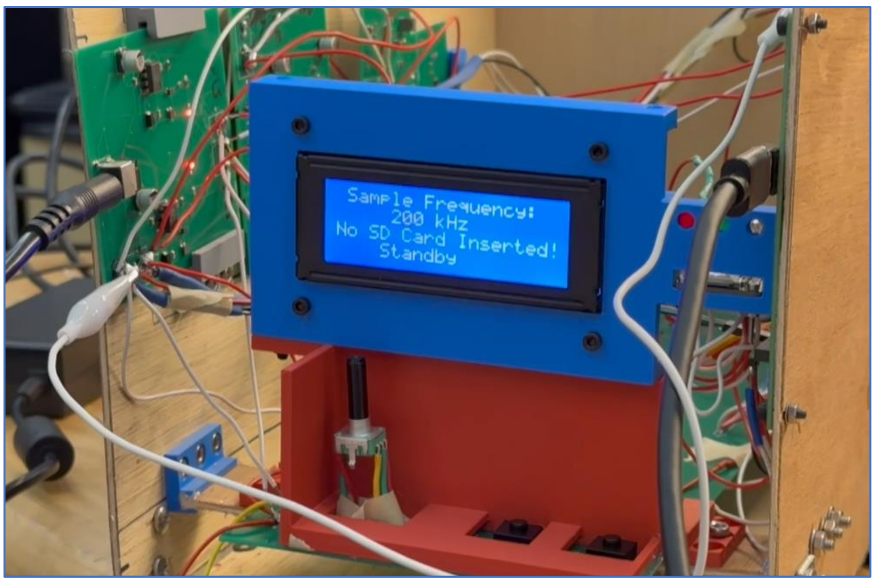

Figure 9-6 *- Picture of the user interface in the final assembly.*

We verify that buttons work by having them toggle an LED, as printing or logging in an interrupt service routine (ISR) is not advised. The rotary encoder dial is tested by displaying the pulse count on the LCD and in the log terminal. In our testing, we noticed that the switch for the rotary encoder dial wasn't working. Using a digital multimeter and probing the voltage at the various pins of the encoder showed that the internal pullup resistor was supplying less than 1V. This proved inadequate and so a 1.6kΩ resistor was used to pull up to 5V. This was the case for the other GPIO connections, and so as a preventative measure the other GPIOs were given external 3.3V pull-up resistors (at 1.6kΩ). After that was solved, we noticed that the switch for the rotary encoder acts like an on-off button rather than a single on-off event. Fortunately, since the ISR triggers on the falling edge, it works like a regular button.

In our final design, we also implemented a graphical user interface (GUI) for the Python program that monitors the UART channel and sends commands to the MCU for software-based control.

9.3.iii Python Testing

The first Python program to test is the data retrieval program that accesses the microcontroller. This is done using the *pyserial* package for serial communication schemes, like UART. Once the UART parameters are set, the program constantly prints the received data to the terminal. Once this was achieved, we set up a tag or flag that would indicate that ADC data would be printed across the UART bridge. This then allows us to parse a set number of lines of data into the Python program. We start by getting the raw ADC conversion data, which are integers from 0 to 4096 (2^{12}). This raw value can then be converted into a voltage reading, but the results were abnormal. This was due to a bug where "2^12" equates to "2+12" in Python, and so the proper way is "pow(2,12)." The formula for conversion is:

$$\text{Eq. 9-1: } v_{out} = d_{out} \cdot \frac{v_{max}}{d_{max}}$$

Where v_{max} is the maximum voltage that the ADC can read given the attenuation mode, and d_{max} is the max raw value of that the ADC can output (2^{12}).

The next Python code to that we can test is the pulse time calculator, and the polarization measurement. Since the polarization measurement requires 4 sets of data, it is not practical to test it until we have access to it. The pulse time calculation, however, can be tested as any sinusoidal signal will have a frequency/pulse time. We consider two main ways to find the pulse time. The 1st is to use calculus to find the extrema of the signal, and then find the time difference between adjacent maxima or minima. The 2nd method is to perform a Fast Fourier Transform (FFT) on the data which would peak at the frequency of the signal.

In the pulse counter redesign, the MCU gives us the raw, cumulative pulse count every sample period. To convert this to number of pulses per period, we subtract adjacent counts to get the number of new pulses. A plot of this is shown in **Figure 9-7** below.

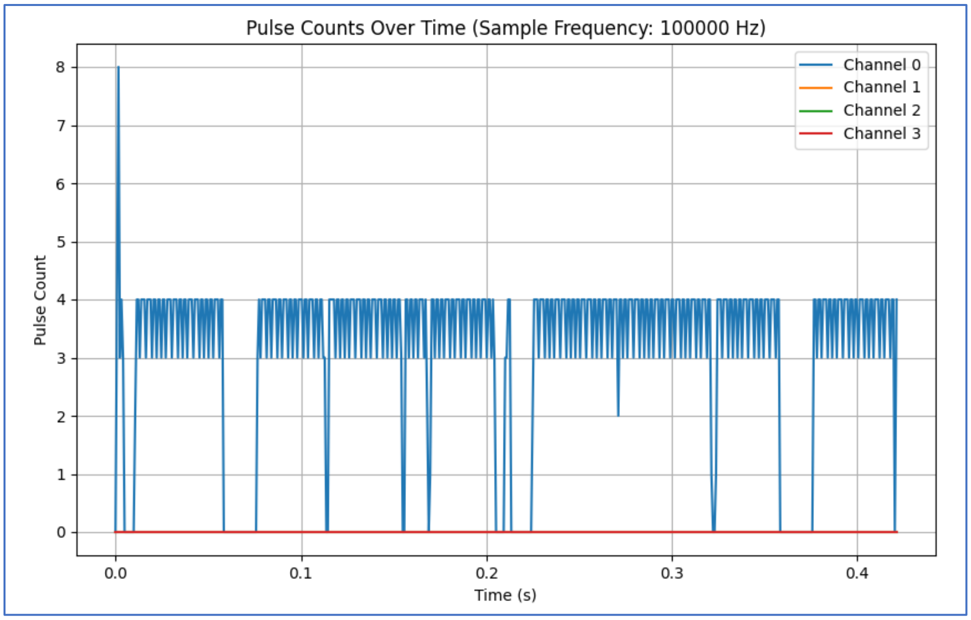

Figure 9-7 *– Plot of pulses after being collected from the MCU. The signal is from the trigger out of the oscilloscope with a representative pulse coming from a function generator.*

9.4 System Performance Evaluation

To evaluate the performance of the system, we will use a linearly polarized light source to test the polarimeter. We use a source with a predictable and known polarization and then compare with our instruments output. For pulse timing, we can use a chopper motor to turn on/off the incident light at a consistent rate and use an oscilloscope to check its frequency/pulse time. This can then be used to compare with the output of the processed data. It is important to note that the function of our system is heavily dependent on the performance of individual parts or sub-assemblies. As such, individual is absolutely essential and closely indicative of the final system performance, even though final tests will need to be conducted to ensure proper integration.

The specifications and location of the Robinson Observatory telescope provide us with a set of performance targets for imaging. Stars seen through the telescope have an angular size of approximately 3 arcsec. For stable tracking, we therefore want the IFOV of our imaging system to be at most 1 arcsec. We need at least 2 arcmin FOV to ensure visibility of stars we can use for tracking and require no more than 5 arcmin. We will test these parameters first in simulation software, then on-sky using the telescope when a prototype is ready.

Another test we can perform, is to find the extinction ratio of the wedged double Wollaston, which tells us how good it is at separating the polarization components. The higher this extinction ratio, the better the separation, and so the accuracy of our measurements would be better. Measurements of sources with a known polarization will give us accurate data on extinction ratio performance. The expected extinction ratio for a Wollaston prism is 1:10,000, so we look for a measured performance of at least this.

Before integration, the photodetectors will need to be characterized so that we have accurate data on performance metrics. Getting a good measurement of the dark count rates for the detectors will give us the best data for calculating the detector error in our measurement. We will measure the signal output when the detectors are isolated from all possible light sources in order to get a measure of the dark count rates. We will also measure the signal when exposed to light sources with a known power. In particular, a dim source with a count rate of approximately 1000 photons per second, emulating the Crab Pulsar. We will accomplish this using a NKT Photonics supercontinuum laser source that outputs 200mW over a 400 – 2400nm spectrum. Placing a series of polarizers and neutral density filters (OD = 9.43) before the polarimeter system reduces the power to the desired level.

Testing will need to be done on the rotating waveplate to determine its usable range of motion, rotation speed, and position accuracy. Using the control software provided with the ELL14K rotation mount, we can send commands and read position data to easily quantify operational parameters.

9.5 Integration Plans for Senior Design II

In Senior Design I, we were able to integrate the power supply with the microcontroller (MCU) to be able to read data from a function generator by using the on-chip analog-to-digital converter (ADC). Separately, we were able to show the polarimeter design using a standard photometer with a HeNe laser as the source. We have all the electronic parts in Fusion 360, and so we will be ready to start our PCB layout for Senior Design II. Our plans for Senior Design II will be to first integrate a single detector with the MCU to read the number of photons incident on the detector per second, which is the photon flux. This will then prove if the data acquisition portion of the project is designed well enough. If the ADC noise becomes problematic, then a minor redesign to add an external ADC chip should remedy this. After one detector has been proven to work with the MCU, we will connect all 4 and test the data handling of the MCU. Additional designs will be implemented to ensure the power supply is able to supply all the correct voltages and currents to their respective peripherals. Within senior Design II we will begin the physical PCB layout for both the PSU and MCU/Control boards using surface mount components, and test multiple of these boards to ensure proper functionality. Creating PCBs will aid in reducing device footprint whilst also creating a professional grade product.

All production for mechanical mountings will be done in Senior Design II once designs and prototyping are completed. Mounting to the telescope is done through standardized equipment and does not require significant engineering design on our part. Mounting of individual optical components within the instrument will be done using standard optical lens and mirror mounts where space allows. In areas where a typical mount is not viable, we will 3D print custom attachments. Circuitry such as wires and PCBs will need to be attached primarily using 3D printed components. Wires especially will need to be held securely in place to avoid shifting as the telescope moves.

While laboratory testing environment is necessary for the construction process, it is no substitute for in the field testing. Using the Robinson Observatory telescope, we will observe standard stars for final calibration and testing. Standard stars have very well-known luminosity and polarization, which allows us to use real observations to calibrate our data acquisition. Real observations are limited by weather, observatory availability, and distance from the construction environment which is why we will stick with the laboratory until necessary to do otherwise.

Chapter 10 – Administrative Content

In this chapter, we look at some of the administrative details pertaining to the whole project. The main topics relate to money, like the budget and financing of the project. A complete bill of materials is included. We then look at how the project was managed, the project milestones, and the work distribution.

Declaration on AI usage: We hereby declare that we have not copied more than 7 pages from a Large Language Model (LLM) for the purposes of writing this paper. We have used an LLM for purposes of comparing during research, and for some proofreading tasks.

10.1 Budget and Financing

Our funding for this project is provided by Dr. Stephen Eikenberry through his Astrophotonics Laboratory. Dr. Eikenberry is a professor at the University of Central Florida, College of Optics and Photonics. Dr. Eikenberry is funding this project in order to further his astrophysics research. The instrument we are going to build will allow him and any other interested scientists access to useful astronomical data.

Dr. Eikenberry is also providing our group with access to laboratory and observatory facilities for testing purposes. Prototype testing will be done in-lab using existing equipment as needed. The telescope at the University of Central Florida's Robinson Observatory is where we will do much of our later stage testing and ultimately the final product integration for our project.

10.2 Bill of Materials

As can be seen in the table below, the optics and related components make up the majority of the expected price tag.

Table 10-1 *- Estimated Cost of Materials*

Part	Part Number	Quantity	Unit Price	Total Cost
Single Photon Avalanche Photodetector	PDA44	4	$1,632.00	$6,528.00
Half Waveplate	AHWP10M-580	1	$1,059.22	$1,059.22
Rotation Mount	ELL14K	1	$600.40	$600.40
Guide Camera	ASI174MM Mini	1	$339.99	$339.99
Wollaston Prisms	WP10-A	2	$679.48	$1358.96
½" Mirror (Square)	BBSQ05-EO2	2	$58.53	$117.06

½" Mirror (Round)	BB05-E02	3	$55.71	$167.13
1" Mirror	BB1-E02	4	$81.22	$324.88
Achromatic Triplet Lenses	TRS254-040-A	5	$92.36	$369.44
PCB Printing	-	1	$100	$100
ESP32	-	1	$10	$10
Prototyping Board	BD-DB-PP-0615	4	$0.570	$2.28
Circuitry Components	-	-	$90.04	$90.04
Housing	-	-	$100	$100
TOTAL	**-**	**-**	**-**	**$11,710.64**

10.3 Project Management

To keep the project on track, it was important to have a good management scheme. The management of the project is based loosely on an Agile or Scrum framework. To this end, we have at least 1 or 2 meetings a week to discuss the status of the final paper, and what sections we will work on for that week. To hit the minimum page count (120), we had to pace ourselves at 16 pages a week. In these meetings, we also discussed the overall project timeline, where we plan out when we want to have certain objectives completed. These objectives mainly followed the deadlines for the divide and conquer report, the 60-page report, and the 120-page report. Outside of these, we had milestones related to completing portions of the design. For example, by July 8th, we wanted to have the design mostly worked out so that we could begin prototyping. As such, we ordered parts the week prior so that we could prototype as soon as they came in. Going forward, the goal will be to have more milestones to ensure that we meet our goals on a timelier basis.

To make meetings run as smoothly and efficiently as possible, a meeting agenda is written out ahead of time. Going forward, this agenda will be sent out to everyone ahead of time and updated after the meeting with the solutions discussed. This will make it clearer for everyone to know what is going on. By implementing these ideas, the already good communication will improve even further.

10.4 Project Milestones

To make sure we are able to come up with a quality project and be able to deliver it in a timely manner, we have come up with key goals and milestones. Our main goals include defining clear objectives and requirements. Dr. Eikenberry is funding this project to further his astrophysics research. The significant PCB design and implementation, along with the 120-page documentation that will accompany our product. At the start of the project, we'll focus on setting clear goals, figuring out what we need, and understanding any limitations. We'll create a detailed plan that outlines when tasks should be completed by creating a

Gantt chart with weekly deliverables that we discuss in biweekly meetings. Coming up with a budget given the specifications of our components needed will be essential. Additionally, we'll conduct initial studies to ensure our ideas are realistic and aligned with our desired outcomes.

Next, we select and acquire the major components, ensuring we have most, if not all, of the essential materials early in the project. During this period, we will test each major part using breadboards or development boards to verify their functionality and compatibility. This will lead to creating a detailed overall schematic design, which will be the basis for our PCB layout design.

Throughout the project, we demonstrate our progress weekly during our twice-a-week meetings. These meetings will serve as checkpoints to ensure we are on track and to address any issues promptly so problems throughout our semester don't get a chance to build up. Additionally, we must produce a certain number of pages per week as deliverables to keep the project documentation on track and meet the 120-page final report requirement.

After the design phase, we move on to the fabrication phase, where custom parts, optical components, and mechanical assemblies will be made according to our specifications. Following this, we will assemble all components into a working prototype. This phase includes careful alignment and calibration procedures to ensure our tool works correctly.

Midway through the project, we conduct a midterm demonstration to get feedback and make necessary adjustments. This step is crucial for identifying any issues early and ensuring we stay on track. As we approach the final stages, we focus on thorough testing to ensure all parts of the project meet our design specifications and performance criteria.

The final phase involves completing all required documentation, including the final report, which must follow specific formatting and content guidelines. We prepare for the final review and live demonstration by thoroughly rehearsing and ensuring all team members are ready to present their contributions effectively. Finally, we participate in the Senior Design Showcase presentation, where we demonstrated our fully functional prototype to faculty reviewers and other stakeholders. By following these goals and milestones, we ensure the project's success and alignment with desired outcomes, ultimately leading to a successful demonstration of our prototype.

Table 10-2 *- Table of Project Milestones and Their Statuses*

	Task	**Contributor**	**Status**
Senior Design 1	Divide and Conquer Document	All	Complete
	Divide and Conquer Revisions	All	Complete
	Polarimeter Research	Vincent	Complete

	Acquisition and Guide Research	David P.	Complete
	Power Supply Research	Ethan	Complete
	Acquisition and Guide Design	David P.	Complete
	ADC Design	David P.	Complete
	Data Handling	David U.	Complete
	Power Supply Design	Ethan	Complete
	Data Processing Software	David U.	Complete
	Polarimeter Design	Vincent	Complete
	60 Page Draft	All	Complete
	60 Page Revisions	All	Complete
	Parts Ordering	All	Complete
	Demo Video	All	Complete
	120 Page Final Report	All	Complete
Senior Design 2	PCB Design	Ethan	Complete
	PCB Manufacturing (Soldering)	All	Complete
	Optical Testing	Vincent, David P.	Complete
	Optical Assembly	Vincent, David P.	Complete
	Software Testing	David P., David U.	Complete
	Final Testing	All	Complete
	Final Demo	All	Complete

10.5 Work Distribution

Below is a table of our work distribution showing the primary and secondary persons involved. It is broken down into areas that align with the different majors – computer, electrical, and photonics engineering. Secondary coverage of the tasks are backed by the most qualified individual after initially assigning the primary task worker.

Table 10-3 *– Work Distribution Table*

Area	**Primary**	**Secondary**
Project Manager	David P.	Ethan Tomzcak
Website Design & Management	David P.	David U.
Polarimeter	Vincent	David P.
Image Acquisition	David P.	Vincent
Embedded Coding	David P.	David U.
Python Package	David U.	David P.

Power Supply	Ethan	David U.
PCB	Ethan	David P.

Chapter 11 – Conclusion

To conclude, we designed, tested, and built an instrument to measure the polarization and pulse timing of visible spectrum astronomical objects. Our specific use case is to observe the pulsar found in the Crab Nebula, as it is a rare visible light pulsar. The light from pulsars is quite dim compared to normal stars, and visible spectrum polarimetry equipment is specialized. Our goal is to help plug the knowledge gap resulting from these two factors.

Our goal with the project is to measure the pulse time and polarization at a temporal resolution of 2 μs (500 kHz frequency). Our other goal is to find the polarization angle to a high degree of accuracy, and high sensitivity to weak signals. This will provide new information for physicists and astronomers. Part of our goals is to also minimize optical power loss and aberrations, which we accomplished in our optical design.

To accomplish our goals, we investigated different technologies in the electrical and optical engineering fields. By analyzing the various technologies out there, we were able to narrow down which technologies have the best tradeoffs that align with our goals and constraints. Product selection was then simplified by having the underlying technology chosen. As we worked on the project, if a particular product would not work in the design, we performed additional research and selected the appropriate product.

We also looked at the standards that were applicable to our project. The main standards were IPC standards for PCB design, and IEEE standards that cover a wide range of electrical design standards. For data interfacing, the USB standard, I2C protocol, and UART protocol impacted how the microcontroller (MCU) and computer would communicate with each other, and how the MCU talks with other ICs or components with I2C. As with all projects, there are constraints on the design that must be accounted for. These are also analyzed, and our biggest limitations were time and budgetary. Despite having a generous sponsor, we want to be respectful and not add unnecessary costs to the design.

For our design, we have three major disciplines involved – electrical, computer, and optics/photonics engineering. As such, there are different design methods and processes used. Optical design usually involves the usage of ray tracing software, Zemax, to quantify aberrations that arise from paraxial simplifications. Electrical design also takes advantage of software, such as LTSpice, that can simulate dynamic circuits and their respective behaviors. Computer programming usually involves identifying the overall problem, and then breaking it apart into smaller pieces that are easier to work with. While not all problems can be broken down effectively, abstracting a problem's complexity can often lead to solutions. There were critical aspects for each disciplines' design. For the optics, it was to use a symmetric lens design to cancel out as much aberration as possible. For electrical this was making a power supply with 4 outputs that would provide and maintain the correct voltages and current output for the MCU, rotating waveplate, photodetectors, and any other peripheral electronics (such as the analog front-end). Additionally, connections of controls to the MCU were created to allow the user to have complete control of the sampling rate and time, and optics calibration. For the software, it was switching from using an Arduino framework, to using the native ESP framework (ESP-IDF). This switch gave us additional control over the MCU's hardware, at the cost of losing the simplicity of Arduino programming. Utilizing tasks in the microcontroller code allowed the program to flow in a more controlled and organized way.

After our design was complete, we ordered parts and assembled the power supply circuits. This ensured that the parts were functional, and that the design theory matches reality. We also hooked up the MCU dev board with the power supply, buttons, LCD and an analog source (function generator). We were successful in testing the output voltage of the regulators and in testing the ADC conversion with the MCU. The hardware UI consisting of an LCD, rotary dial, and some buttons was also tested for adjusting the sample frequency and sample duration. For the optical components, when they arrive, we will test the components to characterize their performance. The performance of the optical components will be the main limitation on the performance of the system.

Unfortunately, we discovered that our analog front-end would be too slow for the detector's pulse output, and so we had to redesign the circuitry to utilize GHz operational amplifiers. This introduced new design challenges, as impendence matching, and proper ground planes become increasingly important at these higher frequencies. This also required the software to switch from using the ADC to using a pulse counter peripheral. This simplified the design somewhat, as we now count photons instead voltage level changes.

Over the course of this project, we were able to achieve a lot of our goals. Top among these achievements is that we were able to work as a team to deliver this design document detailing our efforts working on the design of the project. We did a good job at regularly meeting to discuss the project's progress and work out any problems we found. We were able to build a prototype power supply and hook it up to the microcontroller (MCU), which also was programmed to sample an analog signal at 1MHz. On the optics side, we showed the operating principles of the polarimeter, and manipulation of the input light. Overall, we were able to achieve a prototype of the module, which then will be scaled to our functional specifications.

Along with our achievements, we also learned many lessons along the way. With such a time constraint, it was important early on to make effective use of our time. We did a good job at pacing our writing to meet the final report requirements by averaging 16 pages each week. Unfortunately, at least early on, this came at the cost of us neglecting to start proper designing until after we finished our technology and product research. This meant that most of our designing took place over the last month, making any missteps costly from a lack of time. Our goal was to order parts as soon as we had a solid optical design, but we wanted our sponsor to okay it before ordering costly components. This resulted in delays to ordering. From this we further learn the importance of communication. We also learned to not focus solely on the deliverables, like the design paper, but to also consider the underlying design portions as well.

AI models like ChatGPT proved to be of questionable use during our research and writing process. We analyzed the usefulness of it and similar models in detail to gain a better understanding of how we can augment our workflow with these developing technologies. Our conclusion is that LLMs have a role in guiding our research but cannot replace the use of a normal search engine. They are not suitable for major writing tasks either, and their products should be subject to lots of scrutiny before being included in any final works.

Future work could be to improve the temporal resolution of the instrument. This would require even higher-speed analog circuits. With a faster microcontroller, the temporal resolution could then be in the nanosecond regime. This would of course come with its own challenges, like data processing and storage. At 1 GSPS, 4 detectors would generate close to 8 GB of data per second of continuous sampling.

All in all, we have designed and built an instrument that can be applied to the field of astronomy and astrophysics. Pulsars pulse at a very precise frequency, and so measuring the temporal changes to the intensity will allow us to see the fine details of these pulses. By also finding the polarization, we will give astronomers new information that can provide new insights into the nature of pulsars. By combining both datasets together, we will give more information for astronomers and physicists to learn about our universe.

Appendices

Appendix A – References

[1] J. Baily, D. V. Cotton and L. Kedziora-Chudczer, "A high-precision polarimeter for small telescopes," *Royal Astronomical Society,* vol. 465, no. 2, pp. 1601-1607, Feb 2017.

[2] ThorLabs, "Polarimeter Systems with High Dynamic Range," ThorLabs, [Online]. Available: www.thorlabs.com/newgrouppage9.cfm?objectgroup_id=1564. [Accessed 28 May 2024].

[3] P. C. Cortes and et al., "Interferometric Mapping of Magnetic Fields: The ALMA View of the Massive Star-Forming Clump W43-MM1," *IOPscience,* vol. 825, no. 1, 2016.

[4] "What are Beamsplitters?," ThorLabs, 4 Jun 2024. [Online]. Available: www.edmundoptics.com/knowledge-center/application-notes/optics/what-are-beamsplitters/. [Accessed 4 Jun 2024].

[5] ThorLabs, "Beamsplitter Guide," ThorLabs, [Online]. Available: www.thorlabs.com/newgrouppage9.cfm?objectgroup_id=9028. [Accessed 4 Jun 2024].

[6] D. R. Paschotta, "Beam Splitters," RP Photonics, [Online]. Available: https://doi.org/10.61835/mjw. [Accessed 4 Jun 2024].

[7] "Switchable Mirror / Switchable Glass," Ketn Optronics, 2014. [Online]. Available: www.kentoptronics.com/mirror.html. [Accessed 8 Jun 2024].

[8] "90[deg] Flip Mounts," ThorLabs, [Online]. Available: www.thorlabs.com/newgrouppage9.cfm?objectgroup_id=1447. [Accessed 9 Jun 2024].

[9] "Control 28BYJ-48 Stepper Motor with ULN2003 Driver & Arduino," Last Minute Engineers, 2024. [Online]. Available: lastminuteengineers.com/28byj48-stepper-motor-arduino-tutorial/. [Accessed 25 June 2024].

[10] "Intro to Lithium-ion," FluxPower, 2023. [Online]. Available: www.fluxpower.com/lithium-ion-battery-technology-v2. [Accessed 13 Jun 2024].

[11] J. Chattopadhyay, T. S. Pathak and D. M. Santos, "Applications of Polymer Electrolytes in Lithium-Ion Batteries: A Review," *Polymers(Basel),* vol. 15, no. 3907, 27 Sep 2023.

[12] "The advantages and disadvantages of lithium polymer batttery," A&S Power, 02 07 2021. [Online]. Available: www.szaspower.com/industry-news/The-advantages-and-disadvantag.html. [Accessed 13 June 2024].

[13] A. R. Dehghani-Sanij, E. Tharumalingam, M. B. Dusseault and R. Fraser, "Study of energy storage systems and environmental challenges of batteries," *Renewable and Sustainable Energy Reviews,* vol. 104, pp. 192-208, 2019.

[14] "Lithium vs NiMH Battery Packs," epec Engineered Technologies, 2024. [Online]. Available: www.epectec.com/batteries/lithium-vs-nimh-battery-packs.html. [Accessed 13 June 2024].

[15] "What is a shunt regulator?," MinebeaMitsumi, [Online]. Available: https://product.minebeamitsumi.com/en/technology/ic/shunt-regulate.html. [Accessed 7 July 2024].

[16] "Solar Charge Controller Types," SunWize, [Online]. Available: https://www.sunwize.com/tech-notes/solar-charge-controller-types/. [Accessed 7 July 2024].

[17] ThorLabs, "Wollaston Prisms," ThorLabs, 2024. [Online]. Available: https://www.thorlabs.com/newgrouppage9.cfm?objectgroup_id=917. [Accessed 21 06 2024].

[18] AZO Optics, "Wollaston Prism - Definition and Applications," AZO Optics, 30 04 2014. [Online]. Available: https://www.azooptics.com/Article.aspx?ArticleID=760#:~:text=A%20Wollaston%20prism%20polarizer%20consists,an%20extraordinary%20(E)%20ray.. [Accessed 21 06 2024].

[19] P. W. Meibo Lb, "Ray tracing in Rochon prisms with absorption," *Optics Express,* vol. 25, no. 13, pp. 14676-14690, 2017.

[20] D. R. Paschotta, "RP Photoncis Encyclopedia," RP Photonics, [Online]. Available: https://www.rp-photonics.com/avalanche_photodiodes.html. [Accessed 17 6 2024].

[21] MEETOPTICS LABS, "Single-Photon Avalanche Diode (SPADs)," MEETOPTICS LABS, [Online]. Available: https://www.meetoptics.com/academy/single-photon-avalanche-diode. [Accessed 18 6 2024].

[22] J. P. Y. M. A. G. Verena Mackowiak, "NEP - Noise Equivalent Power," [Online]. Available: https://www.thorlabs.com/images/TabImages/Noise_Equivalent_Power_White_Paper.pdf.

[23] "Quartz Crystal Oscillators," Electronics Tutorials, 2024. [Online]. Available: https://www.electronics-tutorials.ws/oscillator/crystal.html. [Accessed 13 June 2024].

[24] "Switching Regulators," Analog Devices, [Online]. Available: https://www.analog.com/en/product-category/switching-regulators.html. [Accessed 7 July 2024].

[25] "What are buck, boost, and buck-boost DC-DC converters?," TDK-Lambda Americas, 31 July 2020. [Online]. Available: www.us.lambda.tdk.com/resources/blogs/20200731.html. [Accessed 13 June 2024].

[26] "Linear vs. Switching Regulators," Renesas, 2024. [Online]. Available: www.renesas.com/us/en/products/power-power-management/linear-vs-switching-regulators. [Accessed 13 June 2024].

[27] J. Patoux, "Ask The Applications Engineer-37: Low-Dropout Regulators," ADI Analog Dialogue, 2024. [Online]. Available: www.analog.com/en/resources/analog-dialogue/articles/low-dropout-regulators.html. [Accessed 13 June 2024].

[28] "Analog Devices MT-054 Tutorial," 2009. [Online]. Available: https://www.analog.com/media/en/training-seminars/tutorials/mt-054.pdf. [Accessed 7 July 2024].

[29] "High Speed Op Amps (Bandwidth >= 50MHz)," Analog Devices, [Online]. Available: https://www.analog.com/en/product-category/high-speed-op-amps-bandwidth-greaterthanequalto-50mhz.html. [Accessed 7 July 2024].

[30] S. Sarkar, A. Sarrafinazhad and A. Ghoncheh, "Introduction to LNA: Understanding the Fundamentals," Rahsoft, 29 Novemeber 2023. [Online]. Available: https://rahsoft.com/2023/11/29/introduction-to-lna-understanding-the-fundamentals/. [Accessed 7 July 2024].

[31] R. Clifton, "Benefits of Op-Amps with High Output Current," April 2023. [Online]. Available: https://www.ti.com/lit/ab/sboa568/sboa568.pdf?ts=1718917382098. [Accessed 7 July 2024].

[32] "Lens Tutorial," Thorlabs, [Online]. Available: www.thorlabs.com/NewGroupPage9.cfm?ObjectGroup_ID=8790. [Accessed 18 June 2024].

[33] "Home Page of IPC," IPC, [Online]. Available: https://www.ipc.org/. [Accessed 12 July 2024].

[34] "About USB-IF," USB-IF, [Online]. Available: https://usb.org/about. [Accessed 7 July 2024].

[35] "USB Protocol: Architecture, Working, Synchronisation, DataFormat & its Applications," EL-PRO-CUS, [Online]. Available: https://www.elprocus.com/usb-protocol/. [Accessed 7 July 2024].

[36] "USB 3.2 Specification," USB-IF, [Online]. Available: https://usb.org/usb-32-0. [Accessed 7 July 2024].

[37] M. N. Polyanskiy, "Refractiveindex.info database of optical constants," *Sci. Data,* vol. 11, no. 94, 2024.

[38] D. Weiman, "LCD Addressing," Alfred State, 29 Sept 2012. [Online]. Available: https://web.alfredstate.edu/faculty/weimandn/lcd/lcd_addressing/lcd_addressing_index.html. [Accessed 15 July 2024].

Appendix B – Copyright Permissions

7/9/2024

Name of Publication: Crab Pulsar Polarimeter and Pulse Timer (the "Work")

Author: Vincent Miller, David Patenaude, David Urrego, Ethan Tomczak

Publisher: University of Central Florida Senior Design (the "Publisher")

Description or sample of Material: Performance Specification Charts for the following products:

- **Plate Beamsplitter Transmission (BSN04, BSN10, BSN10R, and BSN16)**
- **Cube Beamsplitter Reflection and Transmission (BS025, BS034, BS043)**
- **633nm Beamsplitter Coating Transmission (PBSW-633)**
- **Wollaston Prism Beam Deviation (WP10-A)**
- **Half Wave Plate Comparison (SAHWP05M-1700, AHWP05M-1600)**

(the "Material")

Thorlabs, Inc. hereby grants permission to Publisher under a Creative Commons Attribution License (CC BY) to include the Material in the Work, and in all future editions and revisions thereof, without restriction, and to create derivative and ancillary works therefrom for research and academic purposes only subject to making such derivative work generally available under the grant of a similar license , and to publish such derivative work in all media now known or hereafter discovered throughout the world and in all languages, whether published by Publisher or its licensees.

A credit line to acknowledge use of the material is required and shall reference "Thorlabs, Inc." and the product part number(s).

Agreed and Accepted:

THORLABS, INC.

By:

Date: July 10, 2024

Name: Chris Russo

Title: Senior Corporate Counsel

Appendix C – ChatGPT Prompts & Response

[GPTA]: Prompt: What are some different types of beamsplitters? I need both polarizing and non-polarizing beam splitter options.

Response: Beam splitters are optical devices used to split a beam of light into two or more separate beams. They are commonly used in various optical applications, including laser systems, interferometers, and imaging systems. There are two main categories of beam splitters: polarizing and non-polarizing. Here are some common types from each category:

Non-Polarizing Beam Splitters (NPBS)
1. **Plate Beam Splitters**:
   - **Description**: A thin, flat piece of glass or other transparent material with a partially reflective coating.
   - **Usage**: Suitable for applications where minimal polarization dependence is required.
   - **Pros**: Simple design, easy to manufacture, can handle a wide range of wavelengths.
   - **Cons**: Can introduce beam displacement and unwanted reflections.

2. **Cube Beam Splitters**:
   - **Description**: Consists of two right-angle prisms cemented together with a partially reflective coating on the hypotenuse of one prism.
   - **Usage**: Commonly used in laser applications and optical systems where beam alignment and stability are crucial.
   - **Pros**: Robust, minimal beam displacement, compact.
   - **Cons**: Typically more expensive than plate beam splitters.

3. **Pellicle Beam Splitters**:
   - **Description**: A very thin, transparent membrane stretched over a frame.
   - **Usage**: Used in applications requiring minimal beam displacement and low absorption.
   - **Pros**: Extremely thin, very low absorption, minimal beam displacement.
   - **Cons**: Fragile, sensitive to environmental conditions, limited power handling.

4. **Variable Beam Splitters**:
   - **Description**: Beam splitters with adjustable splitting ratios, often implemented using motorized or manual mechanisms.
   - **Usage**: Used in experimental setups where flexibility in the beam splitting ratio is needed.
   - **Pros**: Adjustable splitting ratio, versatile.
   - **Cons**: Can be complex and expensive.

Polarizing Beam Splitters (PBS)
1. **Polarizing Plate Beam Splitters**:
   - **Description**: Similar to non-polarizing plate beam splitters but with a coating that separates light based on polarization.
   - **Usage**: Used in applications where polarization control is required.
   - **Pros**: Can achieve high polarization extinction ratios.
   - **Cons**: Can introduce beam displacement, coating sensitivity.

2. **Polarizing Cube Beam Splitters**:
   - **Description**: Made from two prisms with a dielectric coating that reflects one polarization while transmitting the other.
   - **Usage**: Common in laser systems and optical setups where precise polarization separation is needed.
   - **Pros**: High extinction ratio, compact, robust.
   - **Cons**: Typically more expensive than polarizing plate beam splitters.

3. **Wollaston and Nomarski Beam Splitters**:
   - **Description**: Consist of two birefringent prisms cemented together, used to separate polarizations with a large angular separation.

- **Usage**: Common in microscopy and interferometry.
- **Pros**: High polarization separation, large angular separation.
- **Cons**: Can be bulky, more complex to align.

4. **Glan-Thompson and Glan-Taylor Prisms**:
- **Description**: High-quality birefringent prisms that provide very high polarization extinction ratios.
- **Usage**: Used in applications requiring extremely pure polarized light.
- **Pros**: Extremely high extinction ratio, excellent optical quality.
- **Cons**: Expensive, limited wavelength range.

Each type of beam splitter has its own advantages and disadvantages, making them suitable for different applications depending on the specific requirements for wavelength range, polarization, beam displacement, and environmental conditions.

[GPTB] Prompt: In a few paragraphs what are some benefits to using generative AI when writing technical engineering documentation?

Response:

Generative AI offers several benefits when it comes to writing technical engineering documentation. One of the primary advantages is enhanced efficiency and productivity. AI can quickly generate large volumes of text based on given inputs, significantly reducing the time and effort required to draft documentation. This capability allows engineers to focus more on their core tasks rather than spending excessive time on writing, ensuring that documentation is produced faster and kept up-to-date with the latest project developments.

Another significant benefit is improved consistency and accuracy. Generative AI can be trained to use specific terminology, formatting, and styles consistently throughout the documentation. This ensures that all documents adhere to the same standards, which is crucial for clarity and professionalism in technical writing. AI can also help in identifying and correcting errors, reducing the risk of misinformation and enhancing the overall quality of the documentation.

Additionally, generative AI can aid in the customization and personalization of documents. AI can tailor content to different audiences, such as creating simplified versions for non-technical stakeholders or detailed technical guides for engineers. This adaptability makes the documentation more accessible and useful to a broader range of readers. Furthermore, AI can integrate and cross-reference information from various sources, creating comprehensive and cohesive documents that cover all necessary aspects of the engineering project.

Finally, using generative AI in technical documentation can foster innovation and collaboration. AI tools can facilitate collaborative writing and editing processes, allowing multiple team members to contribute and refine documents simultaneously. This collaborative approach can lead to the creation of more thorough and accurate documentation. Additionally, the innovative use of AI in documentation can inspire new ways of thinking and working, driving further advancements in both the engineering and documentation fields.

[GPTC] Prompt: In a few paragraphs, what are some negatives for using generative AI for technical engineering writing? [follow up to GPTB]

Response:

While generative AI offers numerous benefits for technical engineering writing, it also presents several challenges and potential drawbacks. One significant concern is the accuracy and reliability of the generated content. AI models can sometimes produce incorrect or misleading information, especially if they are trained on insufficient or biased data. In technical engineering documentation, accuracy is paramount, and any errors could lead to significant misunderstandings or operational issues. This necessitates thorough human review and verification of AI-generated content, which can offset some of the time-saving benefits.

Another issue is the lack of deep contextual understanding. Generative AI, while advanced, may not fully grasp the intricate and nuanced details of complex engineering topics. It can generate plausible-sounding text that lacks the depth and specificity required for high-quality technical documentation. Engineers often need to convey detailed technical specifications, methodologies, and troubleshooting steps that require a level of expertise and context awareness that AI might not yet achieve. This limitation can result in generic or superficial documentation that fails to meet the needs of its intended audience.

Moreover, there are concerns about the potential loss of human expertise and critical thinking. Relying heavily on AI for documentation could lead to engineers becoming less engaged with the writing process and less inclined to develop their technical communication skills. Over time, this could erode the quality of documentation and the ability of engineers to effectively communicate complex concepts. Maintaining a balance between leveraging AI for efficiency and ensuring human expertise is essential to preserving the integrity and quality of technical writing.

Lastly, there are ethical and security considerations. The use of generative AI involves handling sensitive project data, which raises concerns about data privacy and security. Ensuring that AI tools are used in a secure and ethically responsible manner is crucial, particularly when dealing with proprietary or confidential information. Additionally, the deployment of AI in technical documentation must be managed to avoid biases and ensure that the generated content is fair and inclusive, which can be challenging given the inherent biases present in training datasets.

Appendix D – Software Code

The code for this project is available on the GitHub repository for this project, available at this link: https://github.com/AldenP/Pulsar-Instrument-Package. On the repo, is code for the microcontroller, Python data acquisition, and the website created to showcase our project.